CHAPTER IV

RESULTS AND DISCUSSION

In order to find any selective catalyst to preferentially produce SWNT, this research was to focus the effects of supporting materials and catalyst formulations. Moreover, the effect of carbon–containing gases was also considered in this study. In this section, the results were classified according to types of supporting materials, which were silica gel, magnesium oxide and alumina. Each support was studied the effect of feed gases and catalyst formulations. To know both quantitative and qualitative characterizations of produced carbon, the combination of Raman Spectroscopy, TPO, and TEM techniques was used to characterize the carbon deposits.

For the carbon nanotubes characterization, this thesis employs the Raman Spectroscopy technique for a systematic screening of catalyst. It can provide information about purity, distribution of tube diameters, and electronic properties. There are three main signals indicating type of carbon species. First signal, below 300 cm^{-1}, the distribution of tube diameters was shown in the radial breathing mode frequency range (RBM). In this region, It has been shown that for all tube symmetries and SWNT are appeared. Then, in the range of 1,400–1,700 cm^{-1}, the electronic properties, metallic or semiconductor, is shown in the tangential mode (TM). Finally, the level of disordered carbon and amorphous carbon is showed at around 1,350 cm^{-1}.

The TEM technique provides two-dimensional images that suit for studying carbon nanotube structure, diameter, and quality.

The Temperature Programmed Oxidation (TPO) was used to confirm the types of carbonaceous deposits on spent catalysts. Different forms of carbon products are oxidized at different temperatures. In 2000, Kitiyanan and coworkers investigated the oxidation temperature for each type of carbon deposits. The oxidation temperature of amorphous carbon was found in the range of 300–400 °C, while SWNT and MWNT were oxidized around 495–530 °C and 600–700 °C, respectively. Figure 4.1 illustrates the TPO profiles of the carbon produced on the

Co:Mo/SiO$_2$ catalyst. This sample presented a small oxidation peak centered at around 330 °C, which is assigned to amorphous carbon, and a major peak marked in the figure with an arrow, centered at about 510 °C, which is ascribed to the oxidation of SWNT. Two important reference samples were investigated by TPO and their profiles are included in this figure. The first reference was a graphite powder physically mixed with the Co:Mo catalyst. The oxidation of this form of carbon occurred at very high temperatures, starting at about 700 °C, and completed after holding 30 minutes at 800 °C. The second important reference sample investigated was a commercial sample of purified SWNT, obtained from Tubes@Rice (Rice University). The TPO of this sample exhibited two peaks, a low-temperature one that corresponds to the oxidation of the amorphous carbon and a second one centered at 510 °C, which corresponds exactly to the position of SWNT.

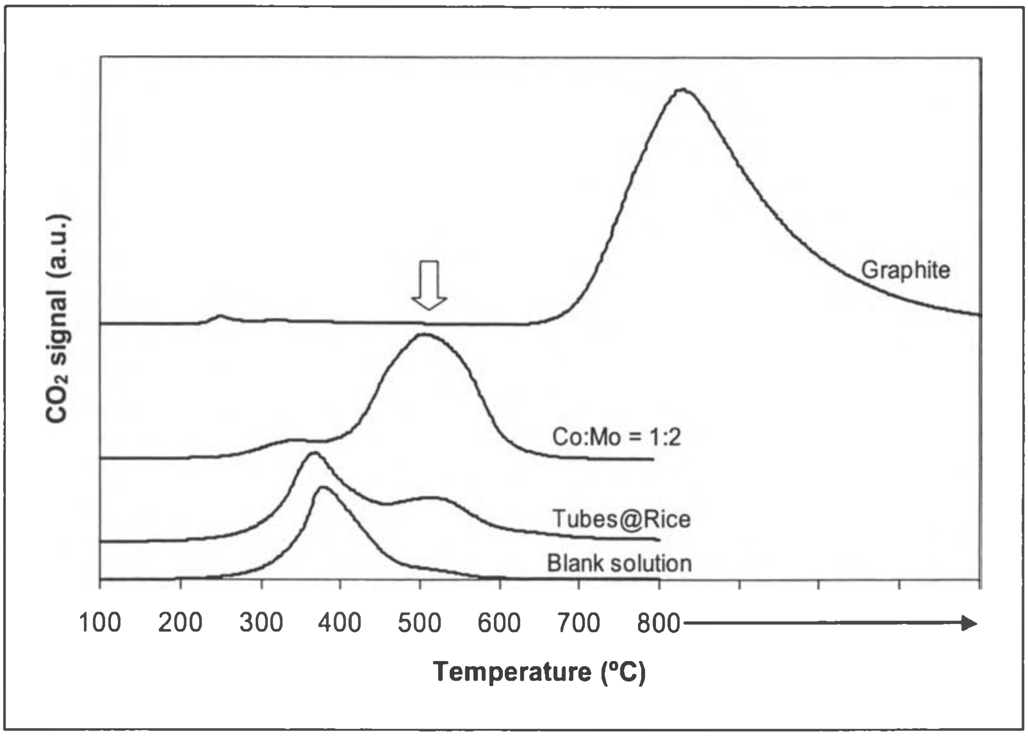

Figure 4.1 TPO of all the carbonaceous species present in the Co-Mo 1:2/SiO$_2$ catalyst compared to similar TPOs of a graphite reference, blank solution, and commercial SWNT obtained from Tubes@Rice (Kitiyanan, 2000)

4.1 The Carbon Nanotubes Formation on Silica Support

Silica support has been showed an interesting result on the carbon nanotubes production. The effects of hydrocarbon–containing gases and catalyst formulations were studied on this support. Table 4.1 summarizes all of the characterization results by using Raman spectroscopy and TPO techniques. The Raman spectrum of carbonaceous product indicate different forms of carbon by comparing the RBM, G-band, and D-band signals. The RBM signal corresponds to the appearance of SWNT, while G-band and D-band indicate graphite-like and disorder carbon, respectively. The intensity of D-band relative to G-band can be used as a qualitative measurement for the formation of undesired forms of carbon. Moreover, the D-band to G-band (D/G) intensity ratio also provides relative amount of disorder carbon to graphite-like carbon. Typically, if the relative intensity ratio (D/G) is low, this can be indicated that the formation of disorder carbon is lower than graphite-like carbon, so it mean that carbon is mostly consist of graphite-like form such as SWNT, MWNT, and nanofiber. On the contrary, if the relative intensity ratio (D/G) is high, this can be implied that the sample is mainly in disorder carbon form.

Table 4.1 Summary of carbon nanotubes production by using different gases and catalyst formulations on silica support.

Samples	D/G Ratio	Carbon Yield (%)	RBM
NiMo 1:1/SiO_2 (CH_4, 750 °C)	0.90	8.51	no
NiMo 1:1/SiO_2 (CO, 750 °C)	0.37	2.05	yes
NiMo 1:1/SiO_2 (CH_4 +CO, 750 °C)	0.79	3.51	no
NiMo 1:2/SiO_2 (CH_4, 750 °C)	0.86	6.16	no
NiMo 1:2/SiO_2 (CO, 750 °C)	0.53	1.90	no
NiMo 1:2/SiO_2 (CH_4 + CO, 750 °C)	0.85	3.25	no
NiMo 2:1/SiO_2 (CH_4, 750 °C)	0.83	7.71	no
NiMo 2:1/SiO_2 (CO, 750 °C)	0.21	2.04	yes
NiMo 2:1/SiO_2 (CH_4+CO, 750 °C)	0.97	5.81	no
CoMo 1:1/SiO_2 (CH_4, 750 °C)	0.85	13.33	no
CoMo 1:1/SiO_2 (CO, 750 °C)	0.06	2.29	yes
CoMo 1:1/SiO_2 (CH_4 +CO, 750 °C)	0.78	6.52	yes
CoMo 1:2/SiO_2 (CH_4, 750 °C)	0.83	15.69	no
CoMo 1:2/SiO_2 (CO, 750 °C)	0.03	1.83	yes
CoMo 1:2/SiO_2 (CH_4 + CO, 750 °C)	0.79	8.42	no
CoMo 2:1/SiO_2 (CH_4, 750 °C)	0.85	14.16	no
CoMo 2:1/SiO_2 (CO, 750 °C)	0.08	1.50	yes
CoMo 2:1/SiO_2 (CH_4+CO, 750 °C)	0.45	6.06	yes
FeMo 1:1/SiO_2 (CH_4, 750 °C)	0.76	13.01	no
FeMo 1:1/SiO_2 (CO, 750 °C)	0.36	1.78	yes
FeMo 1:1/SiO_2 (CO+CH_4, 750 °C)	0.85	3.91	yes
FeMo 1:2/SiO_2 (CH_4, 750 °C)	0.78	16.19	no
FeMo 1:2/SiO_2 (CO, 750 °C)	0.39	1.39	yes
FeMo 1:2/SiO_2 (CO+CH_4, 750 °C)	0.86	4.43	no
FeMo 2:1/SiO_2 (CH_4, 750 °C)	0.82	8.62	no
FeMo 2:1/SiO_2 (CO, 750 °C)	0.33	2.26	yes
FeMo 2:1/SiO_2 (CO+CH_4, 750 °C)	0.20	3.14	yes

Table 4.1 (continued)

Samples	D/G Ratio	Carbon Yield (%)	RBM
Ni/SiO_2 (CH_4, 750 °C)	0.97	0.33	no
Ni/SiO_2 (CO, 750 °C)	0.31	0.43	no
Ni/SiO_2 (CO+CH_4, 750 °C)	0.29	0.31	no
Co/SiO_2 (CH_4, 750 °C)	1.01	0.32	no
Co/SiO_2 (CO, 750 °C)	0.20	0.33	no
Co/SiO_2 (CO+CH_4, 750 °C)	0.26	0.35	no
Fe/SiO_2 (CH_4, 750 °C)	0.90	0.33	no
Fe/SiO_2 (CO, 750 °C)	0.93	0.30	no
Fe/SiO_2 (CO+CH_4, 750 °C)	0.94	0.27	no
Mo/SiO_2 (CH_4, 750 °C)	0.93	0.39	no
Mo/SiO_2 (CO, 750 °C)	0.51	0.86	no
Mo/SiO_2 (CO+CH_4, 750 °C)	0.80	0.45	no

4.1.1 Effects of CH_4, CO, and mixture of CH_4 and CO on the Carbon Nanotubes Formation

The carbon–containing gases have played a very important role for synthesizing carbon nanotubes. During the reaction, the carbon–containing gases, which are methane, carbon monoxide, and the mixture of methane and carbon monoxide, were passed through the tubular reactor packed with different catalysts at 750 °C.

To determine the characteristics of deposited carbon, the Raman spectroscopy and TPO techniques were used to characterize the carbon samples. Figures 4.2–4.13 illustrate the Raman spectra and TPO profiles of carbon samples produced by NiMo, CoMo, and FeMo catalysts over silica support with different gases.

For example, comparing between Raman spectra and TPO profiles in Figures 4.2–4.3 and 4.6–4.7, the Raman spectra of carbon produced by CO disproportionation on 2:1 NiMo and 1:2 CoMo catalysts present RBM peaks, and the D-band intensity is substantially lower than the G-band intensity. Consequently, these spectra may indicate that SWNT were appeared in these samples as well as disordered carbon was formed in very small quantity. On the other hand, carbon obtained by CH_4 decomposition and mixture of CH_4 and CO did not give the RBM signal, and the D-band was also as high as G-band intensity, which possibly mean that carbon product mainly consists of undesirable forms of carbon as shown in Figures 4.2 and 4.6. In agreement with the results obtained from TPO technique in Figures 4.3 and 4.7, the oxidation temperature of carbon produced by CO disproportionation on NiMo is centered at around 500 °C, which due to SWNT, whereas high oxidation temperature peaks of CH_4 and mixed gases are centered above 600 °C, which correspond to MWNT.

From Figures 4.4–4.13, as can be seen to the Raman spectra, most of the carbons produced by CO disproportionation present the RBM signals, so SWNT are appeared in the carbon products. On the other hand, carbon generated by CH_4 decomposition does not give the RBM signals. It gives high intensity of D-band, which is ascribed to too much disordered carbon. For the D-band to G-band intensity ratio, using CH_4 give higher ratio than using CO as a feed gas; therefore, carbon produced by CH_4 decomposition give large amount of disordered carbon as shown in Table 4.1. A mixture of CO and CH_4 also provides high D/G ratio, but some Raman spectra show SWNT as shown in Figures 4.4, 4.8, and 4.12.

Another interesting result can be observed from Figures 4.6 and 4.8. The Raman spectra of carbon produced by CoMo at 1:2 and 2:1 mole ratios can detect the RBM signals when feed CO, CH_4 and their mixtures through these catalysts. Moreover, CoMo at 1:2 mole ratio gives strong intensity of RBM signal and also gives low of undesirable forms of carbon.

The total amount of deposited carbon was determined by TPO technique. Comparing the TPO profiles among CO, CH_4 and their mixtures, the area under CH_4 curve is greater than others, which can be mean that this sample provides high of carbon deposits, while CO curve gives the lowest of carbon deposits. In addition, TPO technique can previously indicate the type of carbon species such as SWNT, MWNT, and amorphous carbon. The results show that most of the samples show the dominant peaks at around 550–650 °C, which due to the oxidation temperature of MWNT.

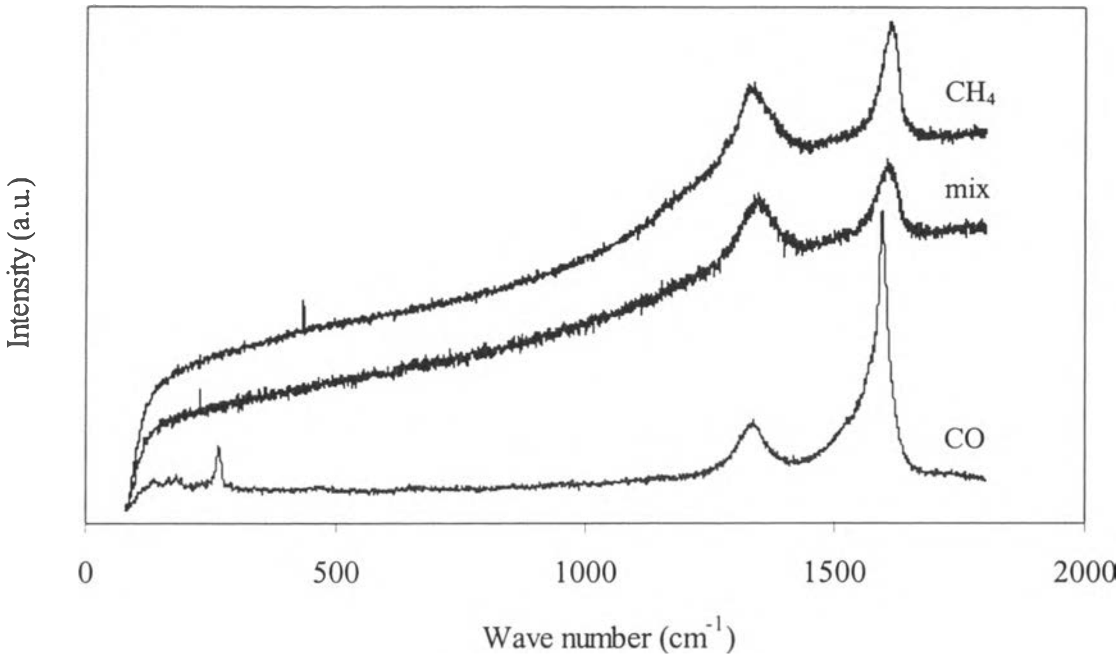

Figure 4.2 Raman spectra of carbon produced by NiMo 2:1 over silica support with CH$_4$, CO, and mixture at 750 °C.

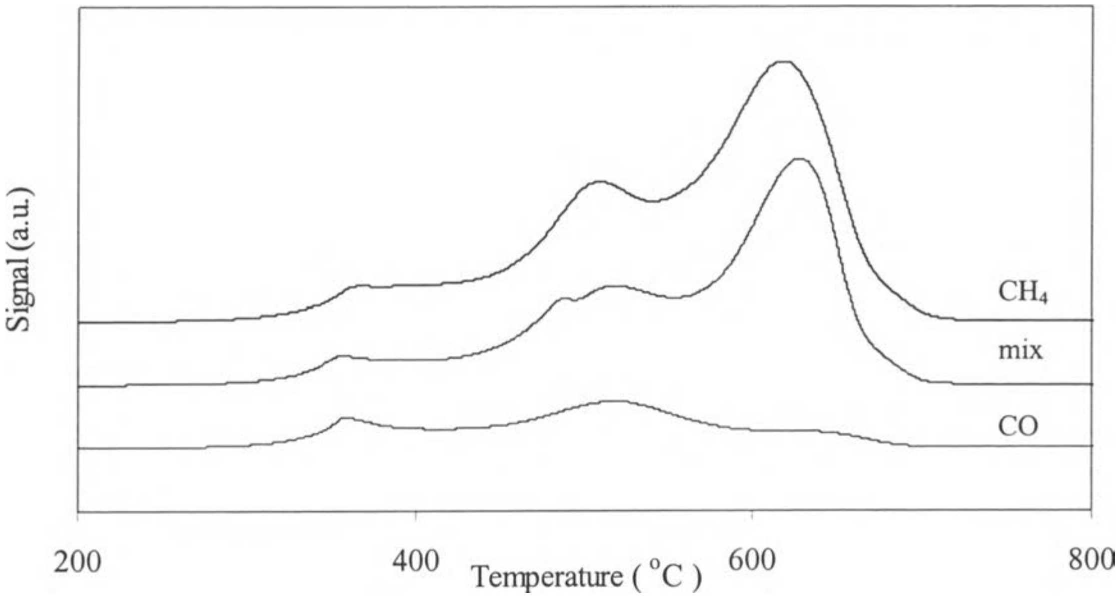

Figure 4.3 TPO profiles of carbon produced by NiMo 2:1 over silica support with CH$_4$, CO, and mixture at 750 °C.

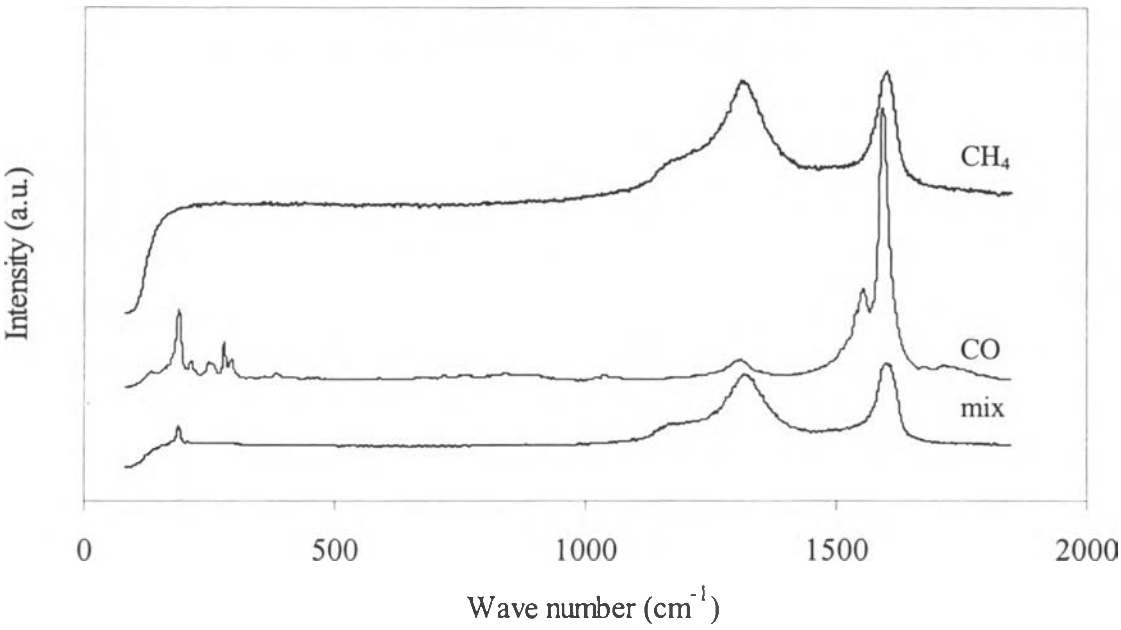

Figure 4.4 Raman spectra of carbon produced by CoMo 1:1 over silica support with CH_4, CO, and mixture at 750 °C.

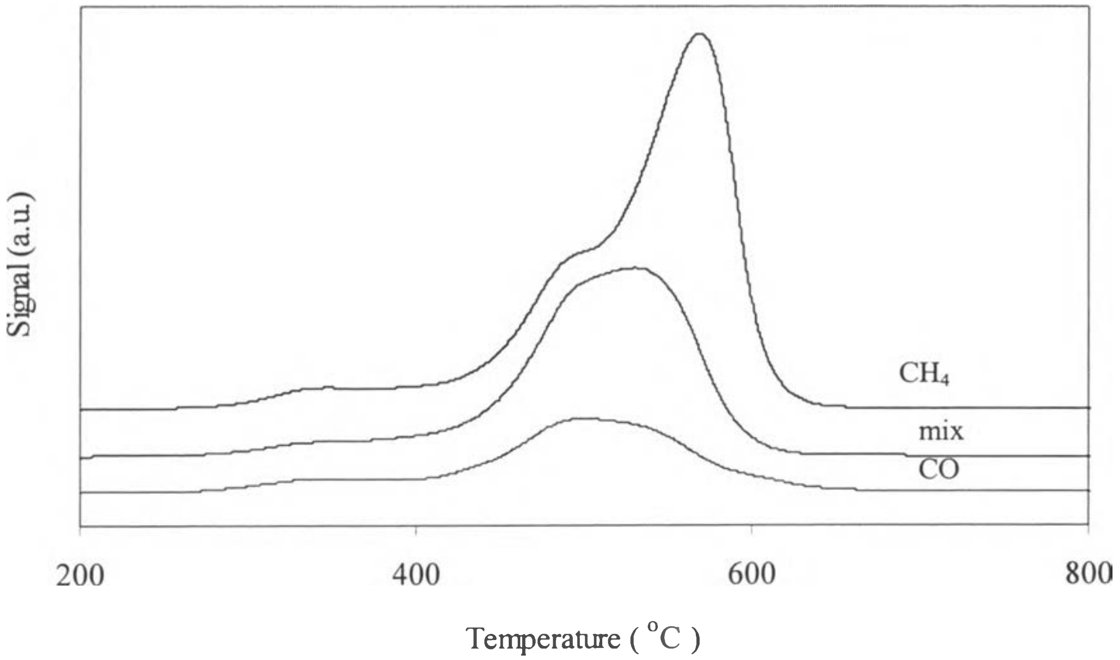

Figure 4.5 TPO profiles of carbon produced by CoMo 1:1 over silica support with CH_4, CO, and mixture at 750 °C.

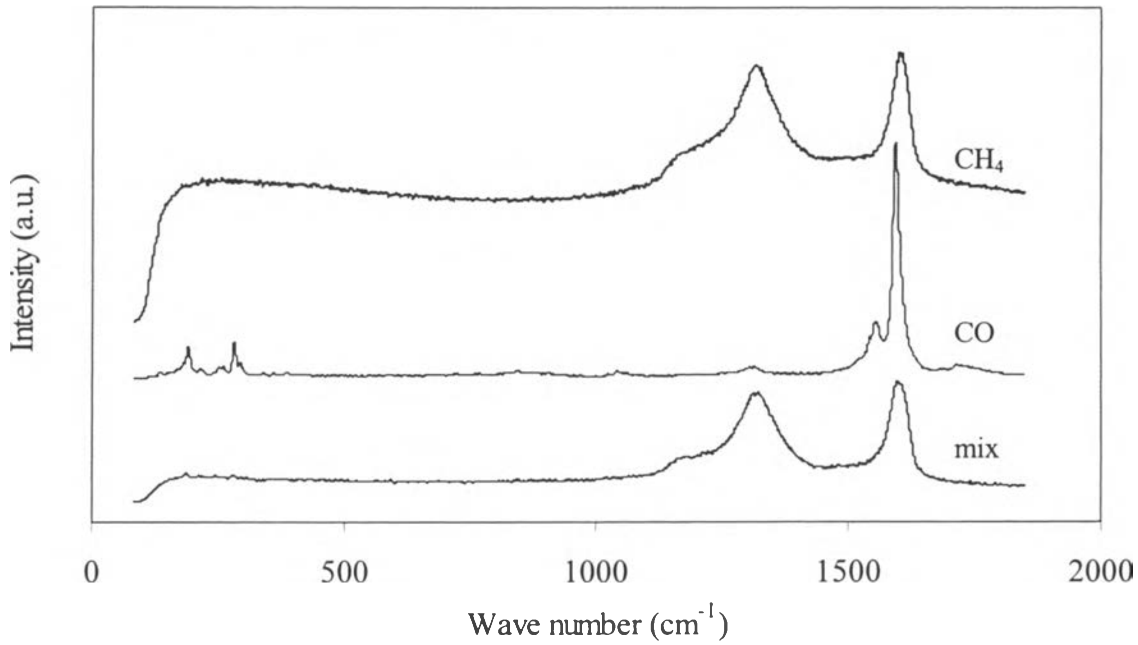

Figure 4.6 Raman spectra of carbon produced by CoMo 1:2 over silica support with CH_4, CO, and mixture at 750 °C.

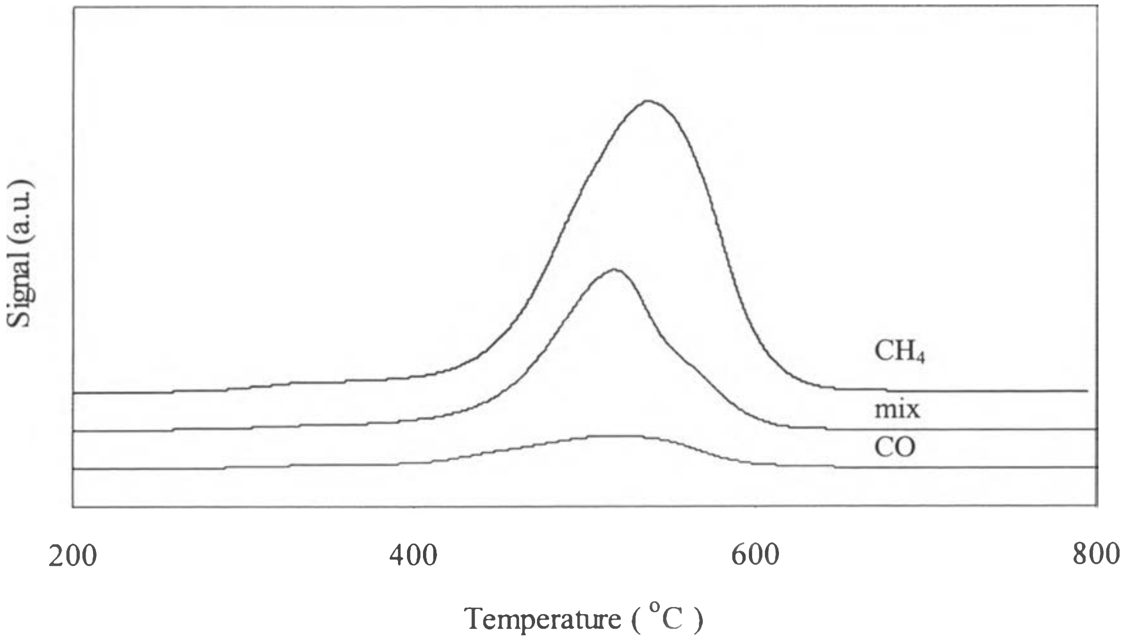

Figure 4.7 TPO profiles of carbon produced by CoMo 1:2 over silica support with CH_4, CO, and mixture at 750 °C.

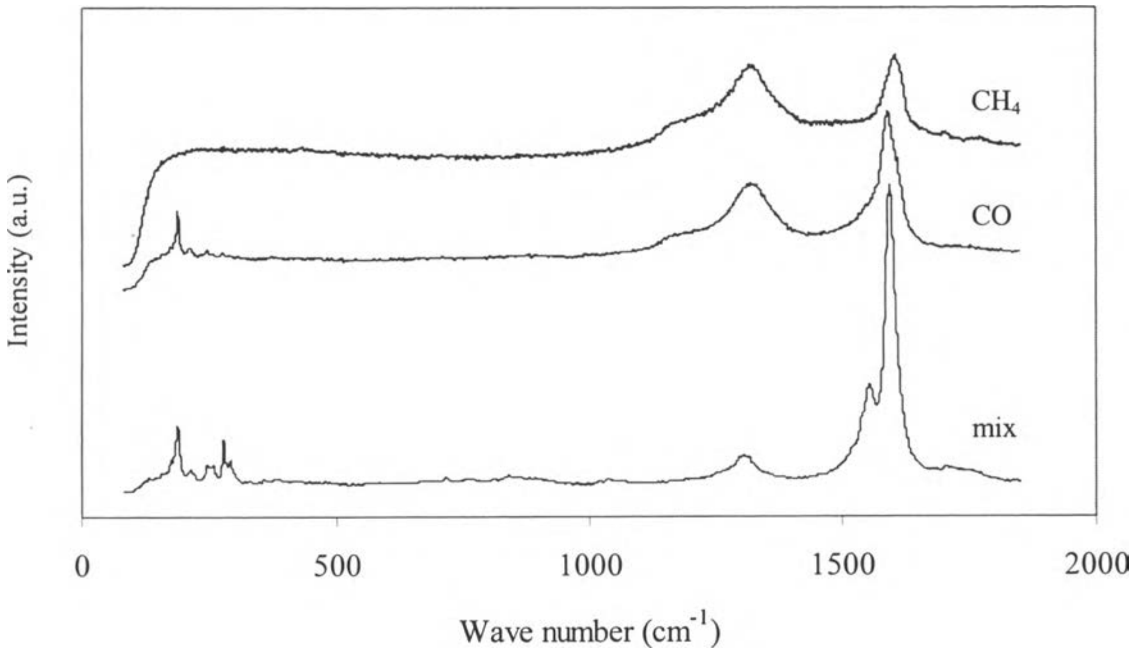

Figure 4.8 Raman spectra of carbon produced by CoMo 2:1 over silica support with CH_4, CO, and mixture at 750 °C.

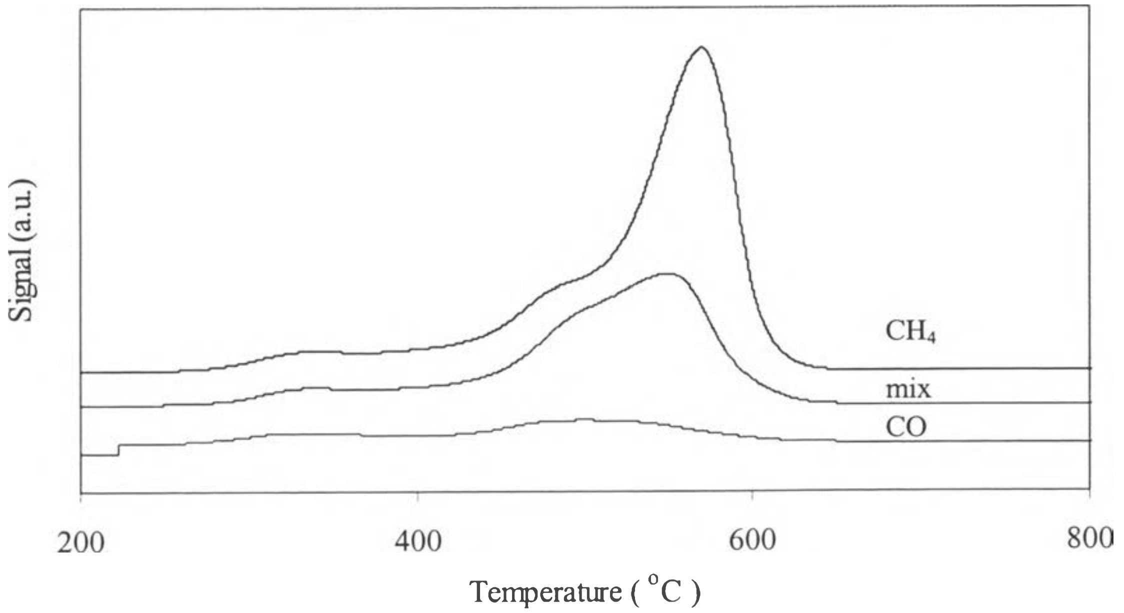

Figure 4.9 TPO profiles of carbon produced by CoMo 2:1 over silica support with CH_4, CO, and mixture at 750 °C.

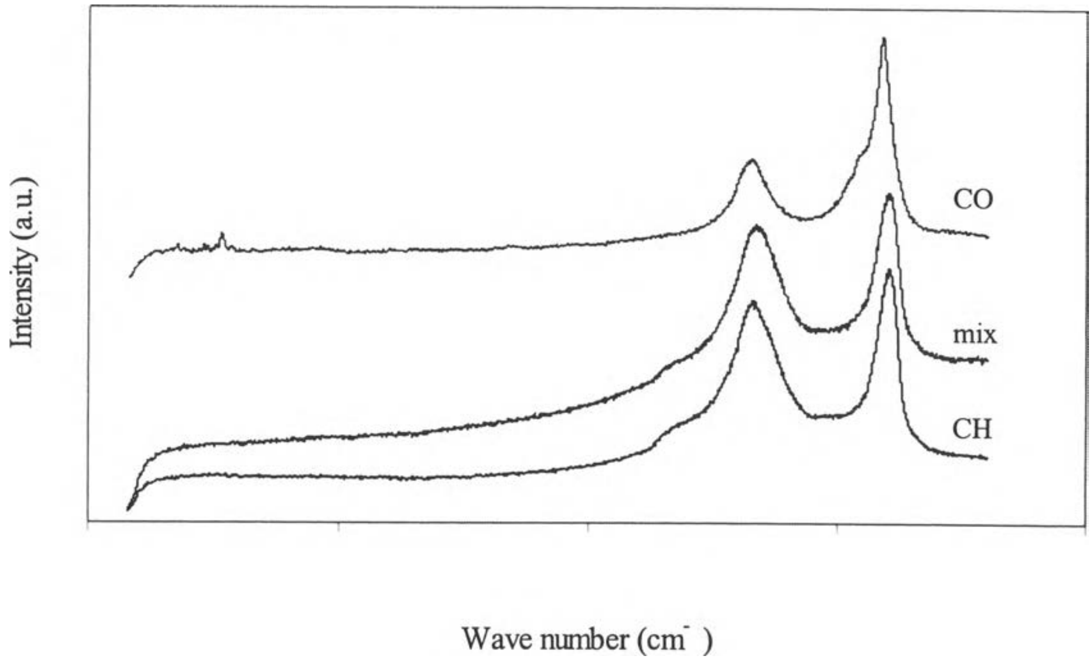

Figure 4.10 Raman spectra of carbons produced by FeMo 1:2 over silica support with CH_4, CO, and mixture at 750 °C.

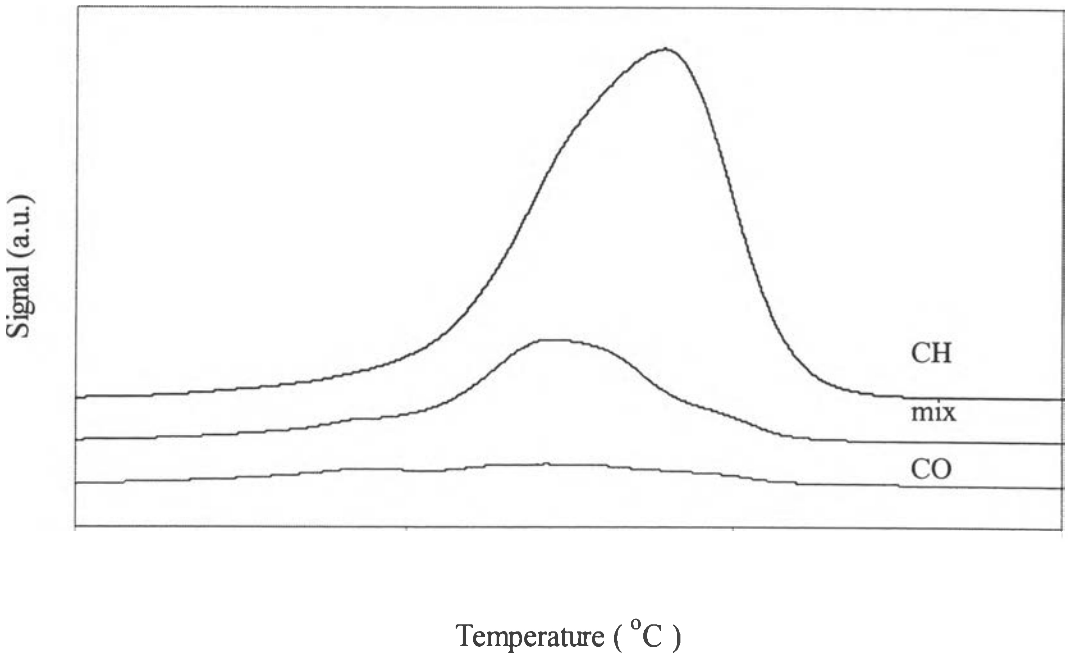

Figure 4.11 TPO profiles of carbons produced by FeMo 1:2 over silica support with CH_4, CO, and mixture at 750 °C.

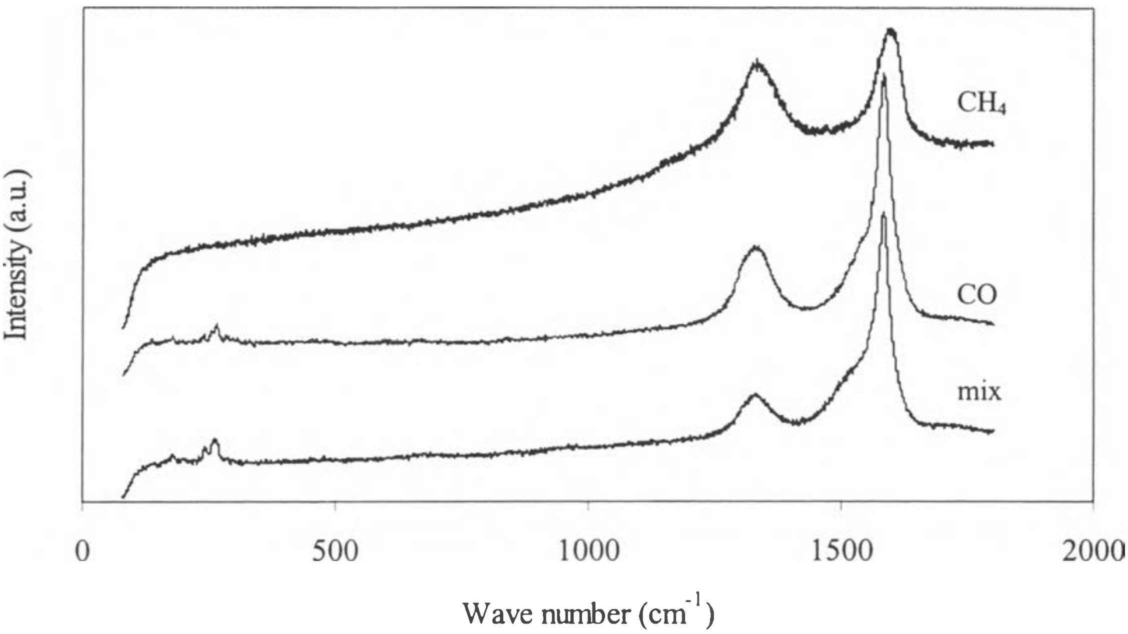

Figure 4.12 Raman spectra of carbon produced by FeMo 2:1 over silica support with CH_4, CO, and mixture at 750 °C.

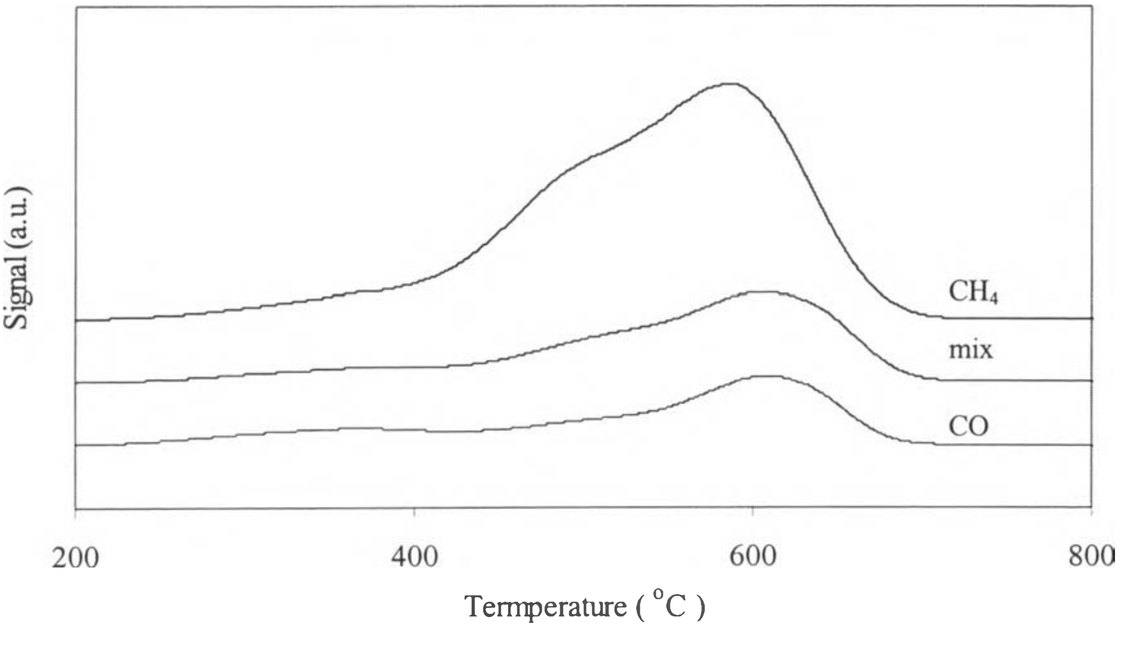

Figure 4.13 TPO profiles of carbon produced by FeMo 2:1 over silica support with CH_4, CO, and mixture at 750 °C.

4.1.2 Effects of Catalyst Formulations on Carbon Nanotube Formation

In this study, Ni, Co, and Fe were used as metal species. They were interacted with Mo to form bi-metallic catalyst—NiMo, CoMo and FeMo. In order to study the effect of catalyst formulations, the effect of metal molar ratio and effect of metal species were investigated. First, the mole ratios at 1:1,1:2, and 2:1 were changed in same feed gas and catalyst as shown some of Raman spectroscopy and TPO results in Figures 4.14–4.25. Second, the metal species of bi-metallic catalysts were changed in same mole ratio and feed gas as showed some examples in Figures 4.26 to 4.29.

For instance, Figures 4.14 and 4.15 show the Raman spectra and TPO profiles of carbon produced by CO disproportionation on NiMo. The result shows that when used the catalyst at 1:1 and 1:2 mole ratios, the RBM signals were observed. Interestingly, the carbon produced by CoMo catalyst with CO disproportionation and mixed gases presented the RBM peaks; moreover, the Raman spectra gave high intensity of RBM signals and low D-band intensity, which indicated that the deposited carbon gave high quality of SWNT as seen in Figure 4.18 and 4.20. For the FeMo series, all of the carbon obtained by CO disproportionation gave the RBM signals as shown in Figures 4.22 and 4.23. Moreover, FeMo 2:1 by mixture of CO and CH_4 can also present this peak as can be seen in Figures 4.24–4.25.

According to Figures 4.26 and 4.27, the Raman spectra and TPO profiles illustrate the difference metal species of bi-metallic catalysts—NiMo, CoMo, and FeMo at 2:1 mole ratio by CO disproportionation. The results showed that all of these catalyst species gave SWNT. Besides, by mixture of CO and CH_4, the carbon produced by CoMo and FeMo catalysts also presented SWNT, yet NiMo cannot give SWNT as shown in Figure 4.28.

Table 4.2 exhibits the Raman spectroscopy resulting on siliga gel support. Unfortunately, when using methane as a feed gas, the RBM signal was not detected. However, most of the carbon produced by CO disproportionation and mixture showed the RBM signals.

Table 4.2 Summary the Raman spectroscopy results on silica gel support

Catalyst/ SiO_2	CH_4			CO			CH_4+CO		
	1:1	1:2	2:1	1:1	1:2	2:1	1:1	1:2	2:1
NiMo	–	–	–	+	–	+	–	–	–
CoMo	–	–	–	+	+	+	+	–	+
FeMo	–	–	–	–	+	+	+	–	+

+ positive RBM signal

– no RBM signal

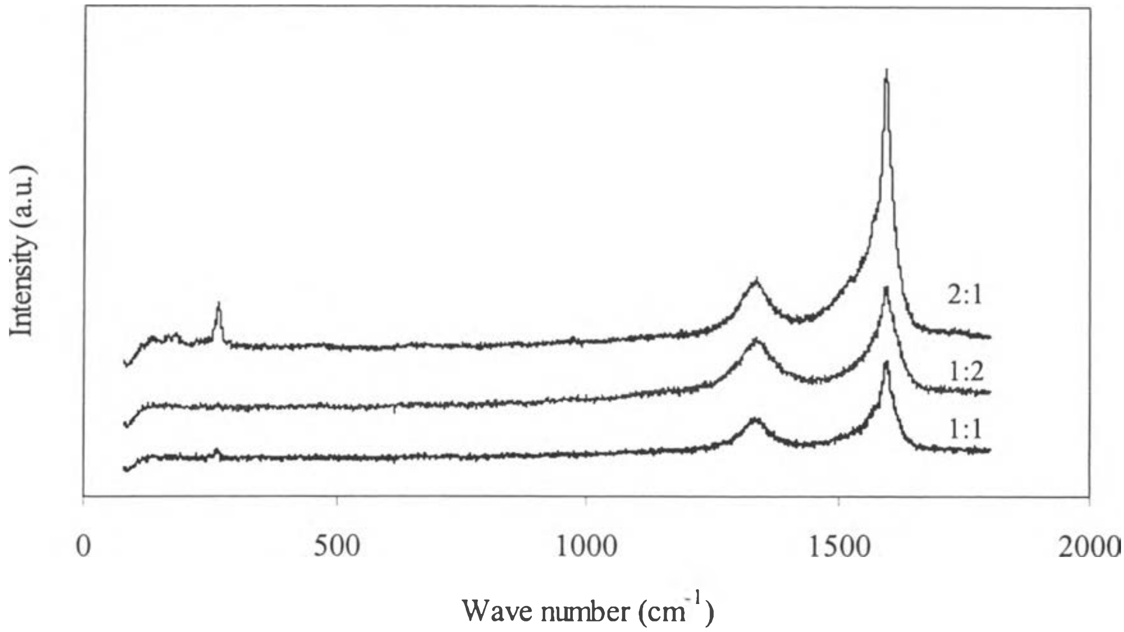

Figure 4.14 Raman spectra of carbon produced by NiMo at 1:1, 1:2, and 2:1 mole ratios over silica support with CO at 750 °C.

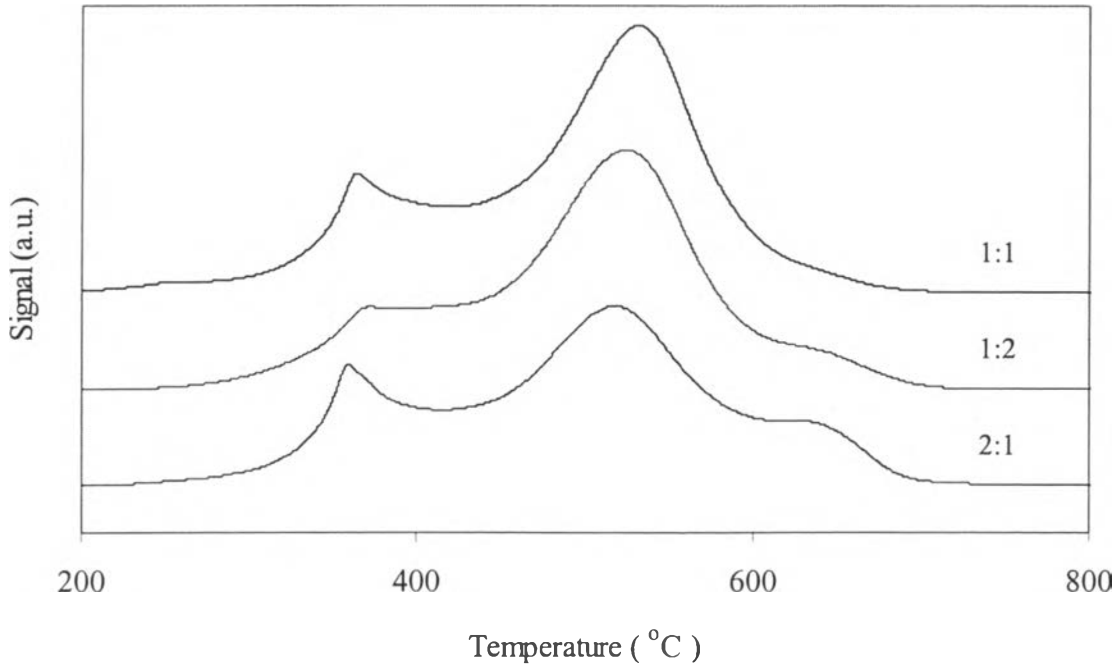

Figure 4.15 TPO profiles of carbon produced by NiMo at 1:1, 1:2, and 2:1 mole ratios over silica support with CO at 750 °C.

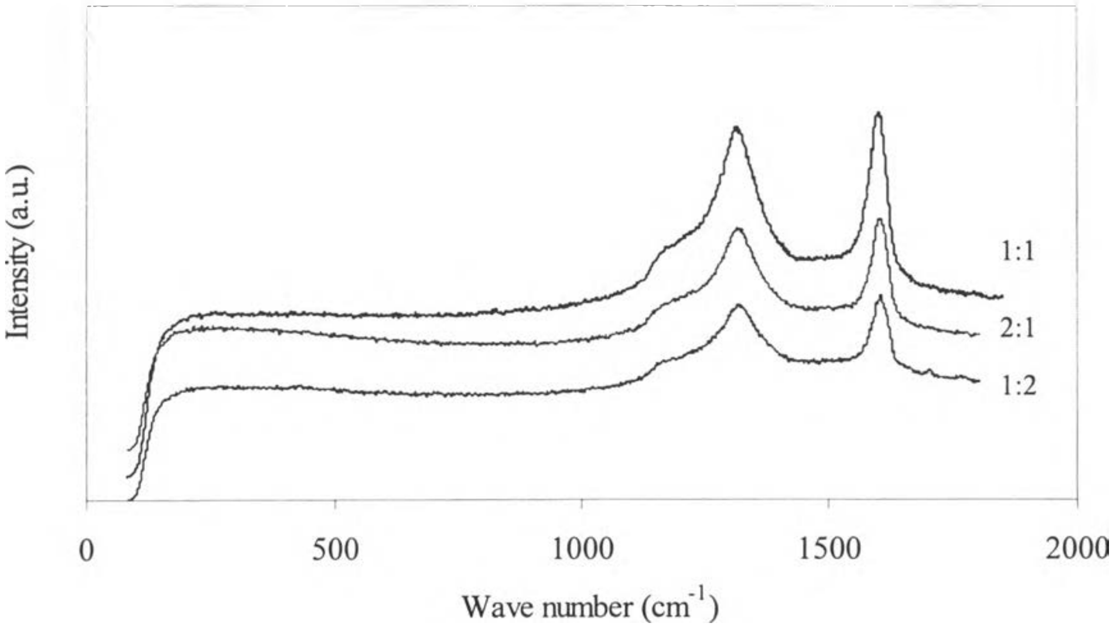

Figure 4.16 Raman spectra of carbon produced by CoMo at 1:1, 1:2, and 2:1 mole ratios over silica support with CH_4 at 750 °C.

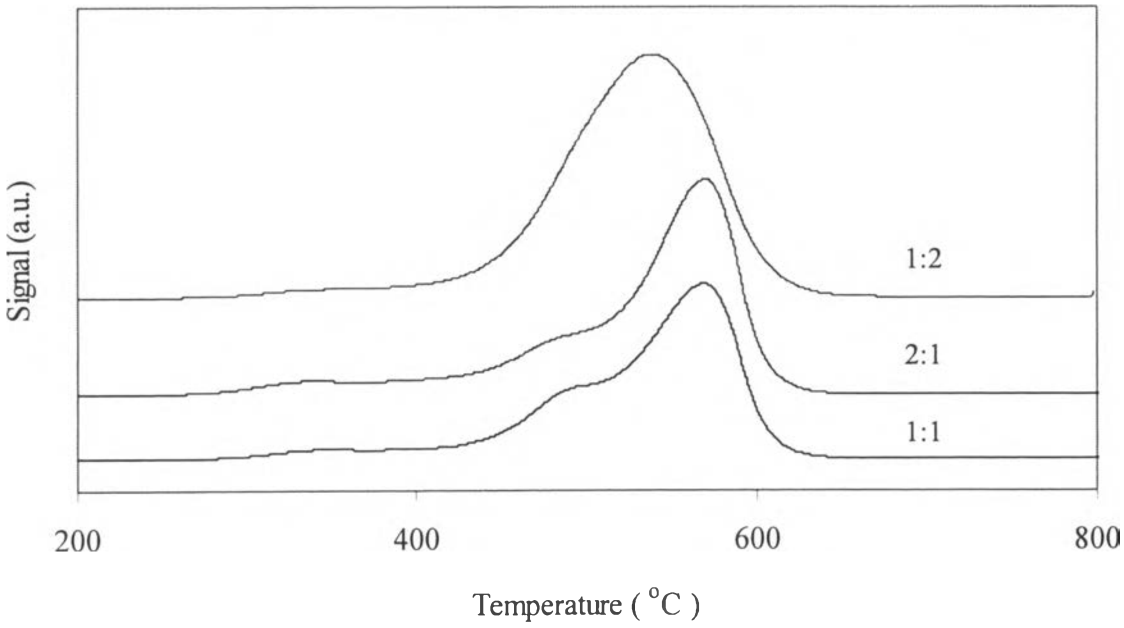

Figure 4.17 TPO profiles of carbon produced by CoMo at 1:1, 1:2, and 2:1 mole ratios over silica support with CH_4 at 750 °C.

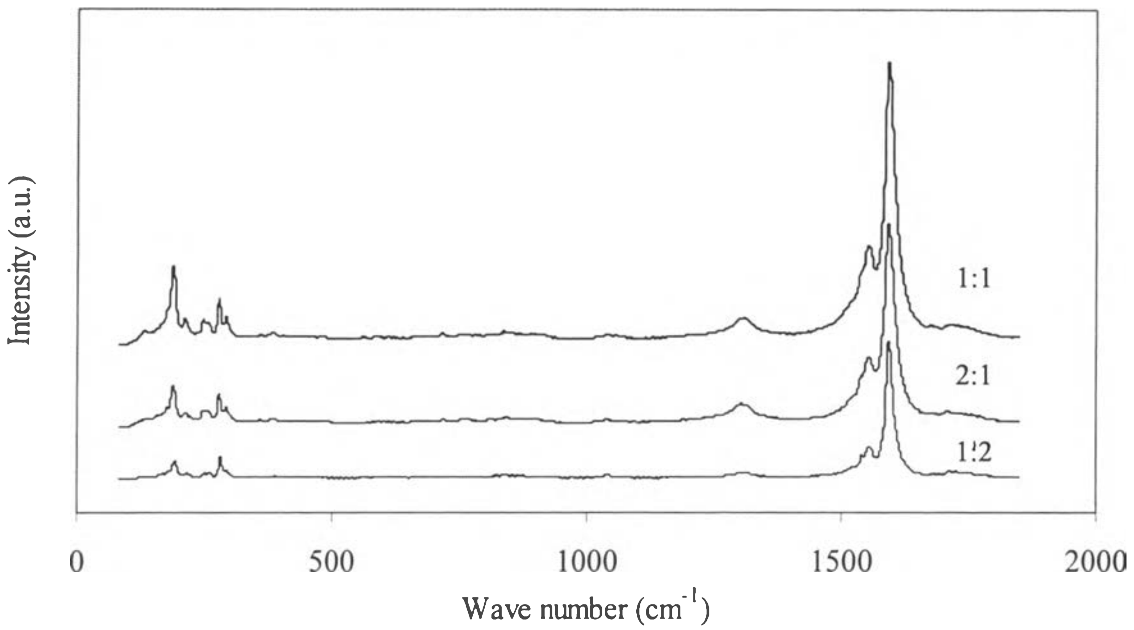

Figure 4.18 Raman spectra of carbon produced by CoMo catalyst at 1:1, 1:2, and 2:1 mole ratios over silica support with CO at 750 °C.

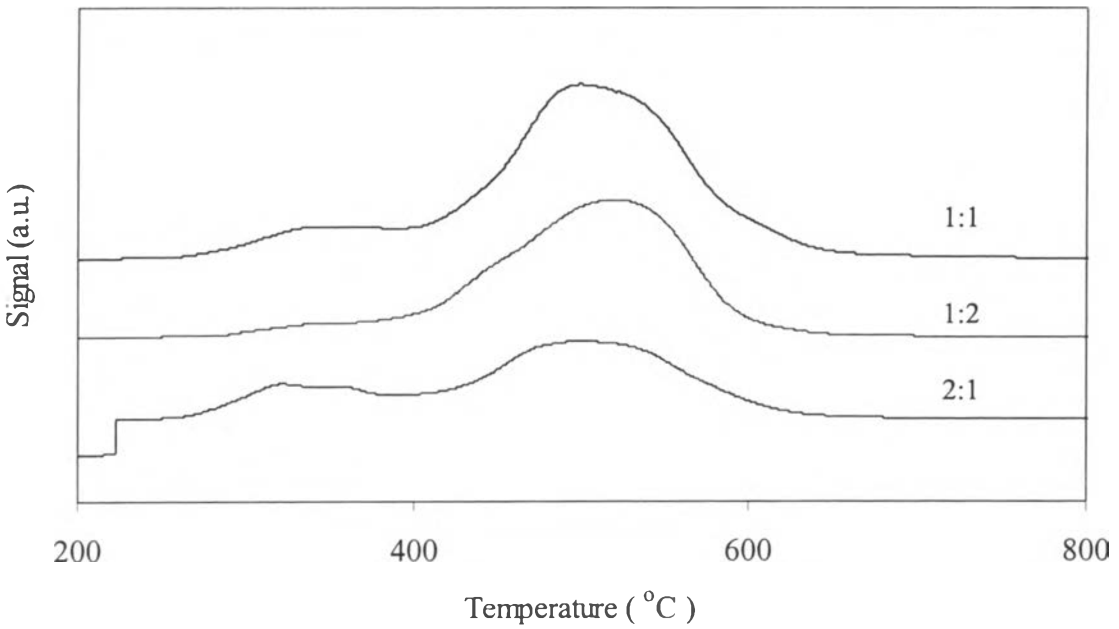

Figure 4.19 TPO profiles of carbon produced by CoMo catalyst at 1:1, 1:2, and 2:1 mole ratios over silica support with CO at 750 °C.

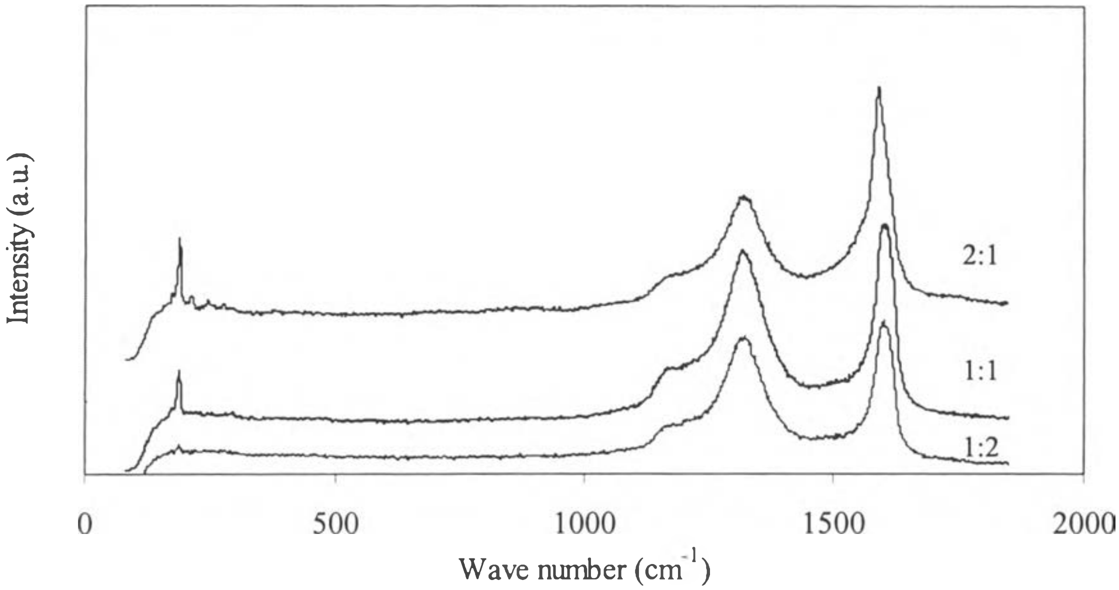

Figure 4.20 Raman spectra of carbon produced by CoMo at 1:1, 1:2, and 2:1 mole ratios over silica support with mixture of CH_4 and CO at 750 °C.

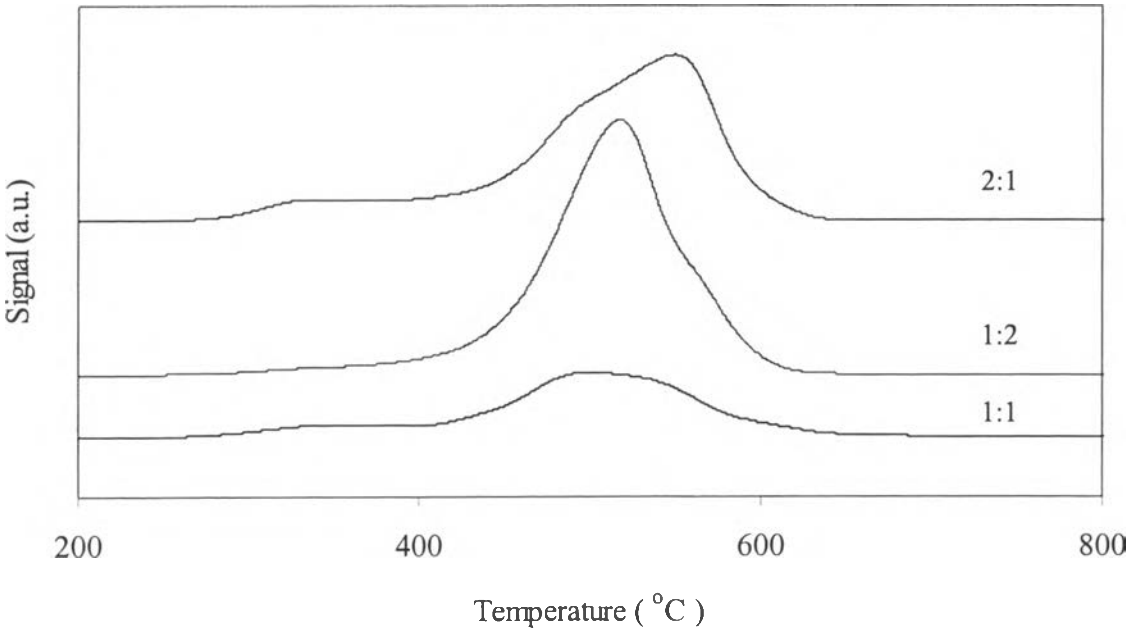

Figure 4.21 TPO profiles of carbon produced by CoMo at 1:1, 1:2, and 2:1 mole ratios over silica support with mixture of CH_4 and CO at 750 °C.

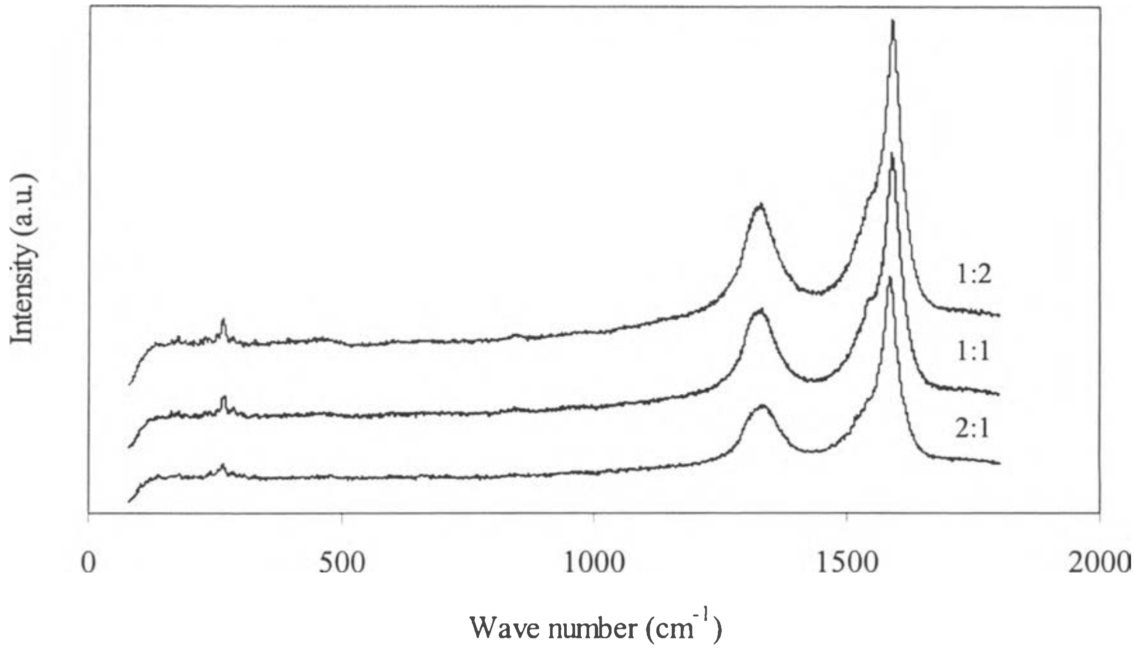

Figure 4.22 Raman spectra of carbon produced by FeMo at 1:1, 1:2, and 2:1 mole ratios over silica support with CO at 750 °C.

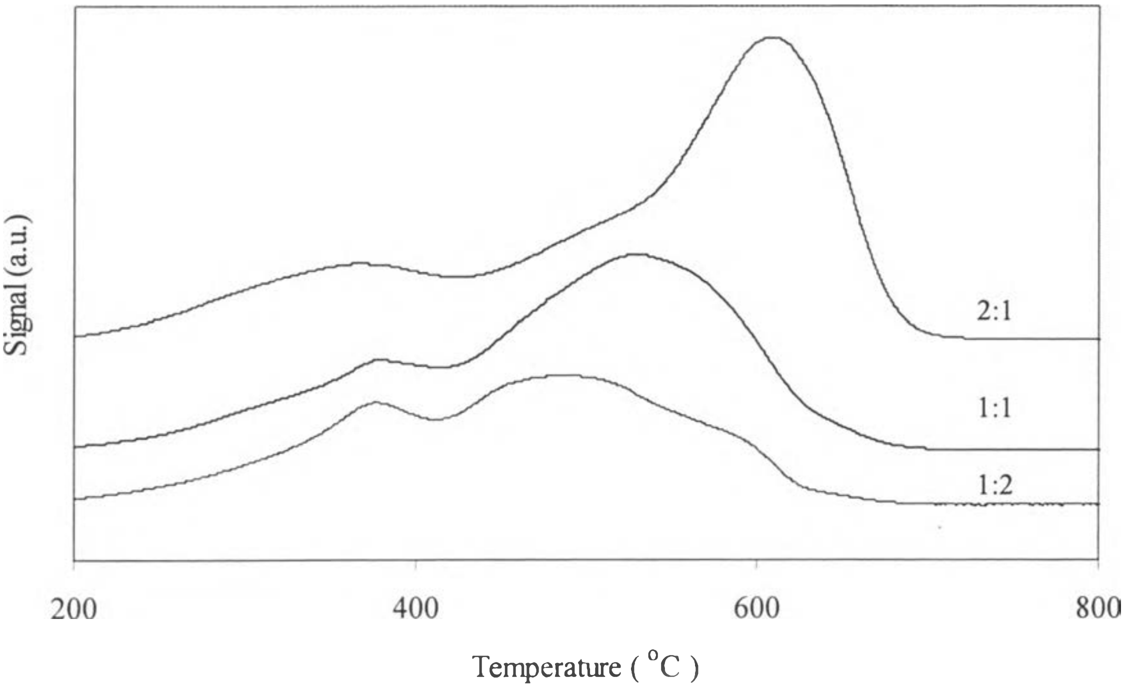

Figure 4.23 TPO profiles of carbon produced by FeMo at 1:1, 1:2, and 2:1 mole ratios over silica support with CO at 750 °C.

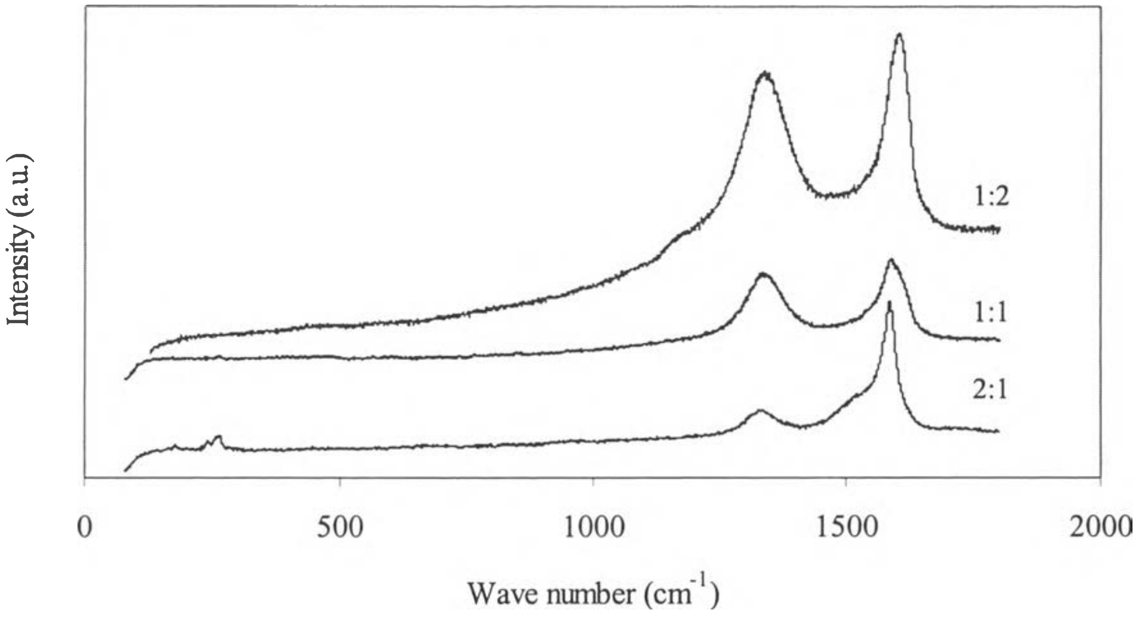

Figure 4.24 Raman spectra of carbon produced by FeMo at 1:1, 1:2, and 2:1 mole ratios over silica support with mixture of CH_4 and CO at 750 °C.

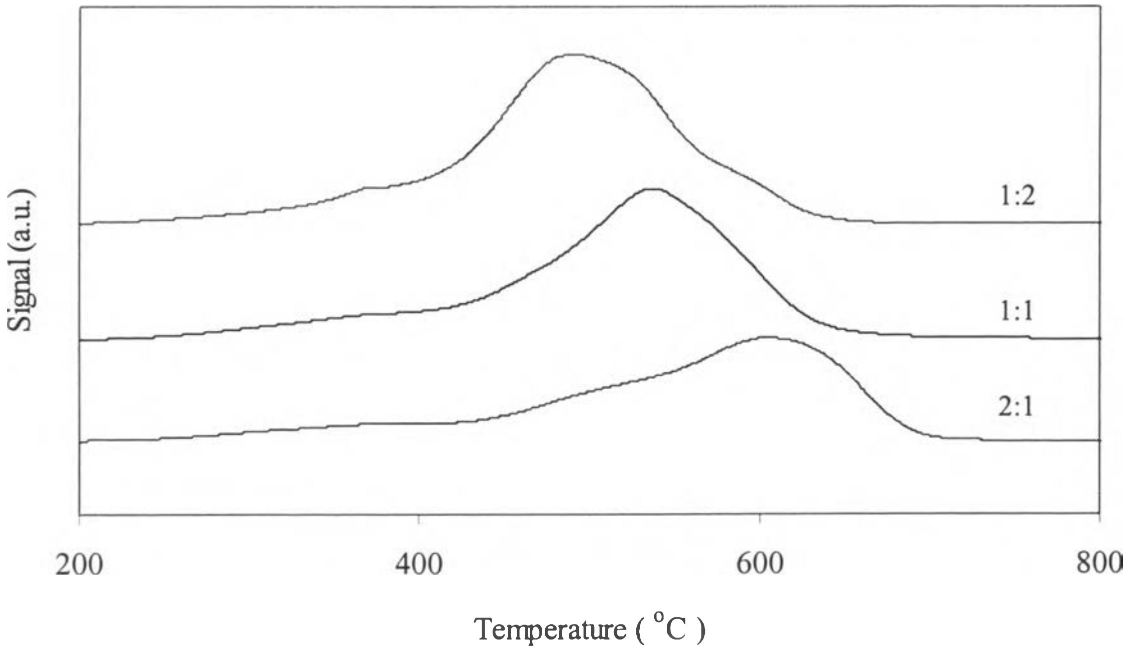

Figure 4.25 TPO profiles of carbon produced by FeMo at 1:1, 1:2, and 2:1 mole ratios over silica support with mixture of CH_4 and CO at 750 °C.

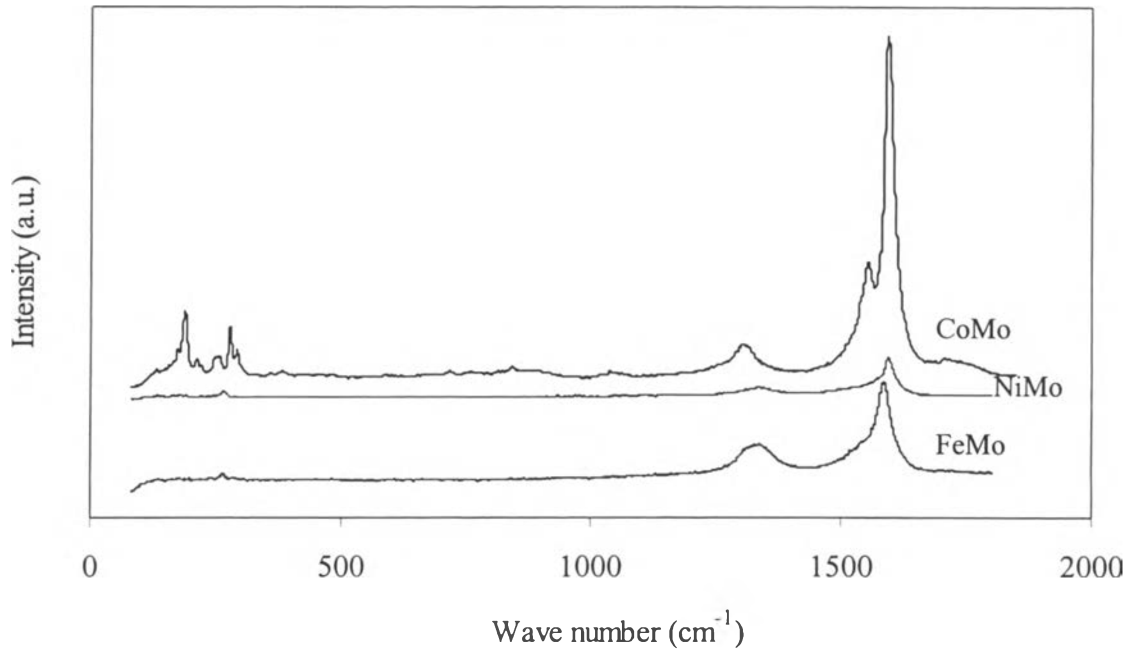

Figure 4.26 Raman spectra of carbon produced by FeMo, CoMo, and NiMo catalysts at 2:1 mole ratio over silica support with CO at 750 °C.

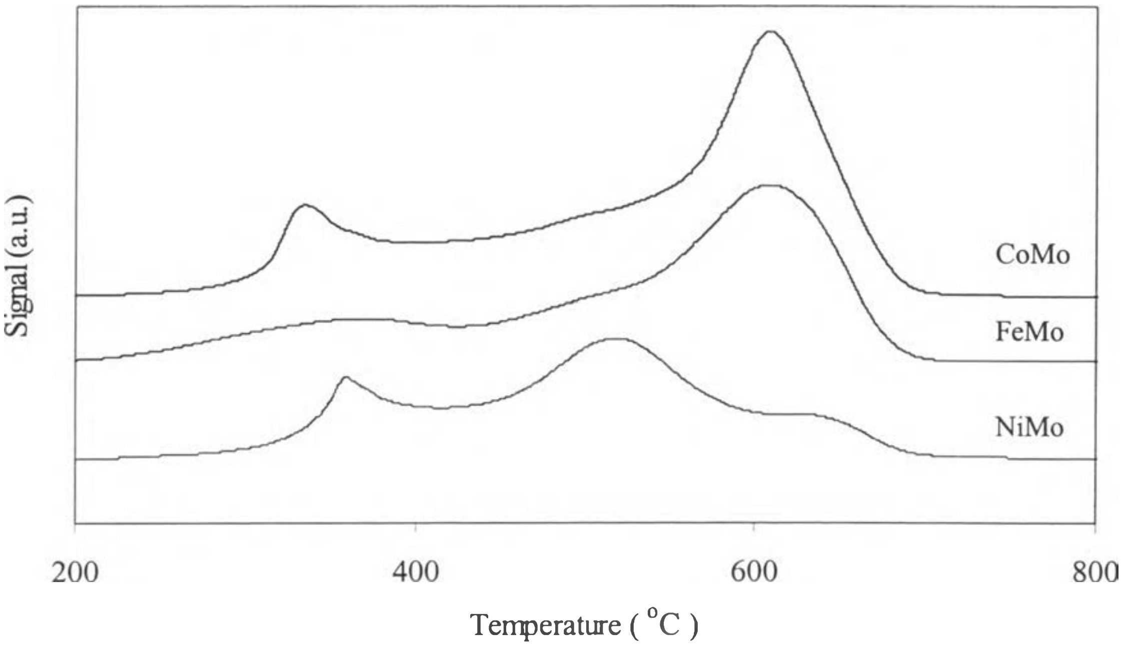

Figure 27 TPO profiles of carbon produced by FeMo, CoMo, and NiMo catalysts at 2:1 mole ratio over silica support with CO at 750 °C.

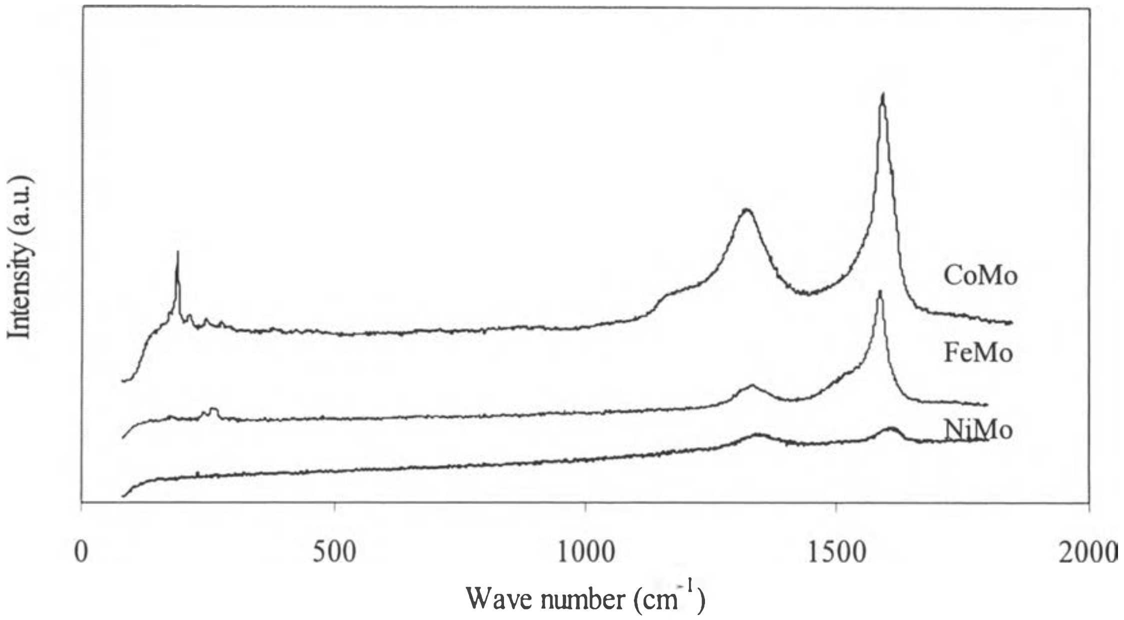

Figure 4.28 Raman spectra of carbon produced by FeMo, CoMo, and NiMo catalysts at 2:1 mole ratio over silica support with mixture of CH_4 and CO at 750 °C.

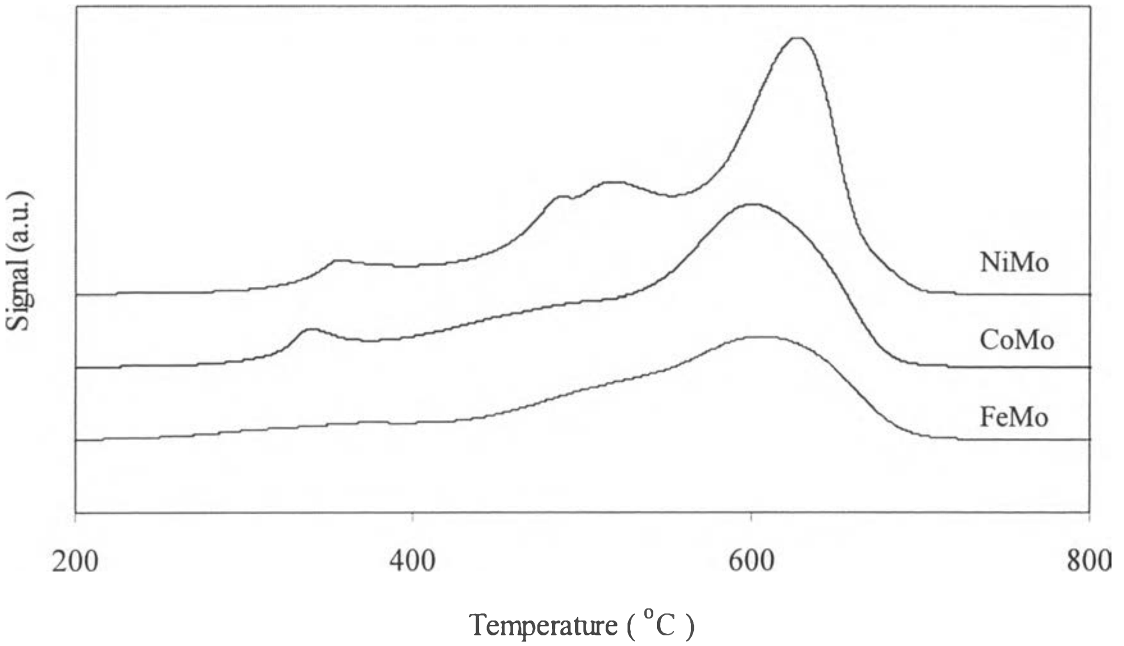

Figure 29 TPO profiles of carbon produced by FeMo, CoMo, and NiMo catalysts at 2:1 mole ratio over silica support with mixture of CH_4 and CO at 750 °C.

Quality Parameter (QP) has been previously used as a quality indicator for carbon products. The QP is defined as 1-D/G, when D is the height of intensity of D-band and G is the height of intensity of G-band. If QP is close to 1, it can be implied that very low D-band relative to G-band, so low amount of disorder carbon and highly graphite-like structure. While QP is less than 1, so it presents high amount of disordered carbon as can be seen from Figure 4.30.

According to Figure 4.30, the comparative bar chart illustrates the quality parameter among using CH_4, CO, and their mixtures as a feed gas over different catalyst formulations on silica gel support. Carbon that gives the RBM signals also provides high quality of SWNT. Interestingly, the quality parameter of carbon produced by CO disproportionation showed this value close to one, so it means that this deposited carbon provided high quality of SWNT. Moreover, the carbon produced by CoMo 1:2 gave the best quality of SWNT as well as this result was in perfect agreement with previous report (Kitiyanan *et al.*, 2000). The results were reported that CoMo catalysts supported on silica gel and having low Co:Mo ratios exhibited the best performance of SWNT. On the other hand, carbon that cannot be observed RBM signal, gave low quality of carbon product. In the same way, it can be concluded that carbon produced by CO disproportionation gave high quality of deposited carbon, while carbon that generated by methane decomposition, most of them did not present SWNT and they provided low quality of deposited carbon as well. On the contrary, as can be seen in Figure 4.31, the comparative bar chart, which compared the total amount of carbon product yields, It showed the results that carbon produced by CO disproportionation gave the lowest percent of total amount of deposited carbon, still methane provided maximum of deposited carbon.

To sum up all results on silica support, From Table 4.3, it can be summarized that a large number of samples produced by CO disproportionation can present SWNT. Consequently, CO is an efficient carbon source for producing high quality of SWNT. In addition, the diameter of SWNT was also showed in this table and calculated by using equation 2.1 from chapter 2. Normally, the diameter of SWNT is around 0.7–2.0 nm. For these results, the distribution of diameter on silica gel support was in the range of 0.8–1.0 nm.

In order to know the quality and quantity of carbon product, besides Raman spectroscopy and TPO techniques, the TEM was used to confirm the results. Figure 4.31 shows the TEM image of NiMo 2:1/SiO_2 catalyst by CO disproportionation.

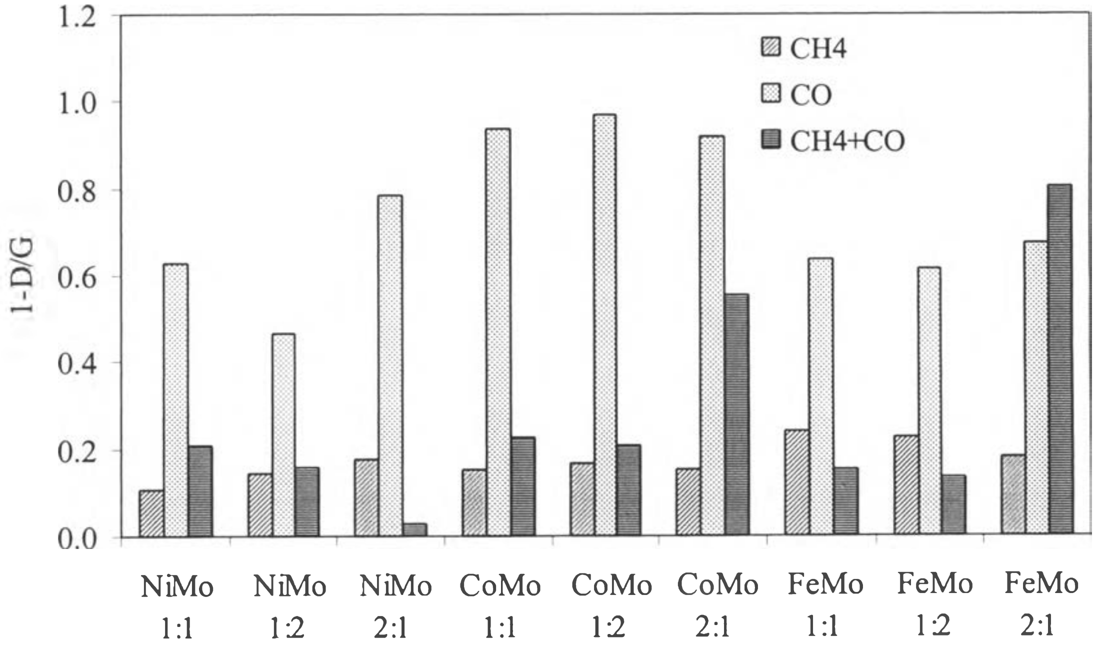

Figure 4.30 the quality parameter of carbon produced by different catalyst formulations over silica support with CH_4, CO, and mixture at 750 °C.

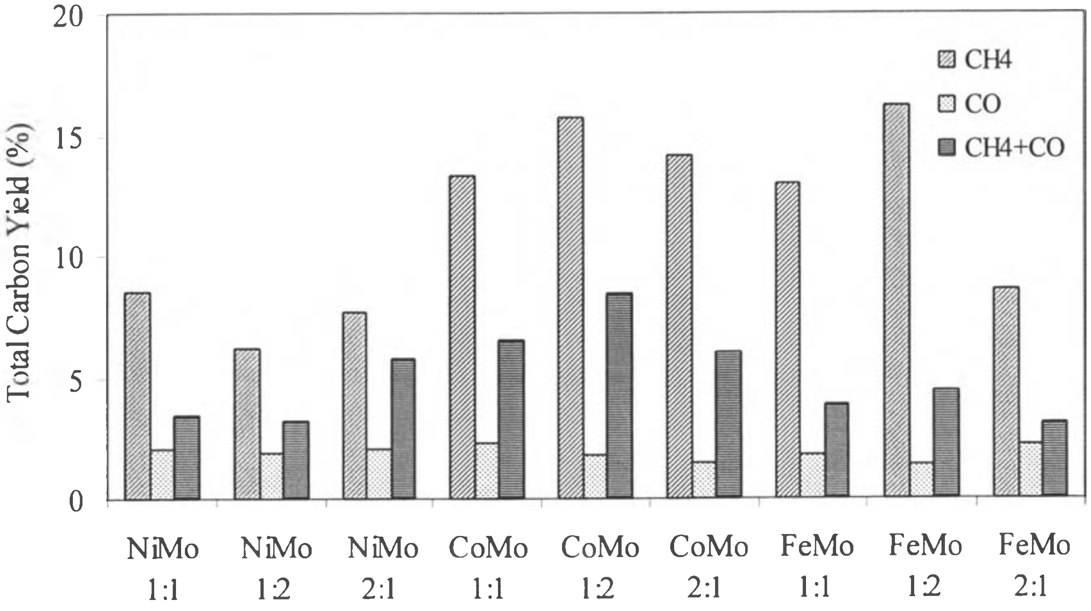

Figure 4.31 the total yields of carbon produced by different catalyst formulations over silica support with CH_4, CO, and mixture at 750 °C.

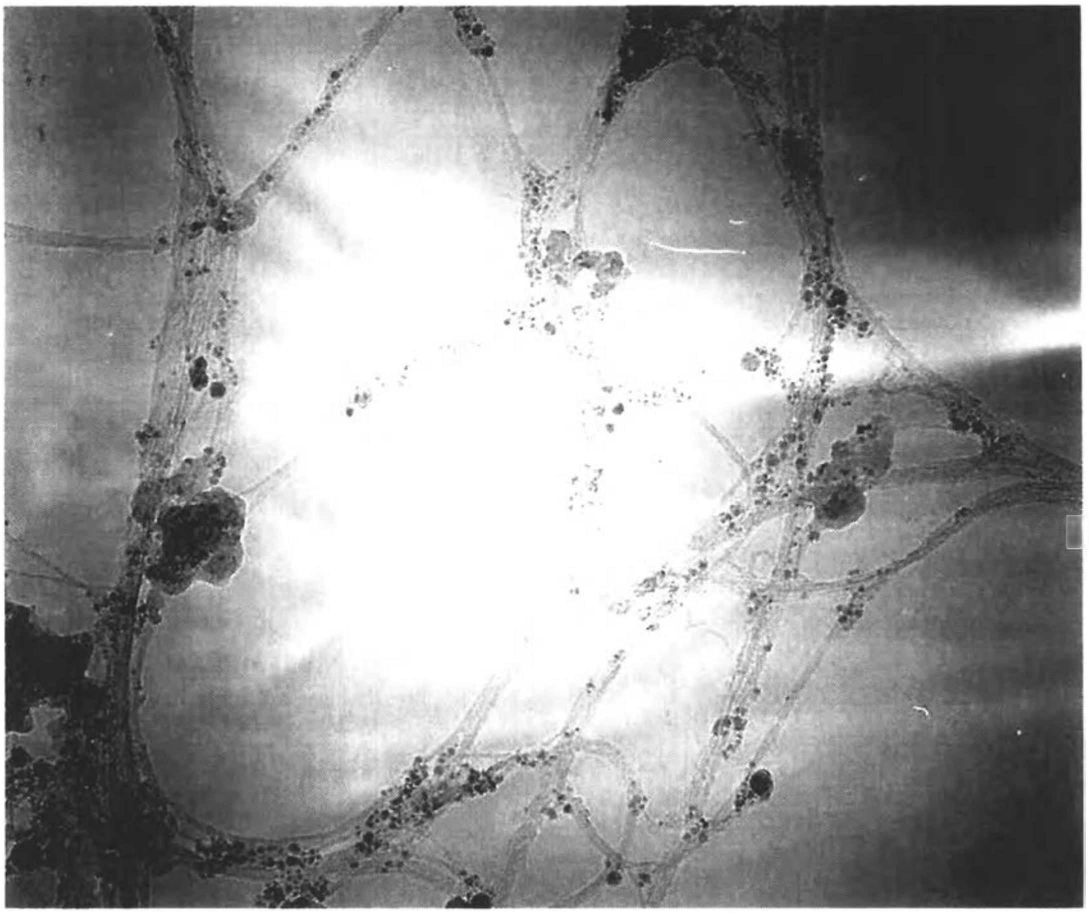

Figure 4.32 TEM image showing a mixture of SWNT and amorphous carbon produced by CO disproportionation on NiMo 2:1/SiO_2 catalyst.

Table 4.3 Summary of SWNT formation on silica gel sorted by quality parameter

Samples	QP (1-D/G)	Carbon Yield (%)	diameter (nm)
CoMo 1:2/SiO_2 (CO, 750 °C)	0.97	1.83	0.83–1.24
CoMo 1:1/SiO_2 (CO, 750 °C)	0.94	2.29	1.16–1.28
CoMo 2:1/SiO_2 (CO, 750 °C)	0.92	1.50	0.84–1.27
FeMo 2:1/SiO_2 (CO+CH_4, 750 °C)	0.80	3.14	0.90–0.93
NiMo 2:1/SiO_2 (CO, 750 °C)	0.79	2.04	0.89
FeMo 2:1/SiO_2 (CO, 750 °C)	0.68	2.26	0.89
FeMo 1:1/SiO_2 (CO, 750 °C)	0.64	1.78	0.82–0.88
NiMo 1:1/SiO_2 (CO, 750 °C)	0.63	2.05	0.89
FeMo 1:2/SiO_2 (CO, 750 °C)	0.61	1.39	0.89
CoMo 2:1/SiO_2 (CH_4+CO, 750 °C)	0.55	6.06	1.28
CoMo 1:1/SiO_2 (CH_4+CO, 750 °C)	0.23	6.52	1.28
FeMo 1:1/SiO_2 (CO+ CH_4, 750 °C)	0.15	3.91	0.84

4.2 The Carbon Nanotubes Formation on Magnesium Oxide Support

The effect of carbon–containing gases and catalyst formulations were studied for several samples on MgO support. The analysis shows that only a few samples can give the RBM signals as shown in Table 4.4. Although using MgO as a support did not present more SWNT, it gave high percent of total carbon yield.

Table 4.4 Summary of carbon nanotubes production by using different gases and catalyst formulations on magnesium oxide support.

Samples	D/G Ratio	Carbon Yield (%)	RBM
NiMo 1:1/MgO (CH_4, 750 °C)	1.55	23.28	no
NiMo 1:1/MgO (CO, 750 °C)	1.24	6.80	no
NiMo 1:1/MgO (CH_4 +CO, 750 °C)	1.57	21.47	no
NiMo 1:2/MgO (CH_4, 750 °C)	1.60	14.47	no
NiMo 1:2/MgO (CO, 750 °C)	1.51	9.02	no
NiMo 1:2/MgO (CH_4 + CO, 750 °C)	1.87	16.34	no
NiMo 2:1/MgO (CH_4, 750 °C)	1.48	14.17	no
NiMo 2:1/MgO (CO, 750 °C)	0.97	14.17	no
NiMo 2:1/MgO (CH_4+CO, 750 °C)	1.66	28.68	no
CoMo 1:1/MgO (CH_4, 750 °C)	1.28	12.60	no
CoMo 1:1/MgO (CO, 750 °C)	1.41	14.65	no
CoMo 1:1/MgO (CH_4 +CO, 750 °C)	1.52	12.37	no
CoMo 1:2/MgO (CH_4, 750 °C)	1.45	8.42	no
CoMo 1:2/MgO (CO, 750 °C)	1.46	13.83	no
CoMo 1:2/MgO (CH_4 + CO, 750 °C)	1.44	11.82	no
CoMo 2:1/MgO (CH_4, 750 °C)	0.70	13.75	yes
CoMo 2:1/MgO (CO, 750 °C)	1.44	11.35	no
CoMo 2:1/MgO (CH_4+CO, 750 °C)	1.34	27.18	no

Table 4.4 (continued)

Samples	D/G Ratio	Carbon Yield (%)	RBM
FeMo 1:1/MgO (CH_4, 750 °C)	1.18	20.49	no
FeMo 1:1/MgO (CO, 750 °C)	1.37	7.63	no
FeMo 1:1/MgO (CO+CH_4, 750 °C)	1.56	16.13	no
FeMo 1:2/MgO (CH_4, 750 °C)	1.35	13.84	no
FeMo 1:2/MgO (CO, 750 °C)	1.47	6.66	no
FeMo 1:2/MgO (CO+CH_4, 750 °C)	1.67	21.70	no
FeMo 2:1/MgO (CH_4, 750 °C)	0.87	18.60	yes
FeMo 2:1/MgO (CO, 750 °C)	0.29	5.49	no
FeMo 2:1/MgO (CO+CH_4, 750 °C)	1.47	14.52	no
Ni/MgO (CH_4, 750 °C)	0.08	0.37	yes
Ni/MgO (CO, 750 °C)	0.07	0.27	no
Ni/MgO (CO+CH_4, 750 °C)	0.09	0.26	no
Co/MgO (CH_4, 750 °C)	0.07	0.61	yes
Co/MgO (CO, 750 °C)	0.07	0.77	yes
Co/MgO (CO+CH_4, 750 °C)	0.14	0.91	yes
Fe/MgO (CH_4, 750 °C)	0.12	0.58	yes
Fe/MgO (CO, 750 °C)	0.07	0.58	no
Fe/MgO (CO+CH_4, 750 °C)	0.06	0.68	no
Mo/MgO (CH_4, 750 °C)	0.19	0.58	no
Mo/MgO (CO, 750 °C)	0.18	1.02	no
Mo/MgO (CO+CH_4, 750 °C)	0.09	0.55	no

4.2.1 Effects of CH_4, CO, and Mixture of CH_4 and CO on the Carbon Nanotubes Formation

In order to study the effect of gases on the carbon nanotubes formation, the Raman spectroscopy and TPO were used to analyze the deposited carbon. All of the samples showed that no RBM signal was observed except CoMo and FeMo at 2:1 mole ratio with CH_4 decomposition. Figures 4.33–4.36 illustrate the Raman spectra and TPO profiles of carbon produced by CoMo and FeMo catalysts with various feed gases on MgO support. As shown in Figures 4.33 and 4.35, the Raman spectra illustrate that carbon generated by CH_4 decomposition gives the small peak in the RBM range, and the D-band is as high as G-band intensity, which was due to deposited carbon mainly consists of disordered carbon. Moreover, both deposited carbon produced by CO disproportionation and a mixture of CH_4 and CO do not show the RBM signal, but provide large amount of disordered carbon. Similarly, the TPO profiles also showed a dominant peak centered on the range of MWNT as shown in Figures 4.34 and 4.36. In addition, this support exhibits the interesting results showing the RBM peak on mono-metallic catalysts. Figures 4.37 and 4.38 show the Raman spectra and TPO profiles which carbon was produced by Co alone, the RBM signal can be observed.

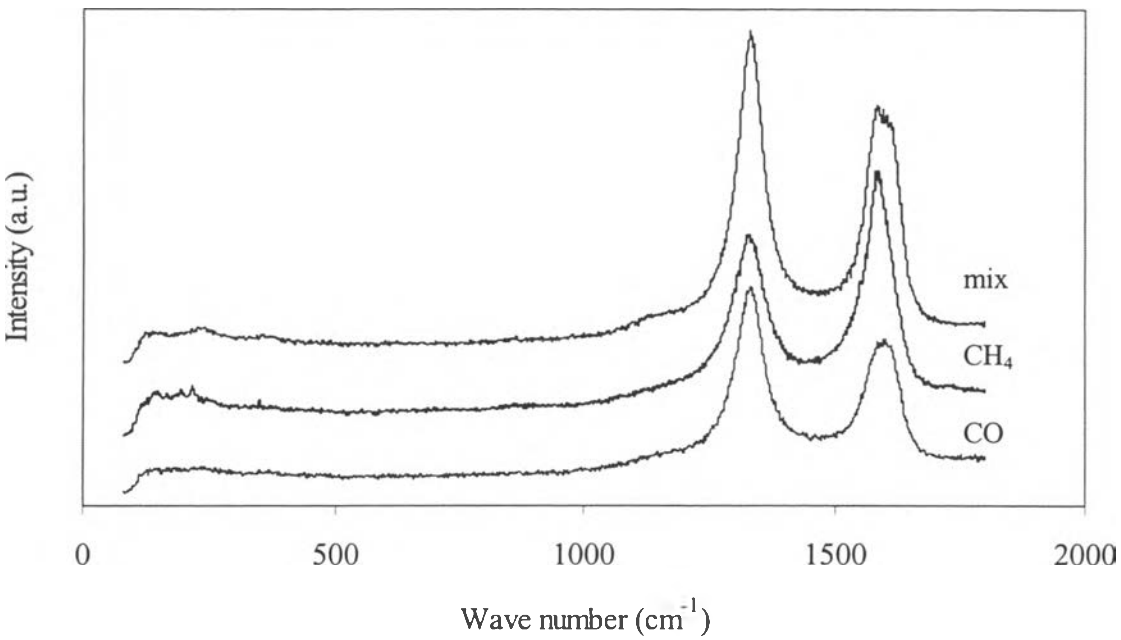

Figure 4.33 Raman spectra of carbon produced by CoMo 2:1 over magnesium oxide support with CH_4, CO, and mixture at 750 °C.

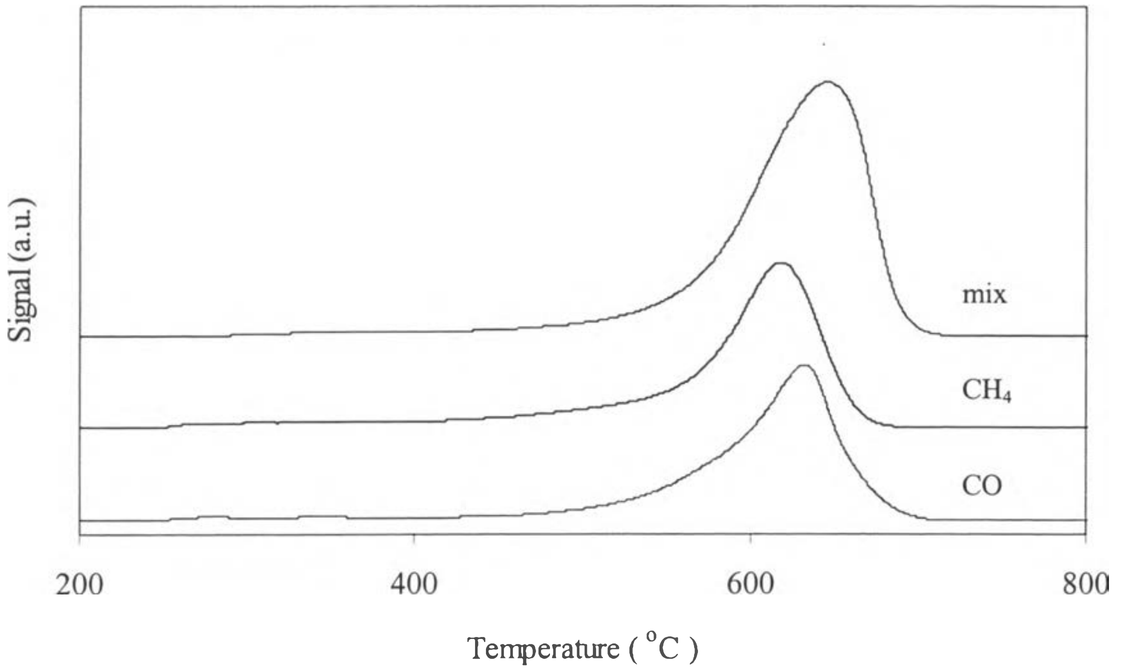

Figure 4.34 TPO profiles of carbon produced by CoMo 2:1 over magnesium oxide support with CH_4, CO, and mixture at 750 °C.

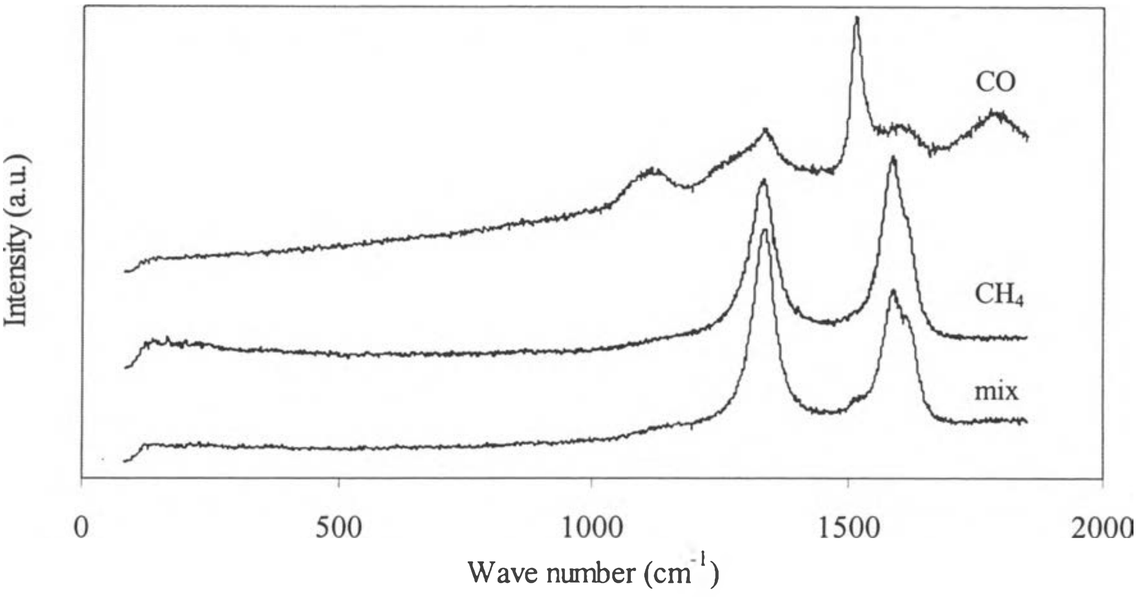

Figure 4.35 Raman spectra of carbon produced by FeMo 2:1 over magnesium oxide support with CH_4, CO, and mixture at 750 °C.

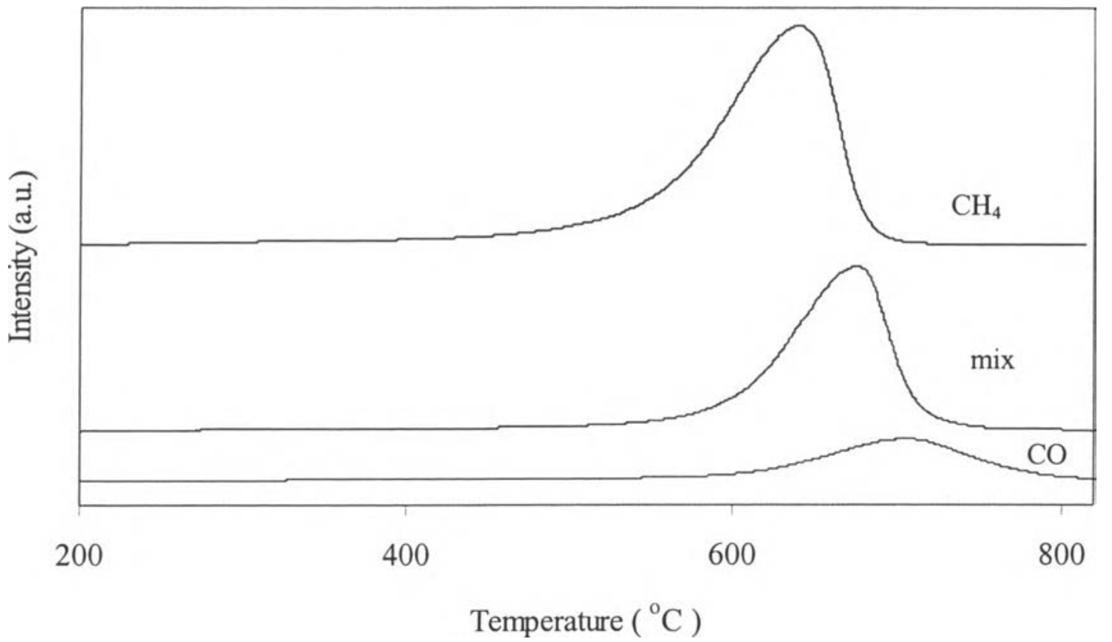

Figure 4.36 TPO profiles of carbon produced by FeMo 2:1 over magnesium oxide support with CH_4, CO, and mixture at 750 °C.

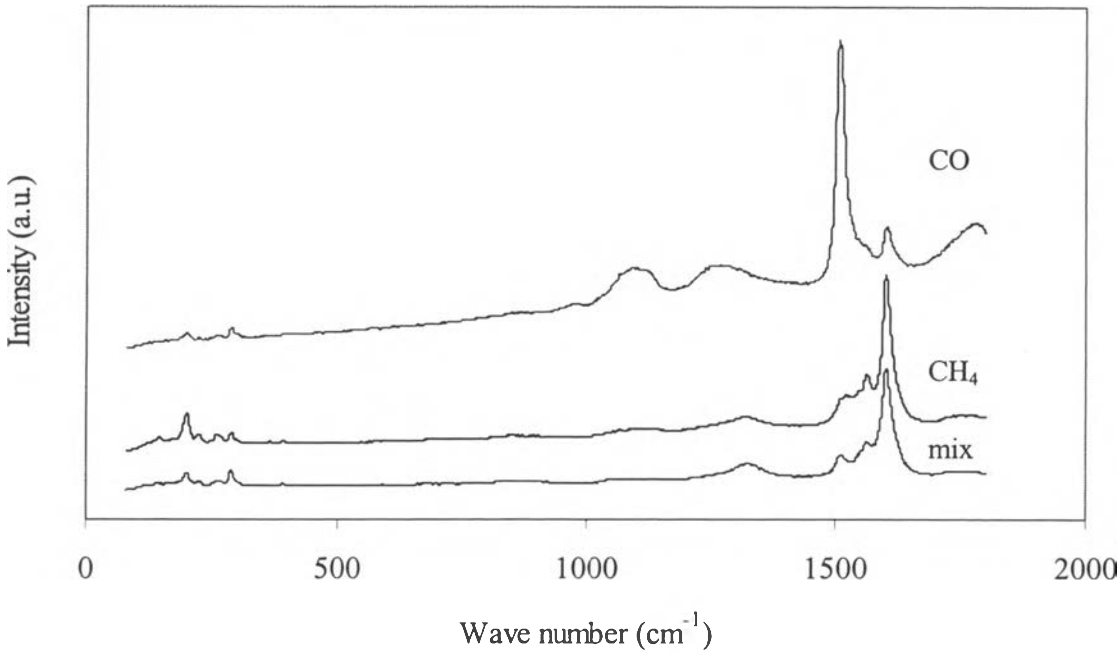

Figure 4.37 Raman spectra of carbon produced by Co catalyst over magnesium oxide support with CH_4, CO, and mixture at 750 °C.

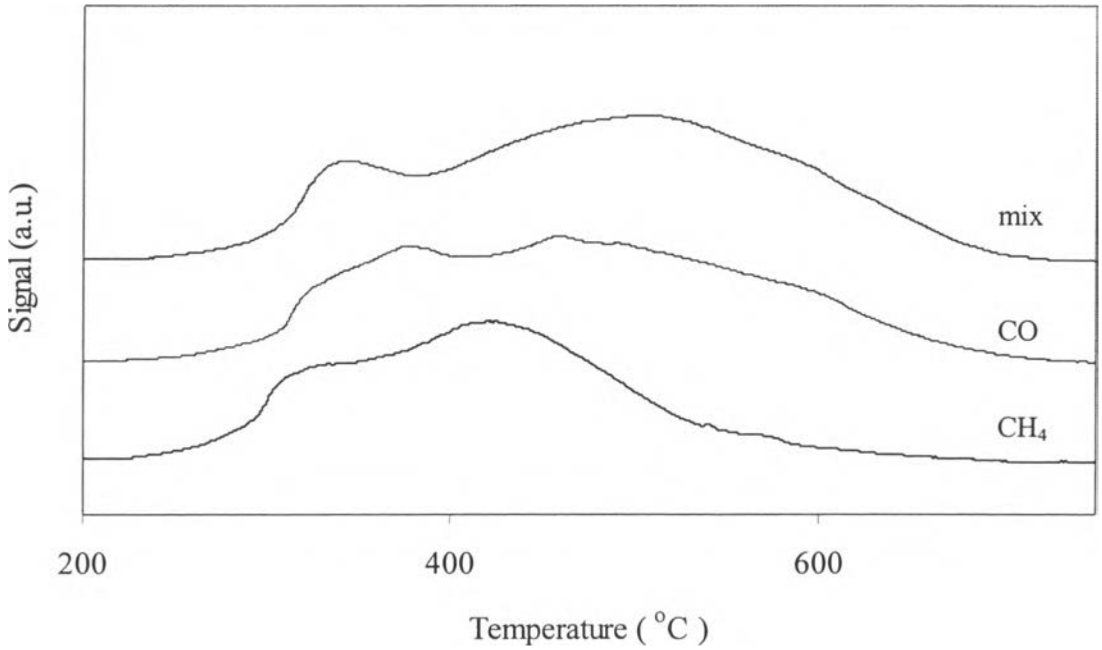

Figure 4.38 TPO profiles at RBM range of carbon produced by Co catalyst over magnesium oxide support with CH_4, CO, and mixture at 750 °C.

4.2.2 Effects of Catalyst Formulations on the Carbon Nanotubes Formation

In these effects, the NiMo, CoMo, and FeMo catalysts were studied with the same feed gas and the mole ratios were changed to 1:1,1:2, and 2:1. The Raman spectra and TPO profiles are illustrated in Figures 4.39–4.42.

The results showed that all of the carbon produced by NiMo series did not give the RBM peak. Moreover, the D-band to G-band intensity ratios are high, which was due to the deposited carbon mostly contained undesirable forms as shown in Table 4.4.

Table 4.5 illustrates the Raman spectroscopy resulted from the MgO support. Only carbon produced by CoMo and FeMo catalysts at 2:1 mole ratio with CH_4 decomposition gives the RBM signals. For instance, the Raman spectra of carbon produced by CH_4 decomposition on FeMo 2:1 give the small RBM signal and also provides high D-band intensity indicating that too much disorder carbon are formed as shown in Figure 4.39. Like the result of Raman spectra, TPO profiles show the dominant peak that centered at around the range of disorder carbon and MWNT.

Besides bimetallic catalysts, carbon made by some mono-metallic catalysts on this support also gives the RBM signals. All of the carbon generated by Co series with CO disproportionation, CH_4 decomposition and mixture of CO and CH_4 show the RBM peaks as seen in Table 4.6. Furthermore, these signals of deposited carbon produced by Ni, Co, and Fe catalysts with CH_4 decomposition can be seen in Figure 4.41. However, Figure 4.42 illustrates the TPO profiles that the peak centered on low oxidation temperature, which corresponds to amorphous carbon.

Table 4.5 Summary the Raman spectroscopy results on magnesium oxide support

Catalyst/ MgO	CH_4			CO			CH_4+CO		
	1:1	1:2	2:1	1:1	1:2	2:1	1:1	1:2	2:1
NiMo	–	–	–	–	–	–	–	–	–
CoMo	–	–	+	–	–	–	–	–	–
FeMo	–	–	+	–	–	–	–	–	–

\+ positive RBM signal
– no RBM signal

Table 4.6 Summary the Raman spectroscopy results of mono-metallic catalysts on magnesium oxide support

Mono-metallic catalyst / MgO	CH_4	CO	CH_4+CO
Ni	+	–	–
Co	+	+	+
Fe	+	–	–
Mo	–	–	–

\+ positive RBM signal
– no RBM signal

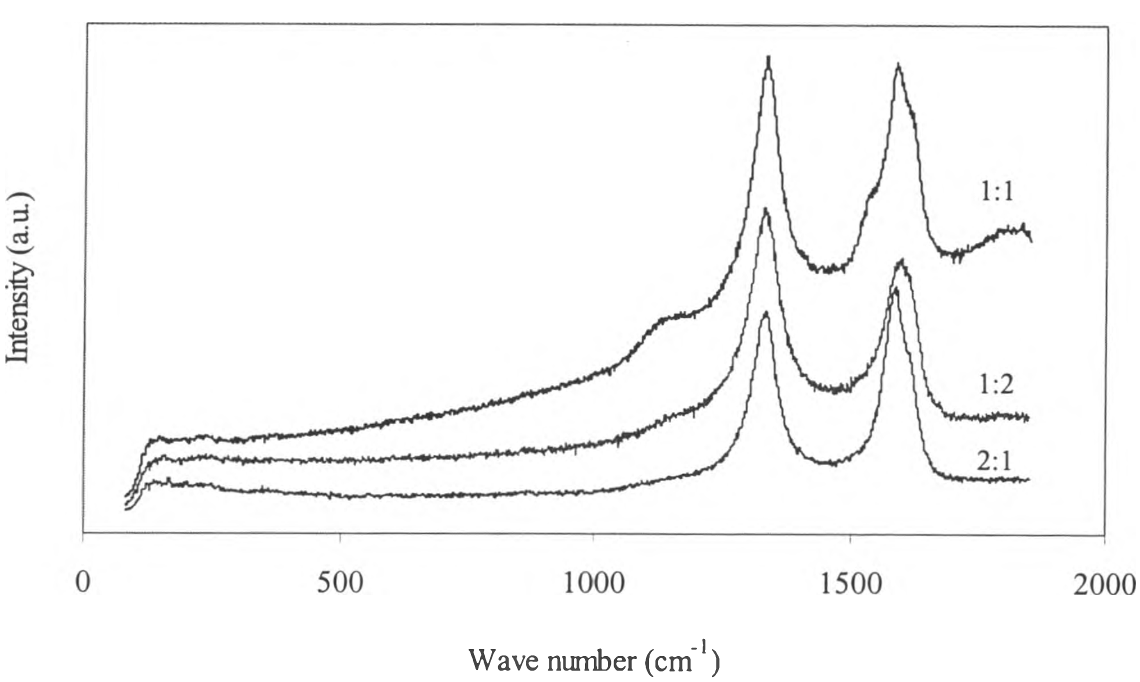

Figure 4.39 Raman spectra of carbon produced by FeMo at 1:1, 1:2, and 2:1 mole ratios over magnesium oxide support with CH_4 at 750 °C.

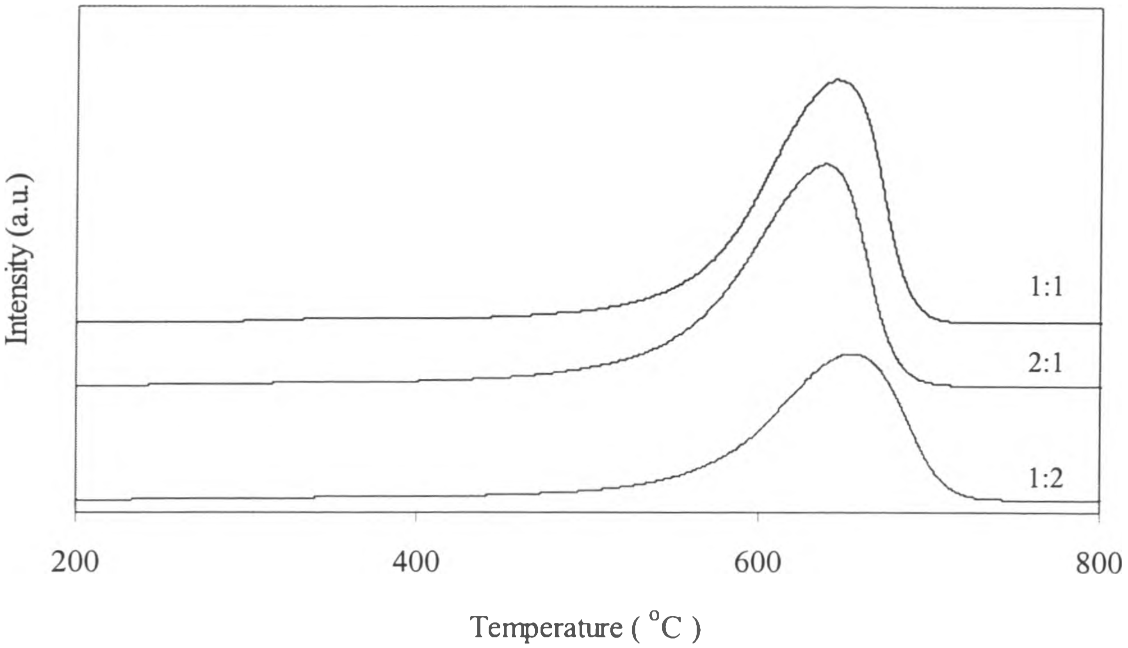

Figure 4.40 TPO profiles of carbon produced by FeMo at 1:1, 1:2, and 2:1 mole ratios over magnesium oxide support with CH_4 at 750 °C.

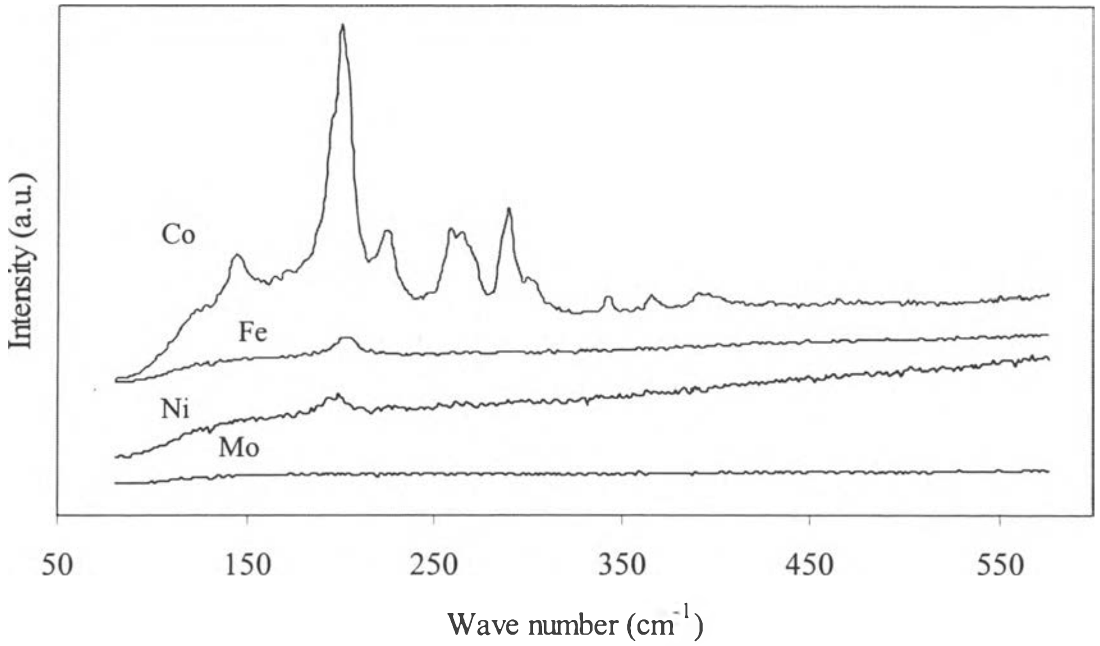

Figure 4.41 Raman spectra at RBM range of carbon produced by Ni, Co, Fe, and Mo catalysts over magnesium oxide support with CH_4 at 750 °C.

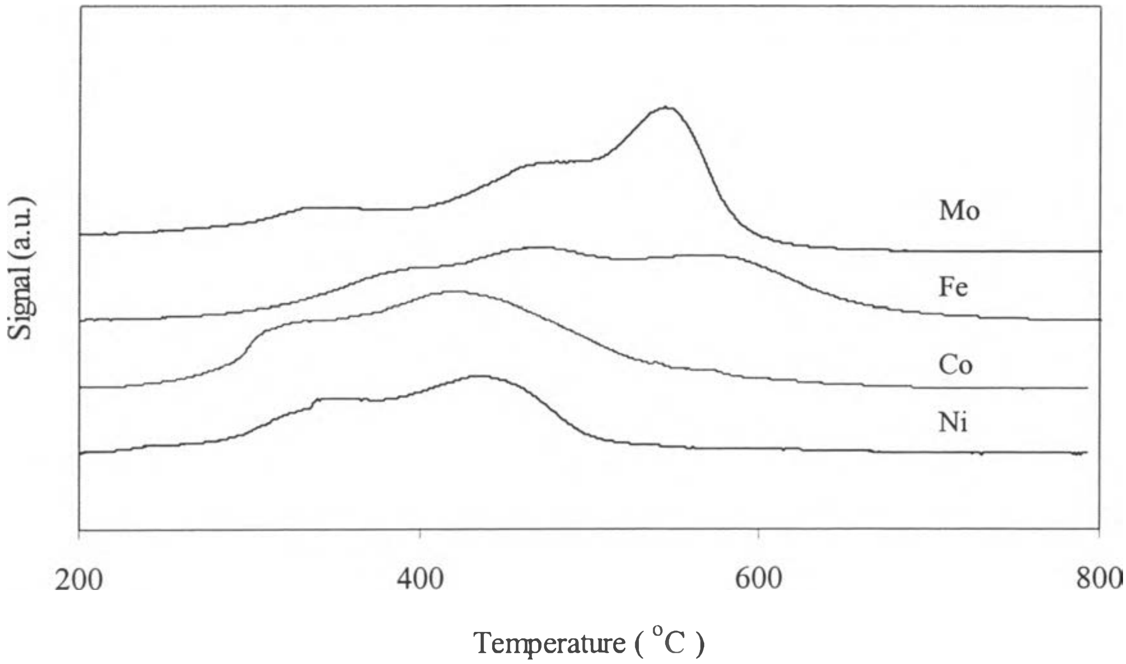

Figure 4.42 TPO profiles at RBM range of carbon produced by Ni, Co, Fe, and Mo catalysts over magnesium oxide support with CH_4 at 750 °C.

A comparison of the quality parameter of carbon produced by CH_4, CO, and mixed gases over different catalyst formulations on MgO support is shown in Figure 4.43. According to this Figure, when using MgO as a support, the quality of carbon products is considerably lower than silica and alumina supports, because most of the quality parameter are less than zero. Although the RBM signals were observed on carbon produced by CoMo and FeMo catalysts at 2:1 mole ratio, deposited carbon has low quality, which mean that these samples were difficult to make SWNT. However, the yields of carbon produced on MgO support are higher than silica and alumina supports as shown in Figure 4.44

Table 4.7 summarizes the results that may present SWNT on MgO support. Although the carbon generated by mono-metallic catalysts gave the RBM signals, yields of carbon are lower than bi-metallic catalysts, so SWNT was difficult to observe in these samples. Moreover, the positions of D-band and G-band cannot be determined the type of carbon species. In perfect agreement with previous study, the deposited carbon produced by FeMo 2:1 with CH_4 decomposition presents the RBM signal as well as provides a high amount of carbon yields (Xuto, 2002). In addition, the prediction of diameter was determined by position of RBM signal as shown in equation 2.1. In this support, a diameter of SWNT is in the range of 0.8–1.4 nm

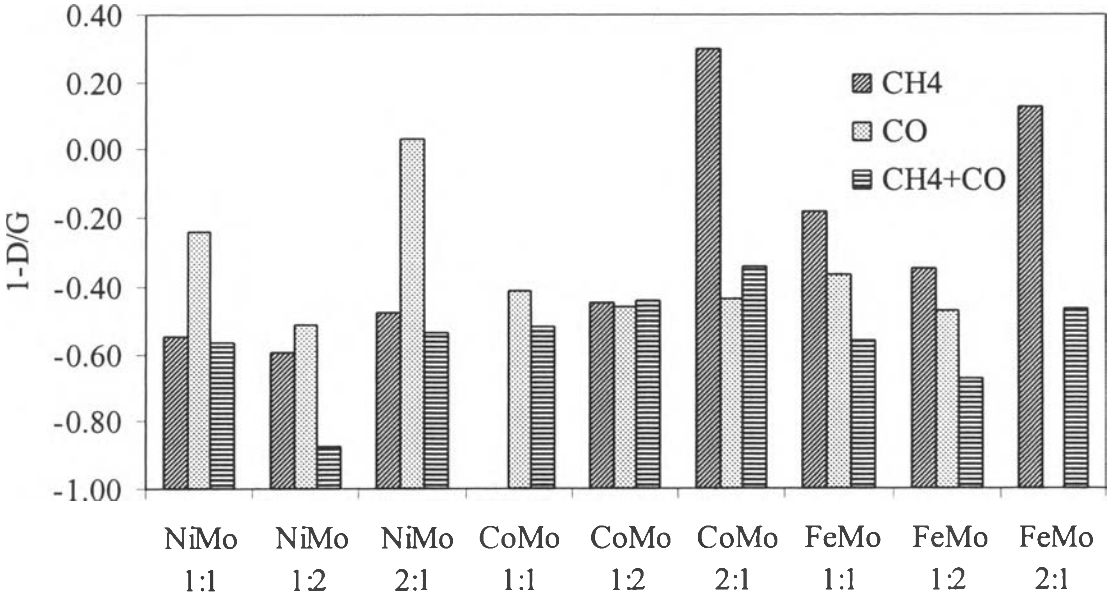

Figure 4.43 the quality parameter of carbon produced by different catalyst formulations over magnesium oxide support with CH_4, CO, and mixture at 750 °C.

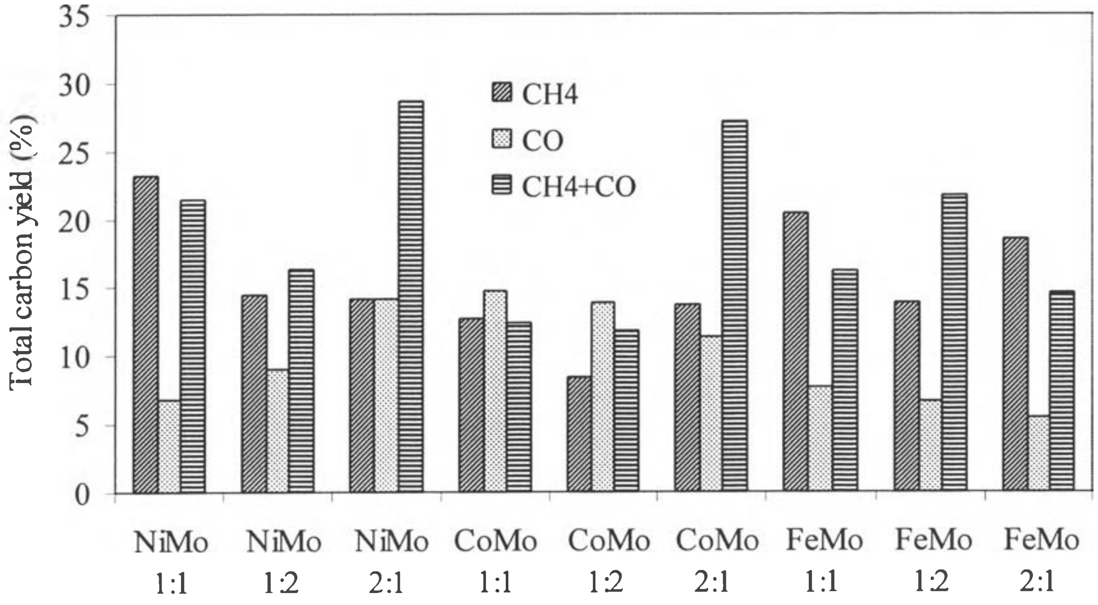

Figure 4.44 the total yields of carbon produced by different catalyst formulations over magnesium oxide support with CH_4, CO, and mixture at 750 °C.

Table 4.7 Summary of SWNT formation on magnesium oxide sorted by quality parameter

Samples	QP (1-D/G)	Carbon Yield (%)	diameter (nm)
Co/MgO (CO, 750 °C)	0.94	0.77	0.81–1.20
Co/MgO (CH_4, 750 °C)	0.93	0.61	0.81–1.16
Ni/MgO (CH_4, 750 °C)	0.92	0.37	1.22
Fe/MgO (CH_4, 750 °C)	0.88	0.58	0.81–1.20
Co/MgO (CO+CH_4, 750 °C)	0.86	0.91	0.81–1.20
CoMo 2:1/MgO (CH_4, 750 °C)	0.30	13.75	0.81–1.20
FeMo 2:1/MgO (CH_4, 750 °C)	0.13	18.60	1.43

4.3 The Carbon Nanotubes Formation on Alumina Support

Alumina support showed fascinating results in the formationtion of carbon nanotubes. Most of the carbons produced on alumina support were SWNT. The summary of carbon nanotubes production by different catalyst formulations and carbon-containing gases are illustrared in Table 4.8.

Table 4.8 Summary of carbon nanotube production by using different gases and catalysts on alumina support

Samples	D/G Ratio	Carbon Yield (%)	RBM
NiMo 1:1/Al_2O_3 (CH_4, 750 °C)	1.05	12.14	no
NiMo 1:1/Al_2O_3 (CO, 750 °C)	0.41	3.56	yes
NiMo 1:1/Al_2O_3 (CH_4+CO, 750 °C)	1.11	11.33	yes
NiMo 1:2/Al_2O_3 (CH_4, 750 °C)	1.15	13.65	no
NiMo 1:2/Al_2O_3 (CO, 750 °C)	0.72	3.60	yes
NiMo 1:2/Al_2O_3 (CH_4 + CO, 750 °C)	1.08	11.54	no
NiMo 2:1/Al_2O_3 (CH_4, 750 °C)	1.08	12.58	no
NiMo 2:1/Al_2O_3 (CO, 750 °C)	0.52	3.90	yes
NiMo 2:1/Al_2O_3 (CH_4+CO, 750 °C)	0.81	10.74	yes
CoMo 1:1/Al_2O_3 (CH_4, 750 °C)	0.90	13.32	yes
CoMo 1:1/Al_2O_3 (CO, 750 °C)	0.14	4.03	yes
CoMo 1:1/Al_2O_3 (CH_4+CO, 750 °C)	0.52	10.43	yes
CoMo 1:2/Al_2O_3 (CH_4, 750 °C)	0.92	12.05	yes
CoMo 1:2/Al_2O_3 (CO, 750 °C)	0.49	3.00	yes
CoMo 1:2/Al_2O_3 (CH_4 + CO, 750 °C)	0.79	11.65	yes
CoMo 2:1/Al_2O_3 (CH_4, 750 °C)	1.00	12.74	no
CoMo 2:1/Al_2O_3 (CO, 750 °C)	0.64	5.06	no
CoMo 2:1/Al_2O_3 (CH_4+CO, 750 °C)	1.17	9.68	yes

Table 4.8 (continued)

Samples	D/G Ratio	Carbon Yield (%)	RBM
FeMo 1:1/Al_2O_3 (CH_4, 750 °C)	0.86	12.10	no
FeMo 1:1/Al_2O_3 (CO, 750 °C)	0.47	3.16	yes
FeMo 1:1/Al_2O_3 (CO+CH_4, 750 °C)	1.02	6.99	no
FeMo 1:2/Al_2O_3 (CH_4, 750 °C)	1.09	11.28	yes
FeMo 1:2/Al_2O_3 (CO, 750 °C)	0.33	3.29	yes
FeMo 1:2/Al_2O_3 (CO+CH_4, 750 °C)	0.96	9.58	no
FeMo 2:1/Al_2O_3 (CH_4, 750 °C)	0.79	14.67	yes
FeMo 2:1/Al_2O_3 (CO, 750 °C)	0.32	3.94	yes
FeMo 2:1/Al_2O_3 (CO+CH_4, 750 °C)	0.44	9.37	yes
Ni/Al_2O_3 (CH_4, 750 °C)	1.16	1.11	no
Ni/Al_2O_3 (CO, 750 °C)	1.02	0.62	no
Ni/Al_2O_3 (CO+CH_4, 750 °C)	1.08	0.99	no
Co/Al_2O_3 (CH_4, 750 °C)	0.69	0.28	no
Co/Al_2O_3 (CO, 750 °C)	0.46	0.14	no
Co/Al_2O_3 (CO+CH_4, 750 °C)	0.99	0.81	no
Fe/Al_2O_3 (CH_4, 750 °C)	1.32	1.04	no
Fe/Al_2O_3 (CO, 750 °C)	1.09	0.12	no
Fe/Al_2O_3 (CO+CH_4, 750 °C)	0.97	0.75	no
Mo/Al_2O_3 (CH_4, 750 °C)	1.01	8.59	no
Mo/Al_2O_3 (CO, 750 °C)	0.98	0.52	no
Mo/Al_2O_3 (CO+CH_4, 750 °C)	0.95	5.09	no

4.3.1 Effects of Effect of CH_4, CO, and Mixture of CH_4 and CO on the Carbon Nanotubes Formation

Figures 4.45–4.61 show the Raman spectra and TPO profiles when using three different feed gases—CH_4, CO, and mixture (CH_4+CO). It is important to be noted that all of the carbons produced by CO disproportionation showed good results for producing SWNT in all series of catalyst. In addition, the carbon produced by CoMo and FeMo catalysts with CH_4 decomposition and mixture of CO and CH_4 gives the RBM signals corresponding to SWNT. However, the D-bands are also as high as G-bands intensity indicating high quantity of undesirable forms of carbon.

For instance, Figures 4.47–4.50 and 4.57–4.58 illustrate the Raman spectra and TPO profiles of bi-metallic catalysts with CO disproportionation, CH_4 decomposition and mixture of CO and CH_4. Only carbon produced by CO disproportionation presented the RBM signals. Other interesting results are illustrated in Figures 4.51–4.54 and 4.61–4.62. All of the Raman results of carbon generated by CoMo 1:1, CoMo 1:2, and FeMo 2:1 catalysts have the RBM signals which correspond to SWNT when using CO, CH_4, and their mixture as reactant gases. The TPO profiles also shows major peak oxidized at high temperature indicating the presence of MWNT.

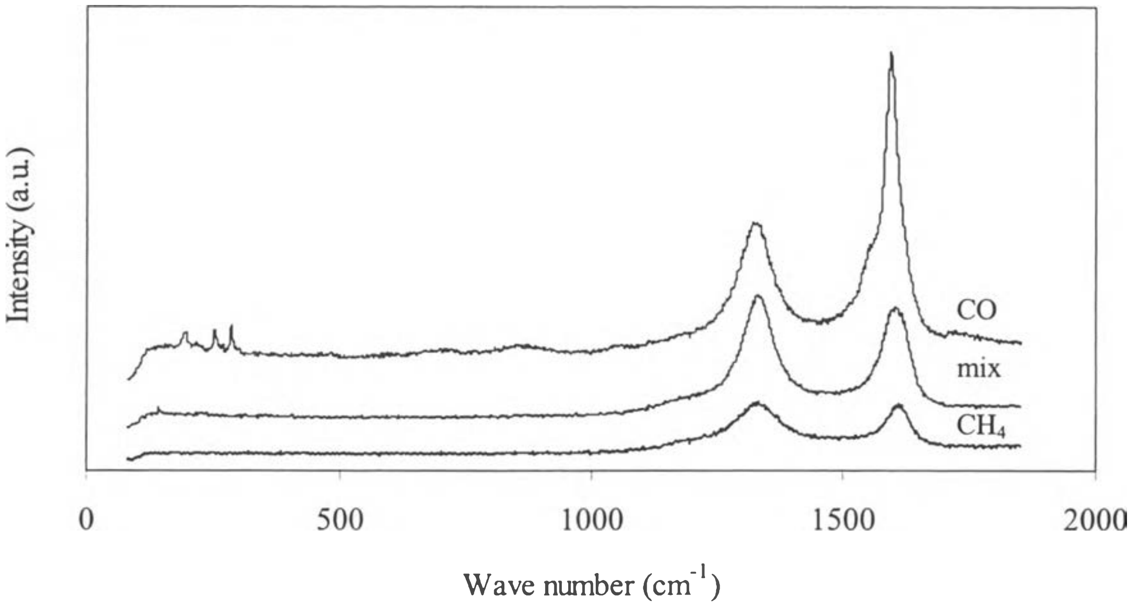

Figure 4.45 Raman spectra of carbon produced by NiMo 1:1 over alumina support with CH_4, CO, and mixture at 750 °C.

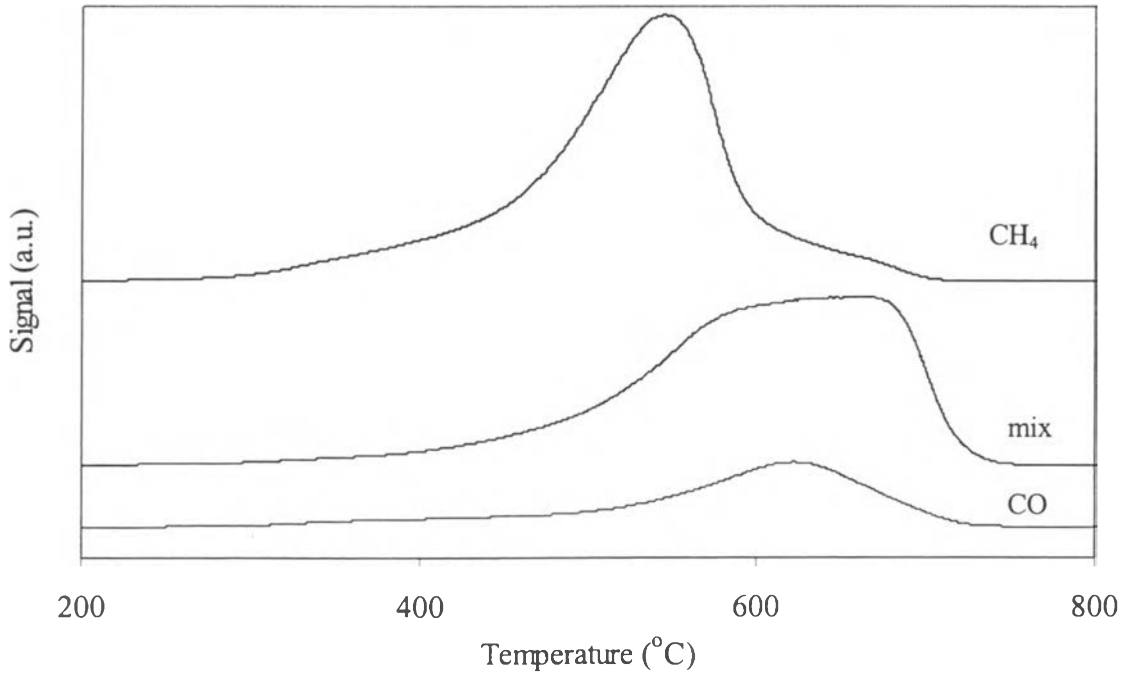

Figure 4.46 TPO profiles of carbon produced by NiMo 1:1 over alumina support with CH_4, CO, and mixture at 750 °C.

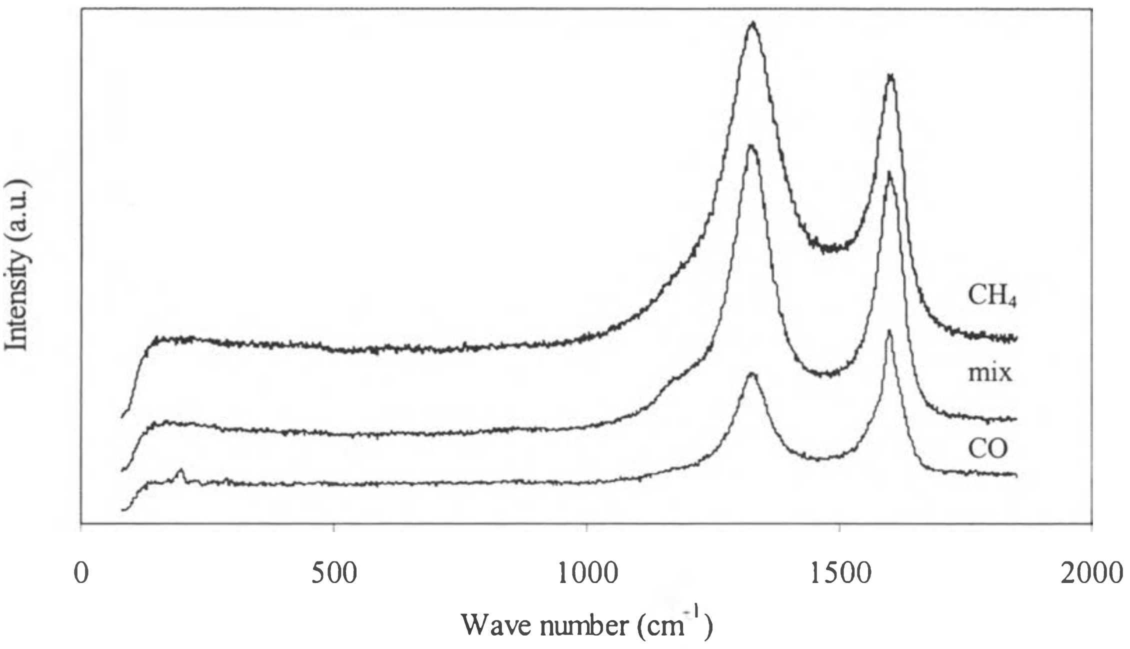

Figure 4.47 Raman spectra of carbon produced by NiMo 1:2 over alumina support with CH_4, CO, and mixture at 750 °C.

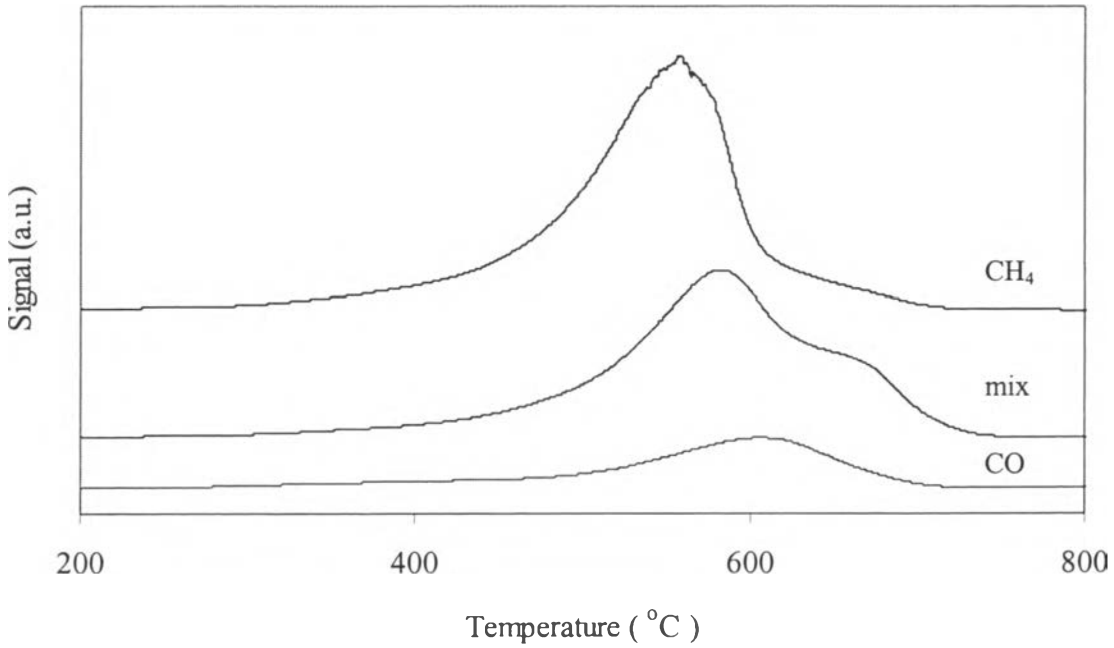

Figure 4.48 TPO profiles of carbon produced by NiMo 1:2 over alumina support with CH_4, CO, and mixture at 750 °C.

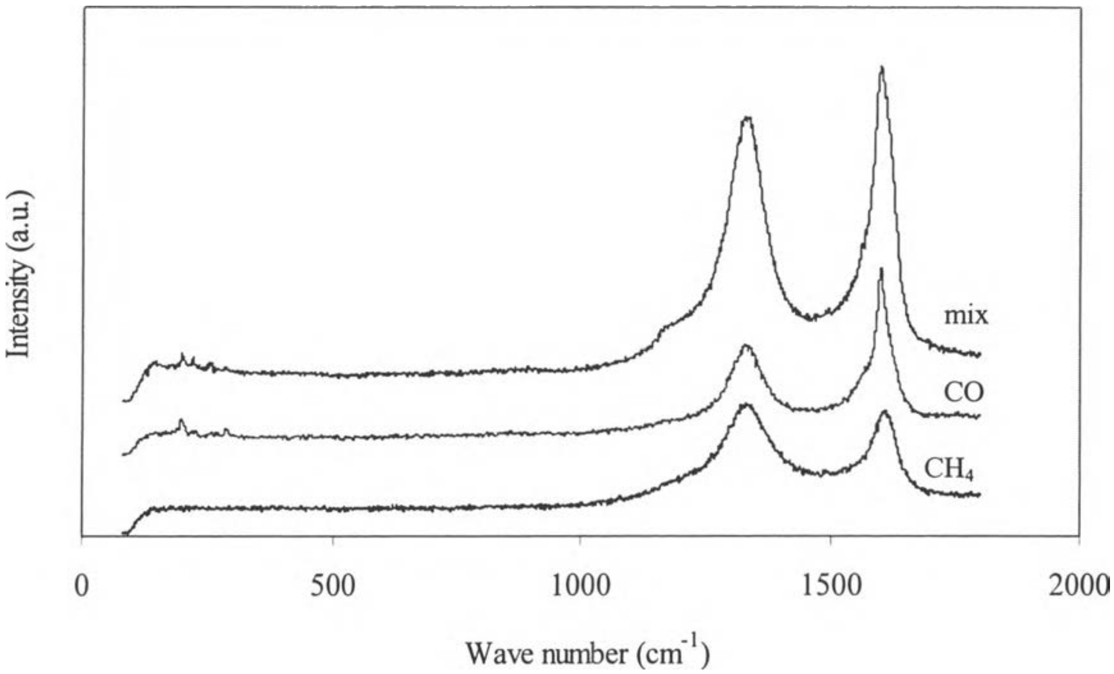

Figure 4.49 Raman spectra of carbon produced by NiMo 2:1 over alumina support with CH_4, CO, and mixture at 750 °C.

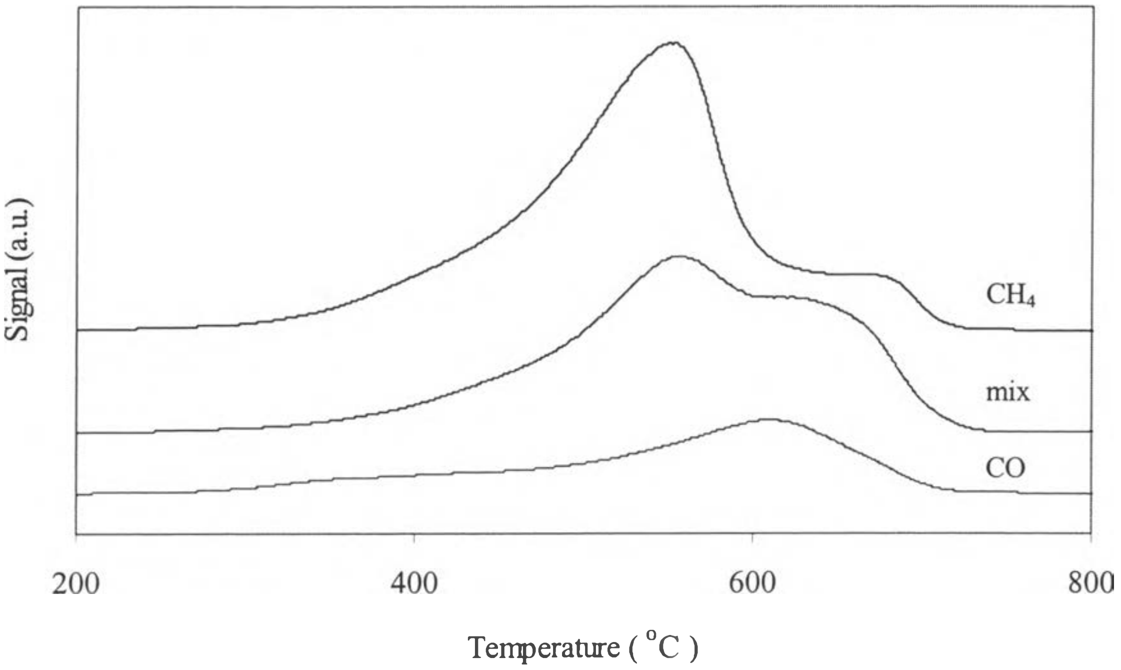

Figure 4.50 TPO profiles of carbon produced by NiMo 2:1 over alumina support with CH_4, CO, and mixture at 750 °C.

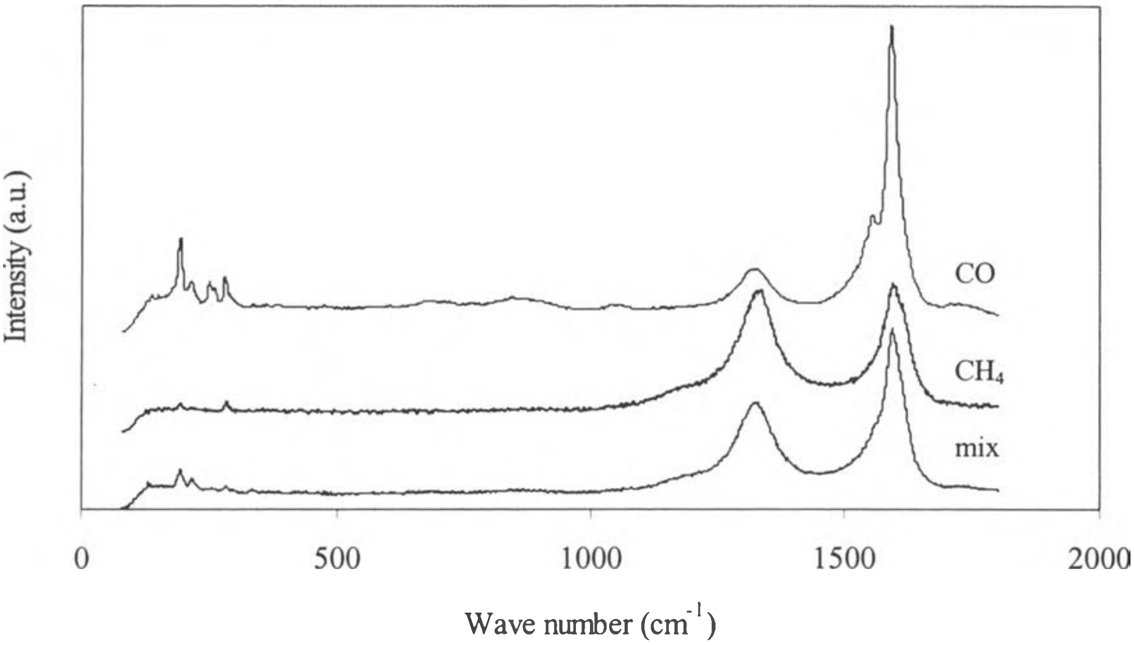

Figure 4.51 Raman spectra of carbon produced by CoMo 1:1 over alumina support with CH_4, CO, and mixture at 750 °C.

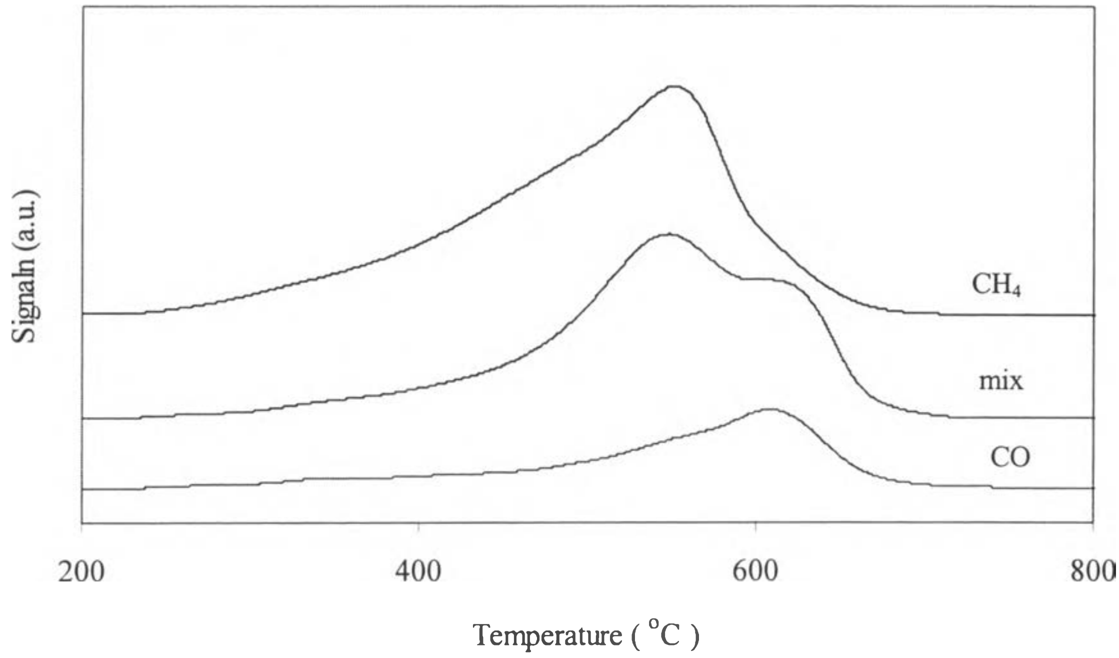

Figure 4.52 TPO profiles of carbon produced by CoMo 1:1 over alumina support with CH_4, CO, and mixture at 750 °C.

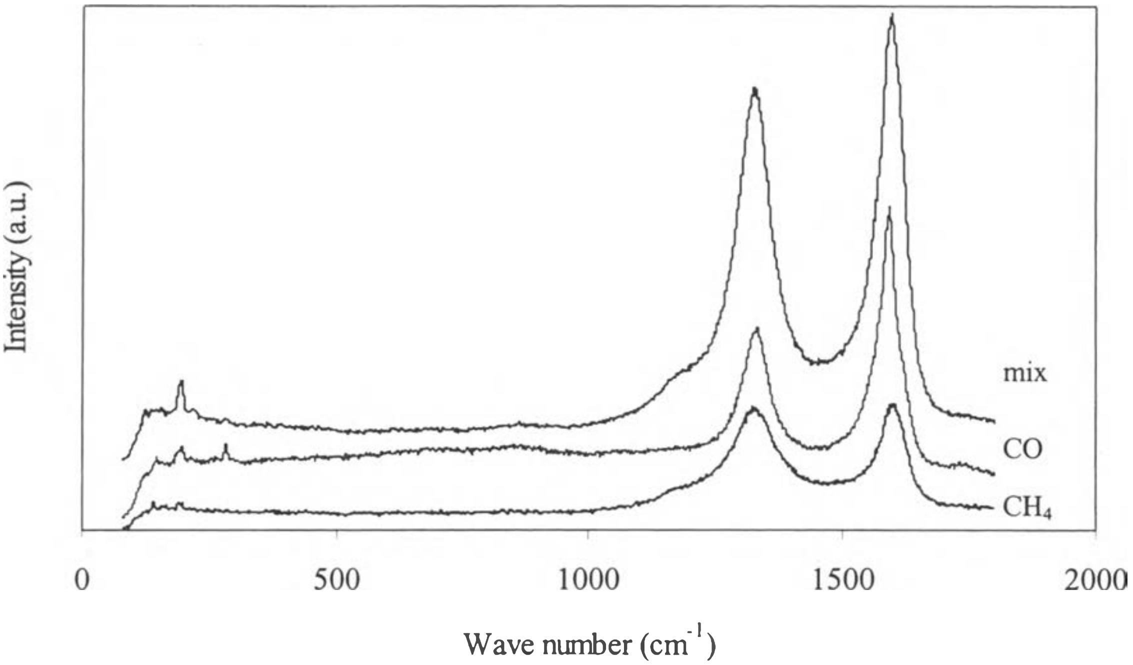

Figure 4.53 Raman spectra of carbon produced by CoMo 1:2 over alumina support with CH_4, CO, and mixture at 750 °C.

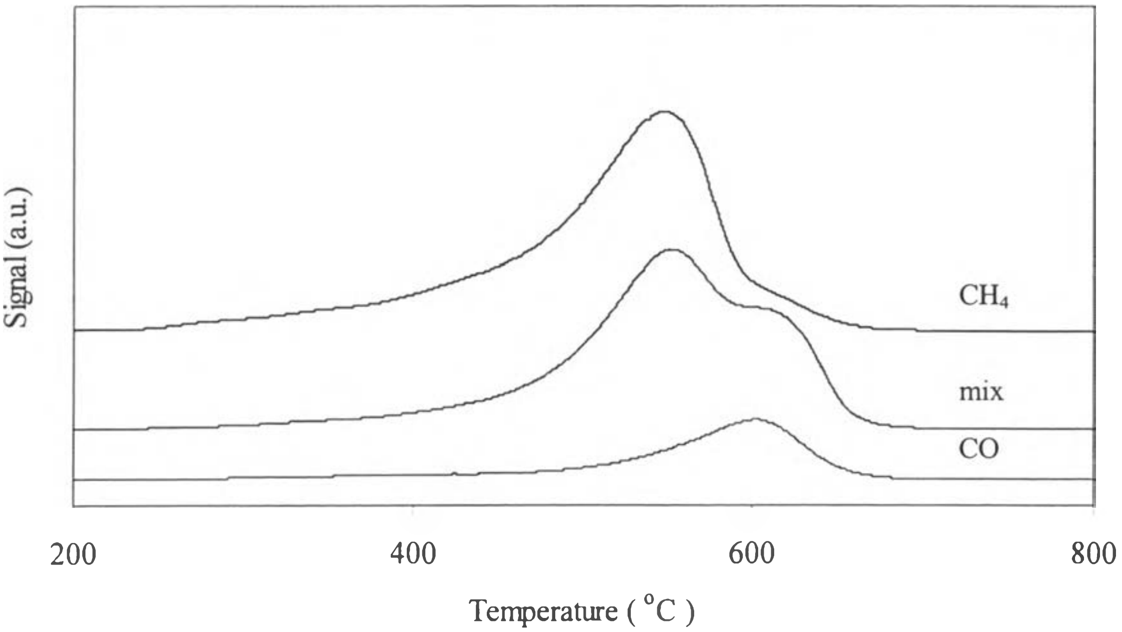

Figure 4.54 TPO profiles of carbon produced by CoMo 1:2 over alumina support with CH_4, CO, and mixture at 750 °C.

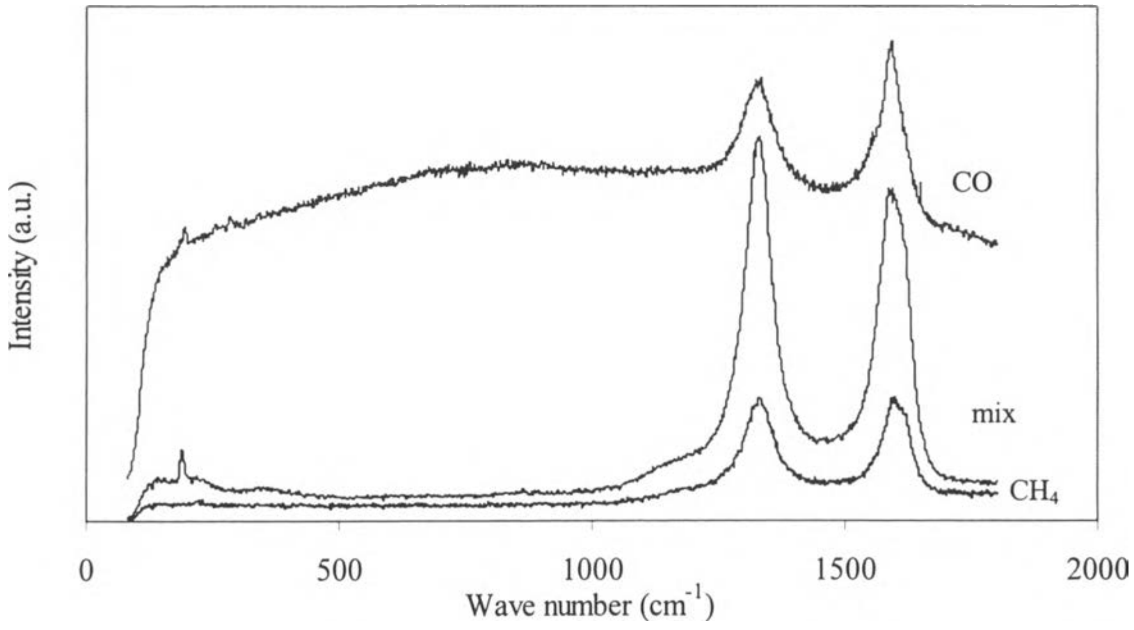

Figure 4.55 Raman spectra of carbon produced by CoMo 2:1 over alumina support with CH_4, CO, and mixture at 750 °C.

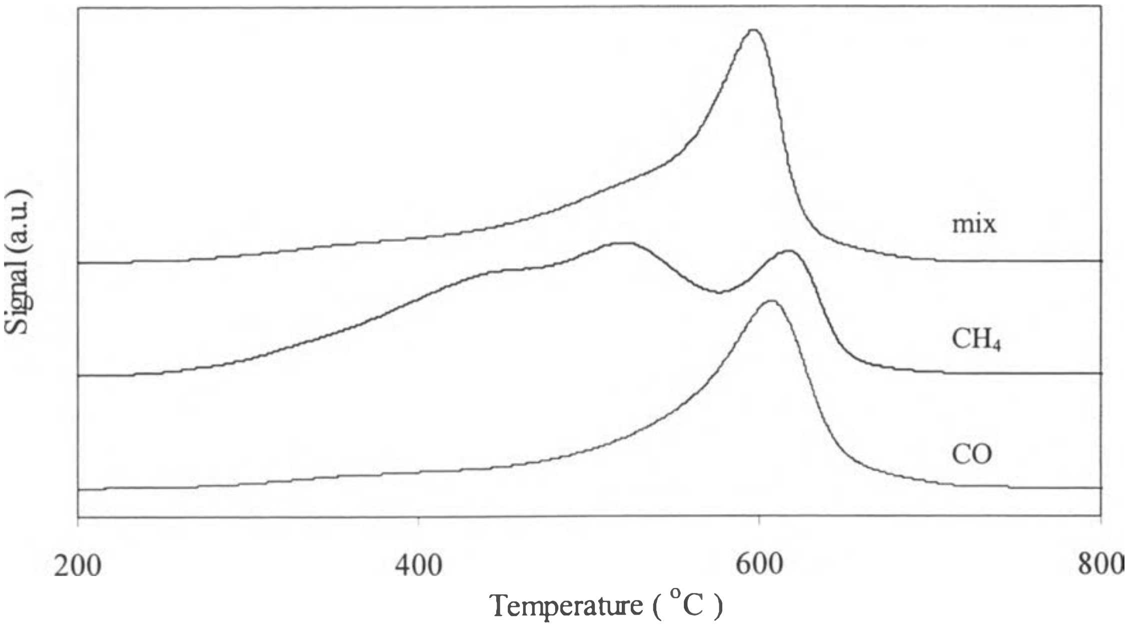

Figure 4.56 TPO profiles of carbon produced by CoMo 2:1 over alumina support with CH_4, CO, and mixture at 750 °C.

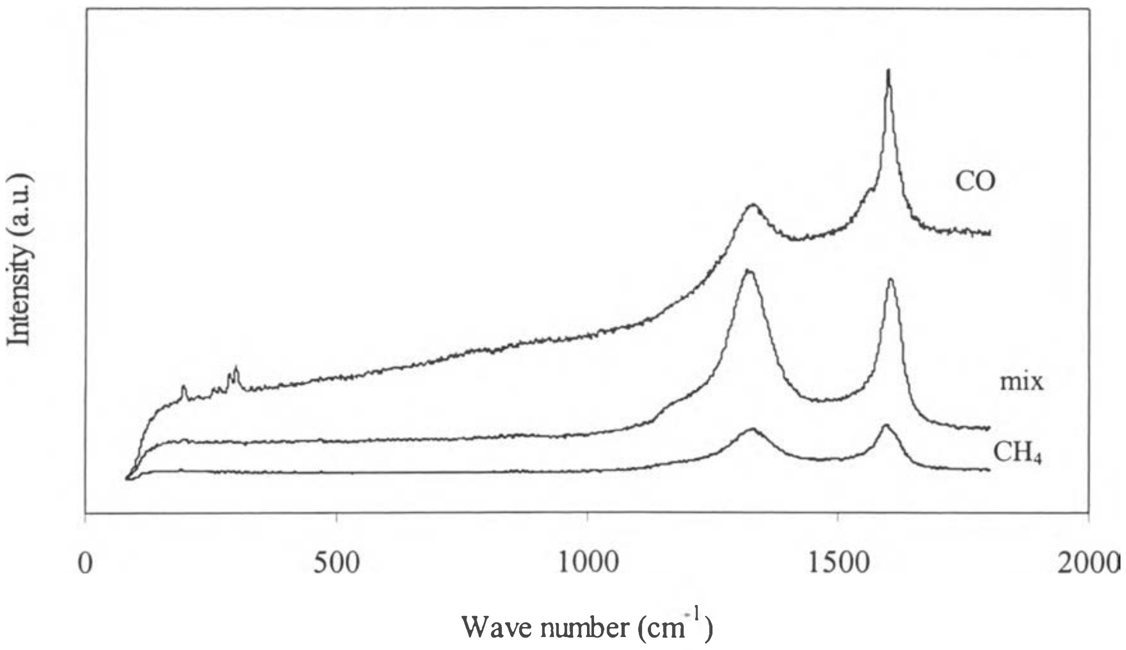

Figure 4.57 Raman spectra of carbon produced by FeMo 1:1 over alumina support with CH_4, CO, and mixture at 750 °C.

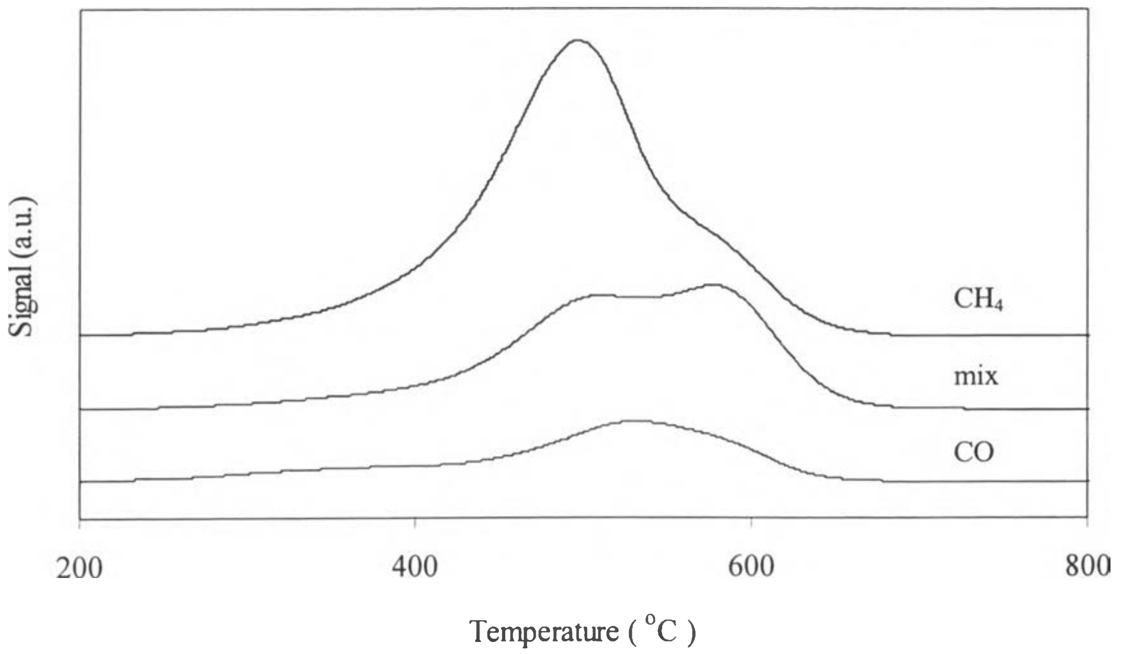

Figure 4.58 TPO profiles of carbon produced by FeMo 1:1 over alumina support with CH_4, CO, and mixture at 750 °C.

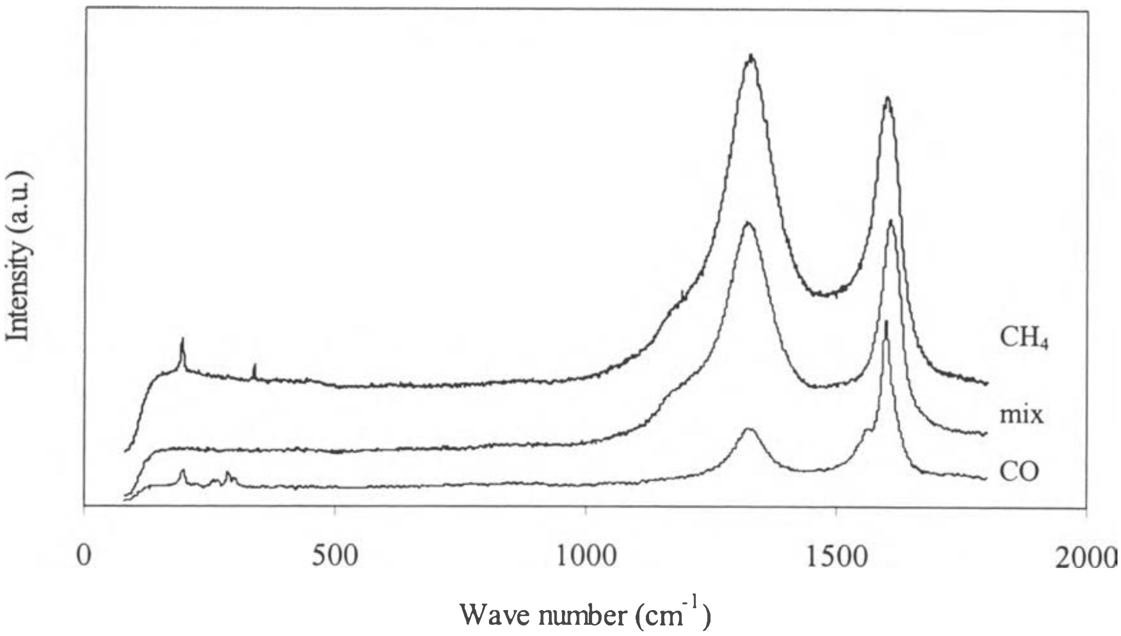

Figure 4.59 Raman spectra of carbon produced by FeMo 1:2 over alumina support with CH_4, CO, and mixture at 750 °C.

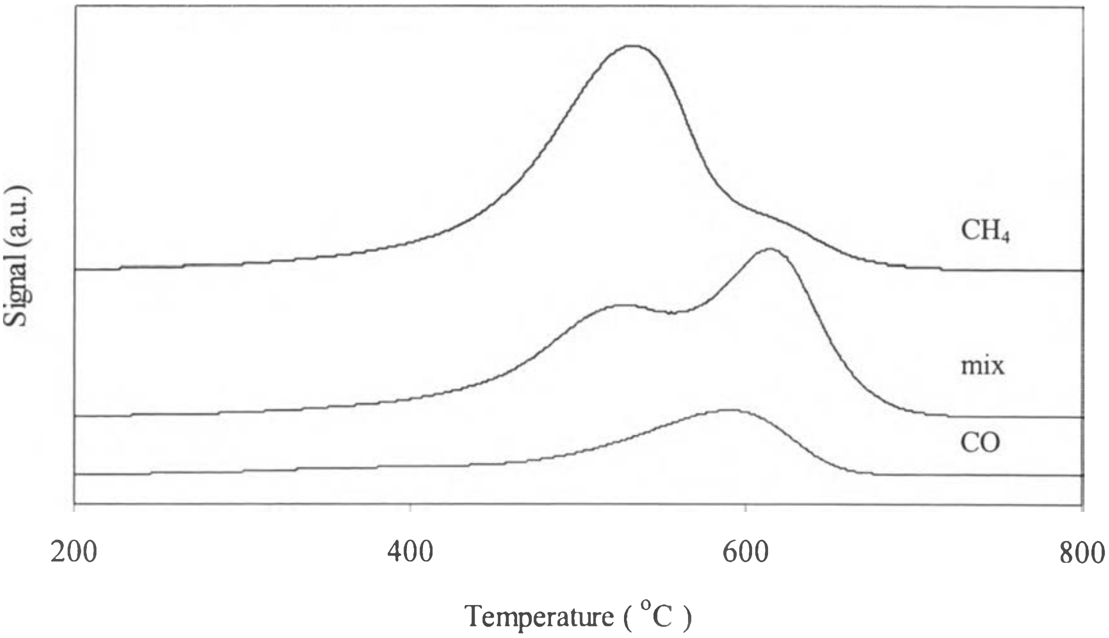

Figure 4.60 TPO profiles of carbon produced by FeMo 1:2 over alumina support with CH_4, CO, and mixture at 750 °C.

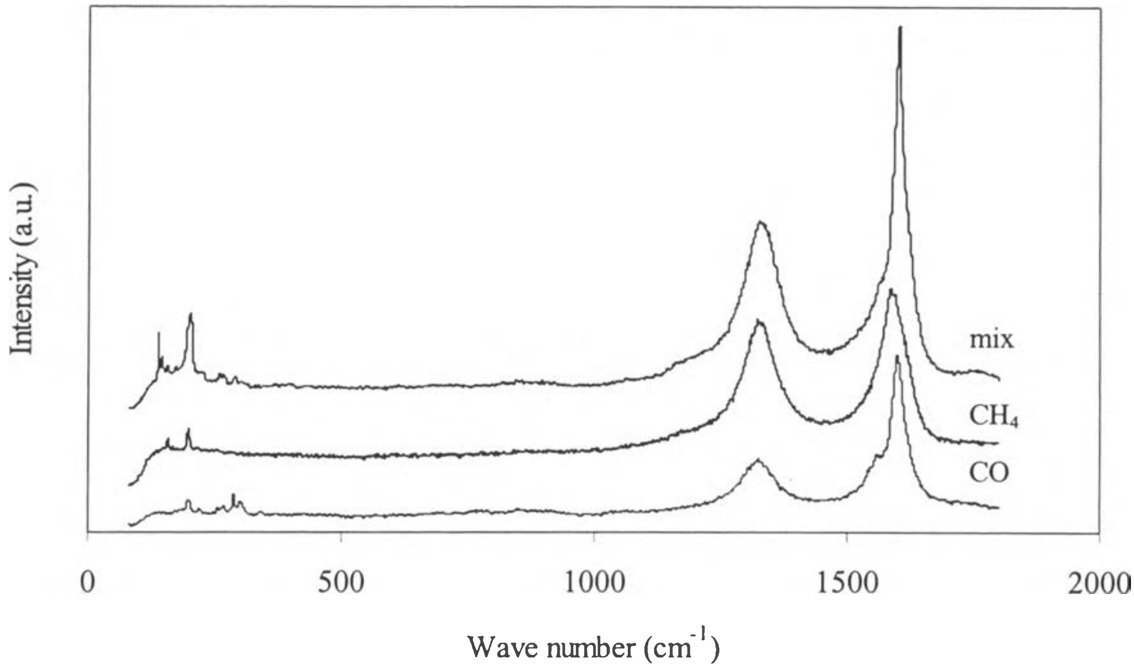

Figure 4.61 Raman spectra of carbon produced by FeMo 2:1 over alumina support with CH_4, CO, and mixture at 750 °C.

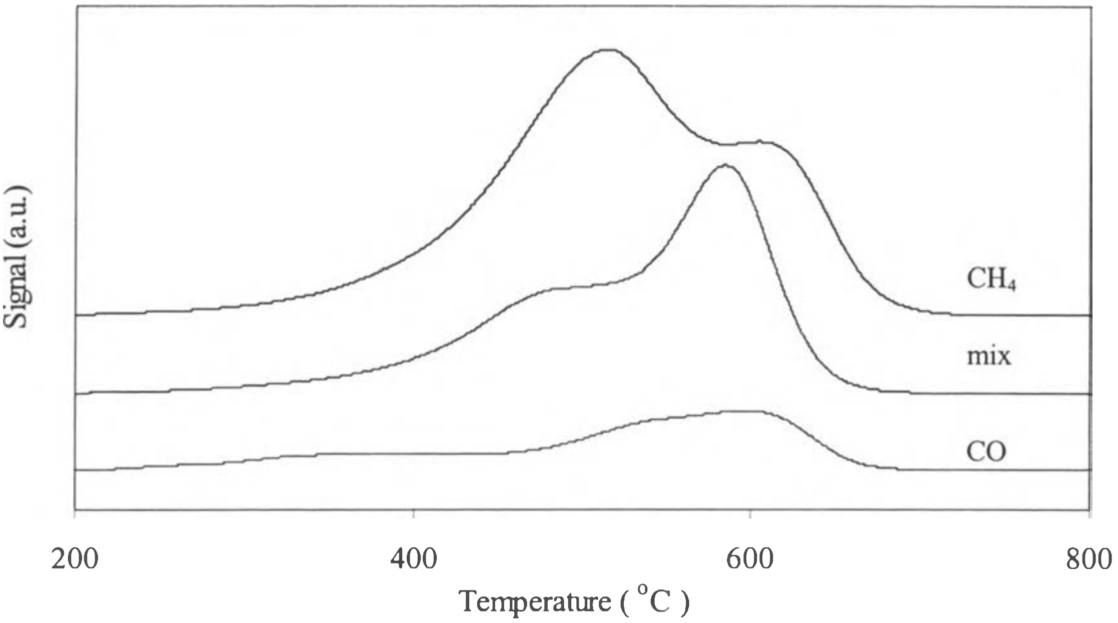

Figure 4.62 TPO profiles of carbon produced by FeMo 2:1 over alumina support with CH_4, CO, and mixture at 750 °C.

4.3.2 Effects of Catalyst Formulations on Carbon Nanotubes Formation

The effect of mole ratios on carbon nanotubes production was also considered. Figures 4.63–4.77 illustrate the Raman spectra and TPO profiles of carbon produced by CoMo, NiMo, and FeMo catalysts by varying the mole ratios at 1:1,1:2, and 2:1 on alumina support. The results of Raman spectroscopy are summarized in Table 4.9. It showed that most of the samples with RBM signals can be observed when using alumina as a support.

In NiMo series, the mole ratios at 1:1,1:2, and 2:1 by CO disproportionation showed good results presenting RBM peaks as well as giving low D-band intensity peaks as shown in Figure 4.63 and 4.64. Moreover, the carbon deposits generated by NiMo 1:1 and 2:1 catalysts with mixture of CH_4 and CO also presented SWNT, but gave high D/G ratios, which provide large of undesirable forms of carbon as can be seen in Figures 4.65 and 4.66. On the other hand, no RBM signals were observed when using CH_4 as a feed gas and high quantity of disordered carbon was formed.

Favorably, RBM signals were detected on the Raman spectra in CoMo series. The carbon species produced by CoMo catalyst at 1:1,1:2, and 2:1 mole ratios with mixture of CH_4 and CO showed SWNT, yet gave high D-band signals indicating high amount of disordered carbon. Furthermore, the carbon deposites made by CoMo 1:1 and 1:2 catalysts with CH_4 decomposition and CO disproportionation also present the RBM signals as can be seen from Figures 4.67–4.72.

According to Figures 4.73–4.78, the RBM signals were appeared when the carbon is produced by FeMo catalyst at 1:1, 1:2, and 2:1 mole ratios with CO disproportionation. It was also observed that the deposited carbon provided low quantity of disordered carbon. Meanwhile, the carbon produced by FeMo 1:2 by CH_4 decomposition and FeMo 2:1 by CO and CH_4 mixture also presented SWNT, but gave high amount of undisirable forms of carbon.

Changing the catalyst series—NiMo, CoMo, and FeMo in same ratio and feed gas were studied to understand the effect of metal species. Figures 4.79–4.80 exhibit the Raman spectra and TPO profiles of NiMo, CoMo, and FeMo catalysts at 2:1 mole ratio by mixture of CO and CH_4. As a result, SWNT are observed in all of the catalyst series at 2:1 mole ratio. Similarly, the carbon produced by all of the catalyst series at 1:2 mole ratio by CO disproportionation also presented SWNT as shown in Figure 4.81.

In contrast, the RBM peaks were not observed on mono-metalllic catalyst series implying absence of SWNT. It also gave the lowest yield of deposited carbon.

Table 4.9 Summary the Raman spectroscopy results on alumina support

Catalyst/ Al_2O_3	CH_4			CO			CH_4+CO		
	1:1	1:2	2:1	1:1	1:2	2:1	1:1	1:2	2:1
NiMo	-	-	-	+	+	+	+	-	+
CoMo	+	+	-	+	+	-	+	+	+
FeMo	-	+	+	+	+	+	-	-	+

\+ positive RBM signal

– no RBM signal

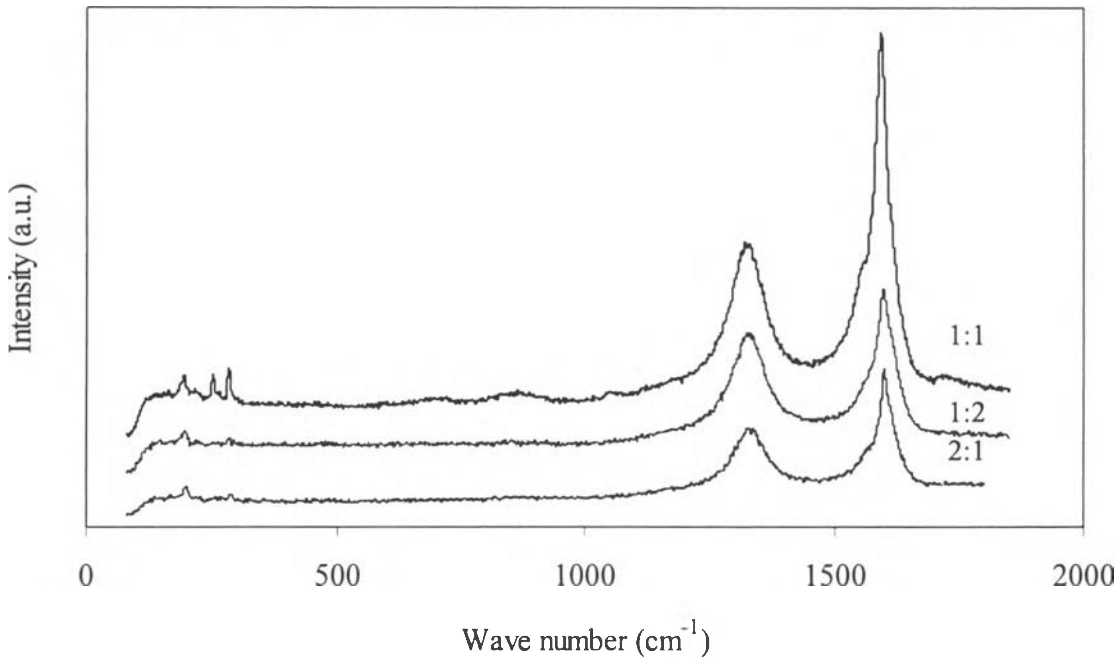

Figure 4.63 Raman spectra of carbon produced by NiMo at 1:1, 1:2, and 2:1 mole ratios over alumina support with CO at 750 °C.

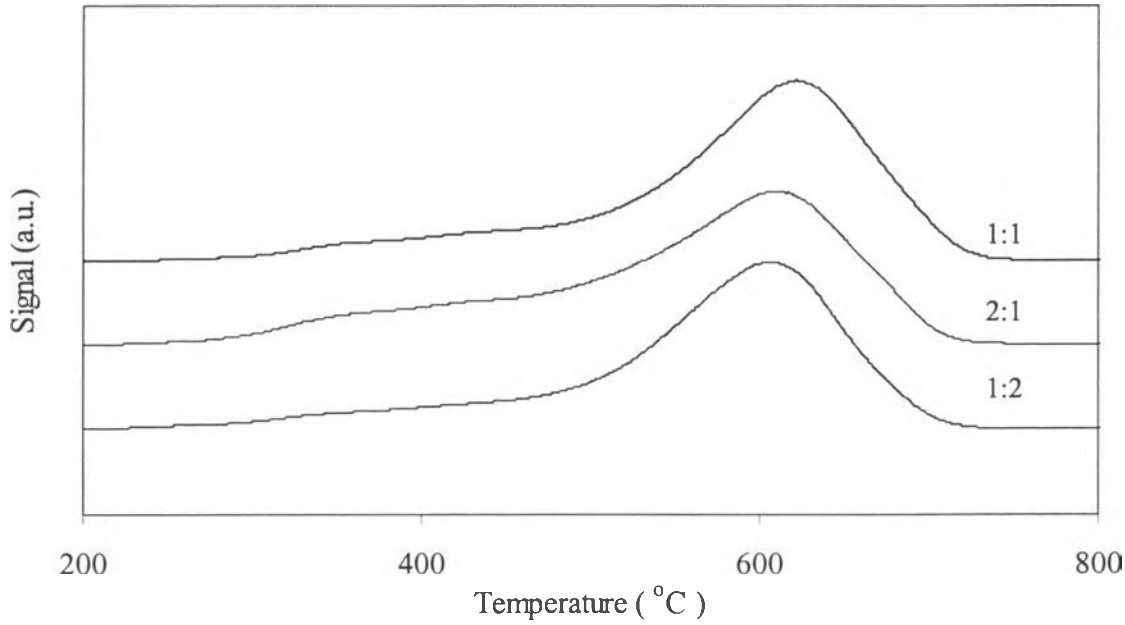

Figure 4.64 TPO profiles of carbon produced by NiMo at 1:1, 1:2, and 2:1 mole ratios over alumina support with CO at 750 °C.

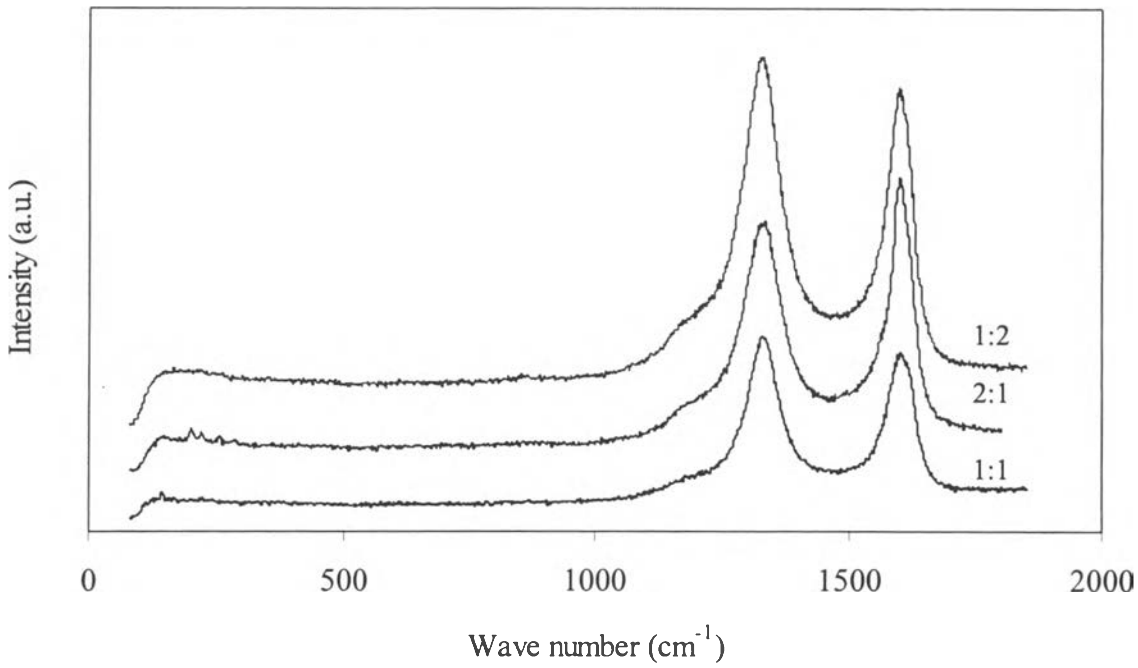

Figure 4.65 Raman spectra of carbon produced by NiMo at 1:1, 1:2, and 2:1 mole ratios over alumina support with mixture of CH_4 and CO at 750 °C.

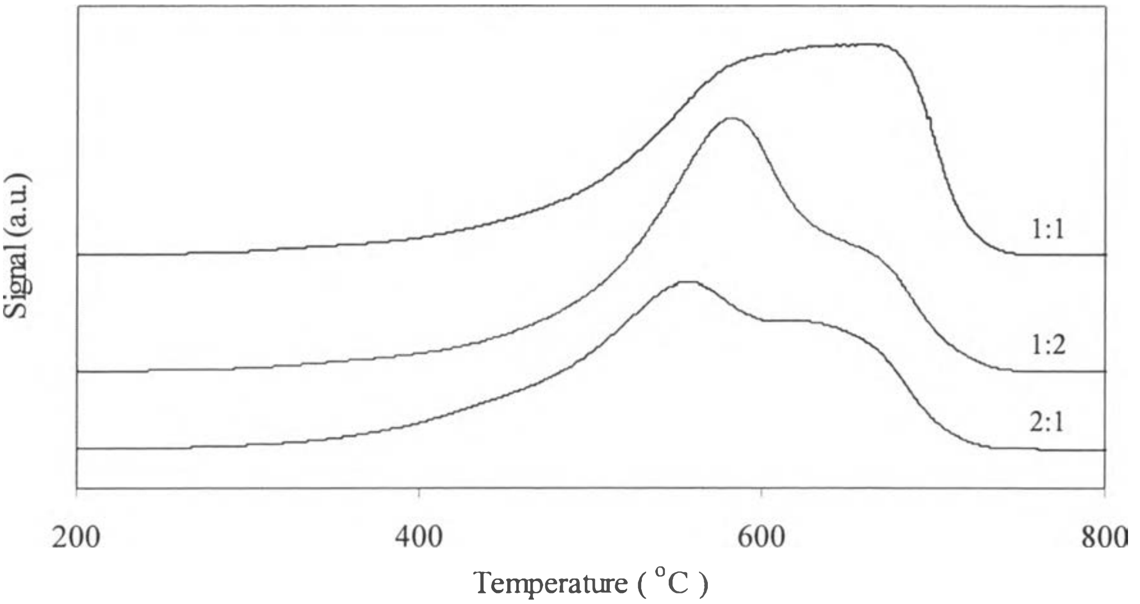

Figure 4.66 TPO profiles of carbon produced by NiMo at 1:1, 1:2, and 2:1 mole ratios over alumina support with mixture of CH_4 and CO at 750 °C.

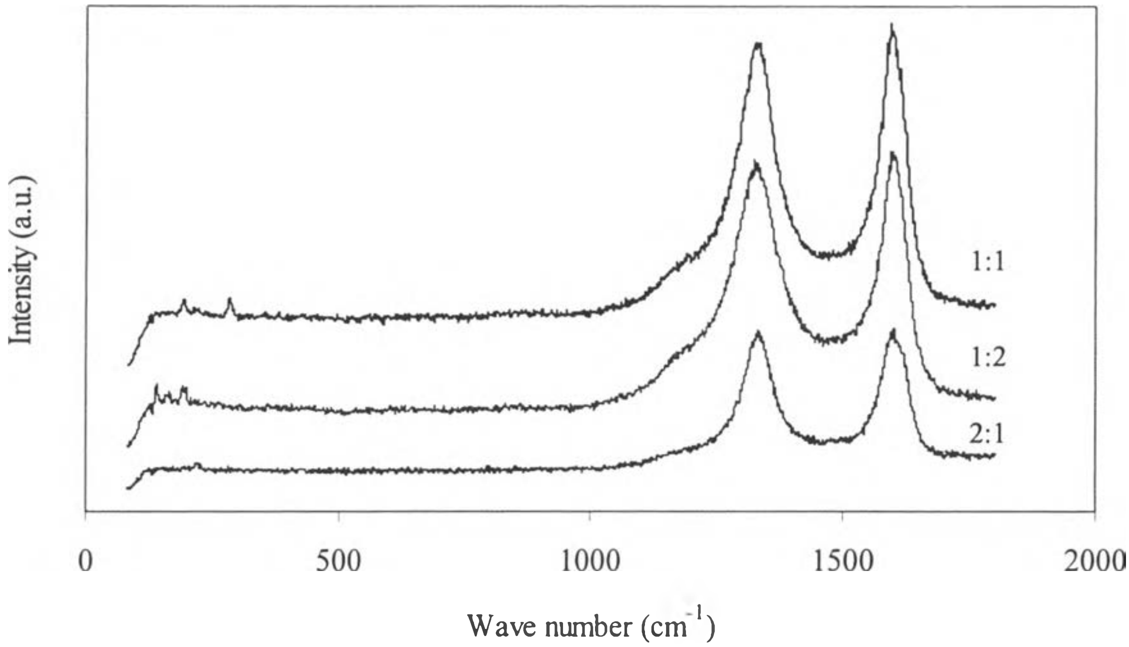

Figure 4.67 Raman spectra of carbon produced by CoMo at 1:1, 1:2, and 2:1 mole ratios over alumina support with CH_4 at 750 °C.

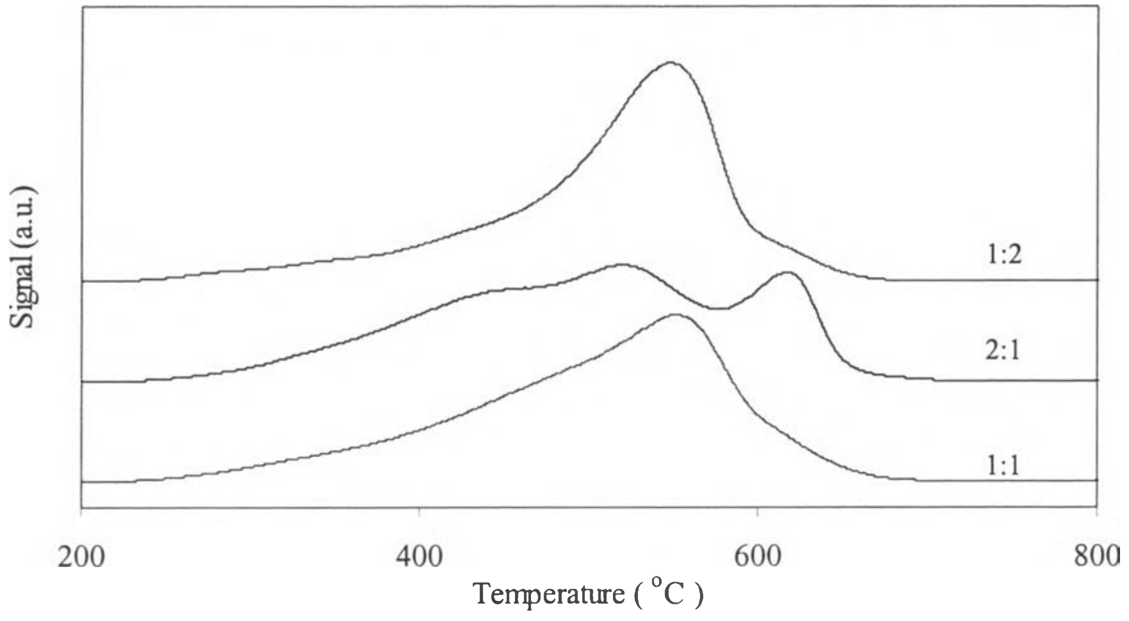

Figure 4.68 TPO profiles of carbon produced by CoMo at 1:1, 1:2, and 2:1 mole ratios over alumina support with CH_4 at 750 °C.

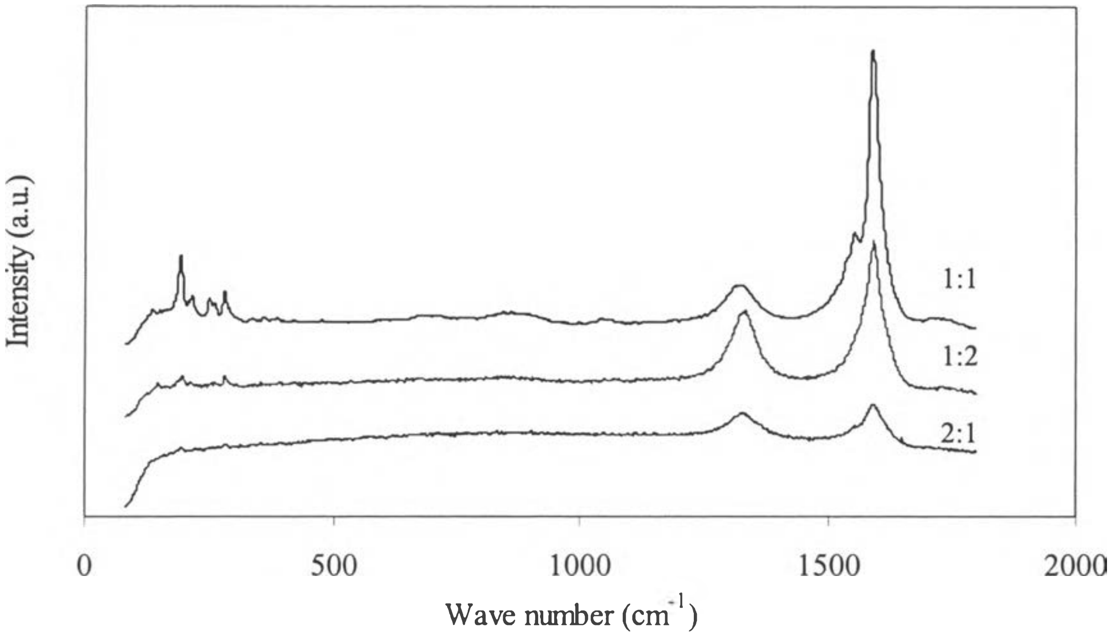

Figure 4.69 Raman spectra of carbon produced by CoMo at 1:1, 1:2, and 2:1 mole ratios over alumina support with CO at 750 °C.

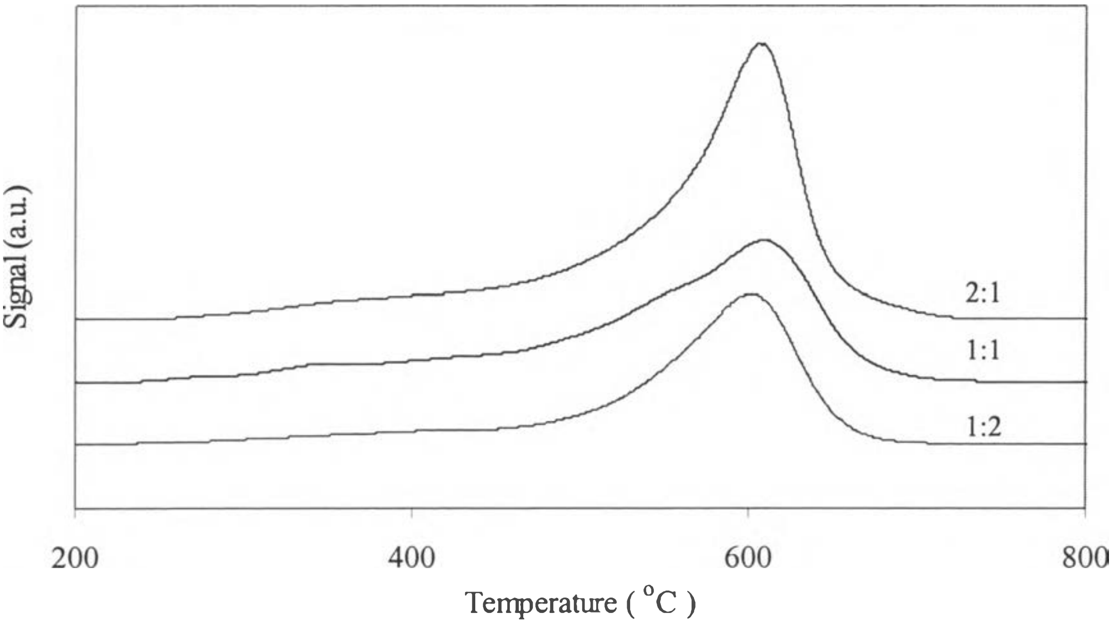

Figure 4.70 TPO profiles of carbon produced by CoMo at 1:1, 1:2, and 2:1 mole ratios over alumina support with CO at 750 °C.

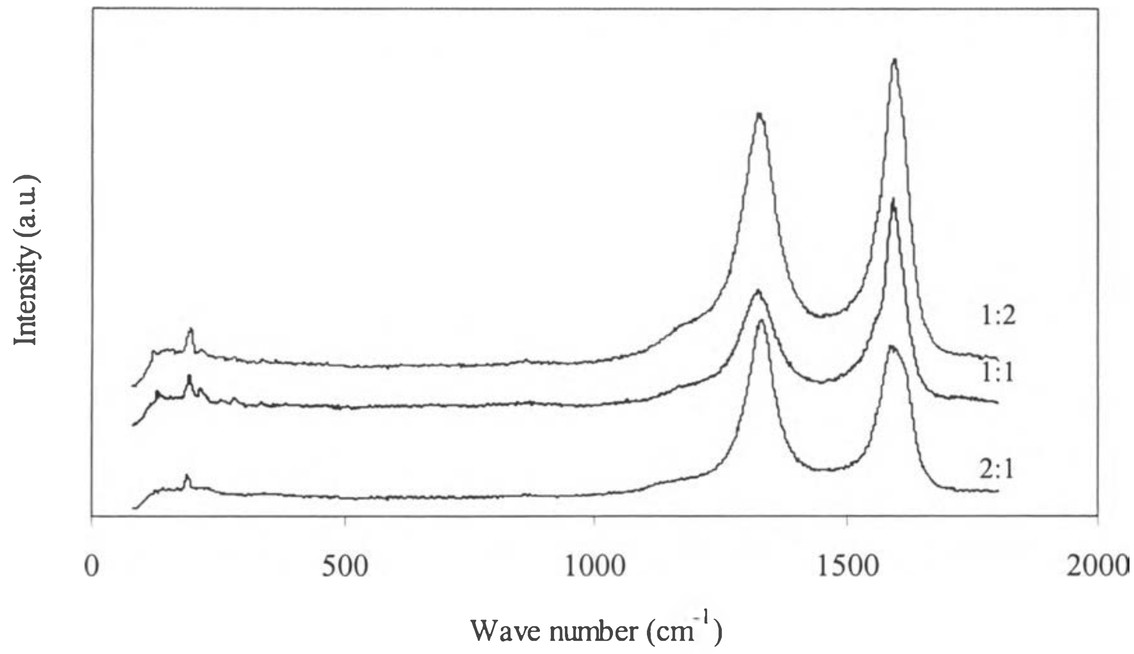

Figure 4.71 Raman spectra of carbon produced by CoMo at 1:1, 1:2, and 2:1 mole ratios over alumina support with mixture of CH_4 and CO at 750 °C.

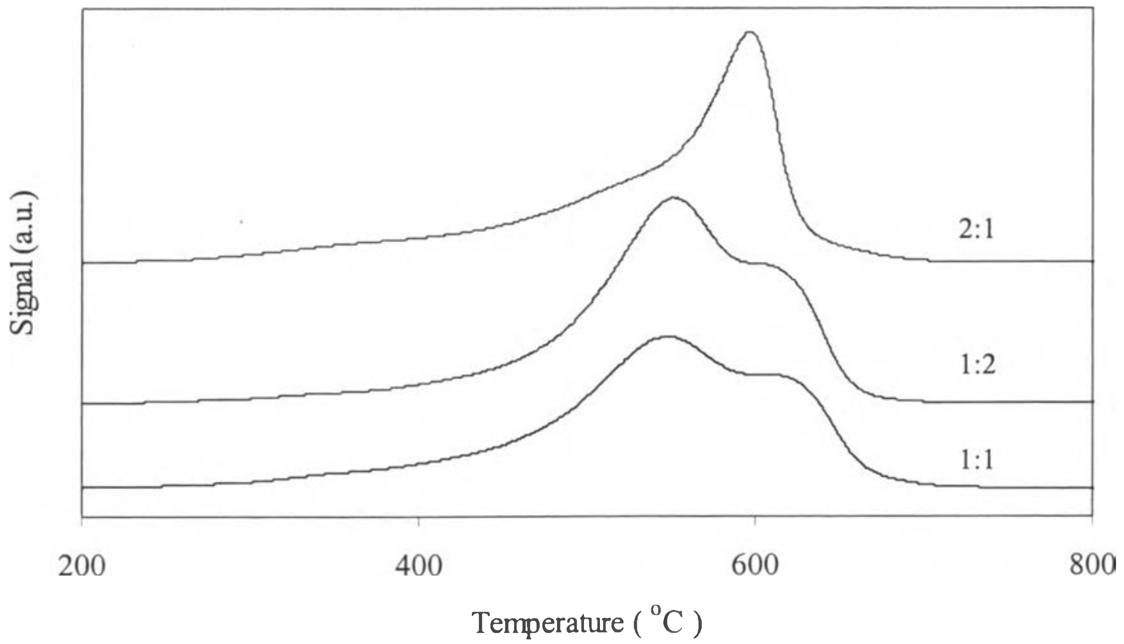

Figure 4.72 Raman spectra of carbon produced by CoMo at 1:1, 1:2, and 2:1 mole ratios over alumina support with mixture of CH_4 and CO at 750 °C.

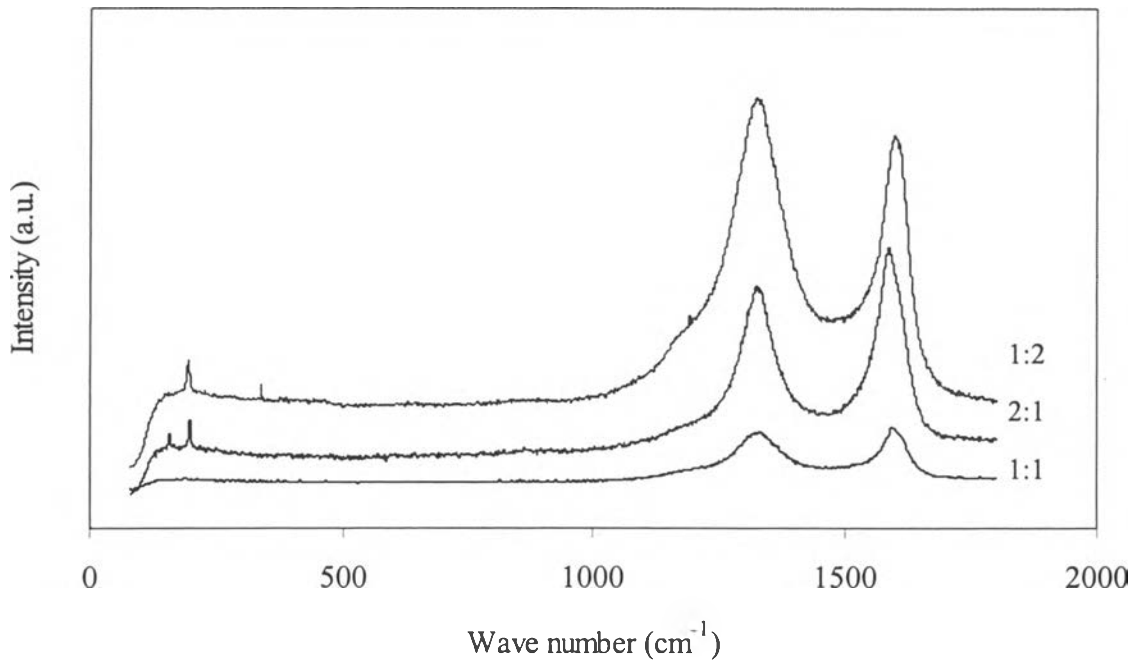

Figure 4.73 Raman spectra of carbon produced by FeMo at 1:1, 1:2, and 2:1 mole ratios over alumina support with CH_4 at 750 °C.

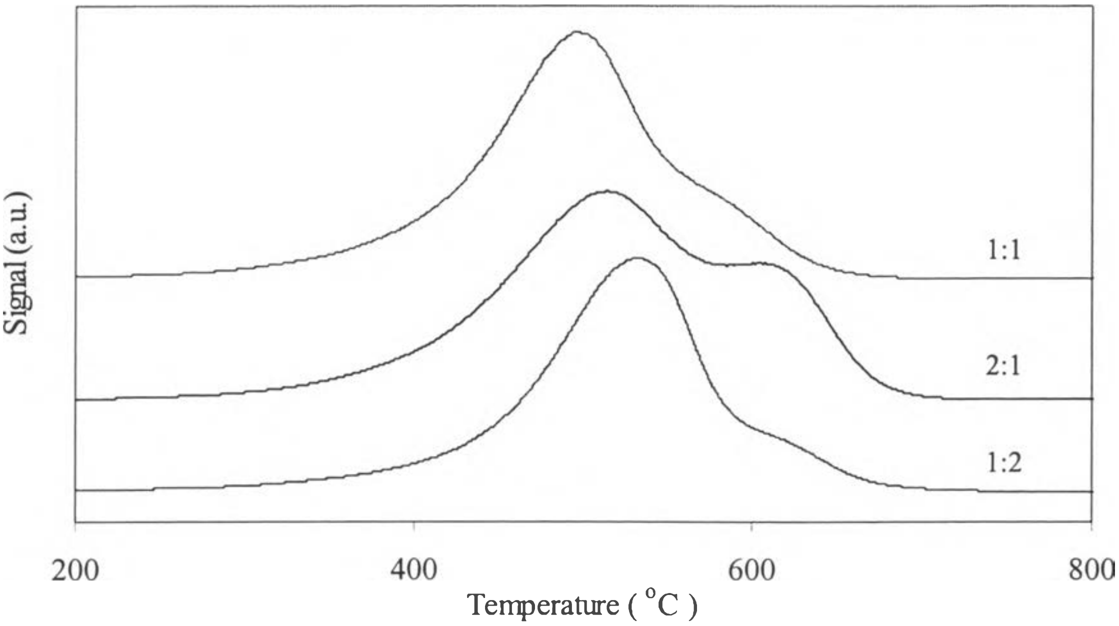

Figure 4.74 TPO profiles of carbon produced by FeMo at 1:1, 1:2, and 2:1 mole ratios over alumina support with CH_4 at 750 °C.

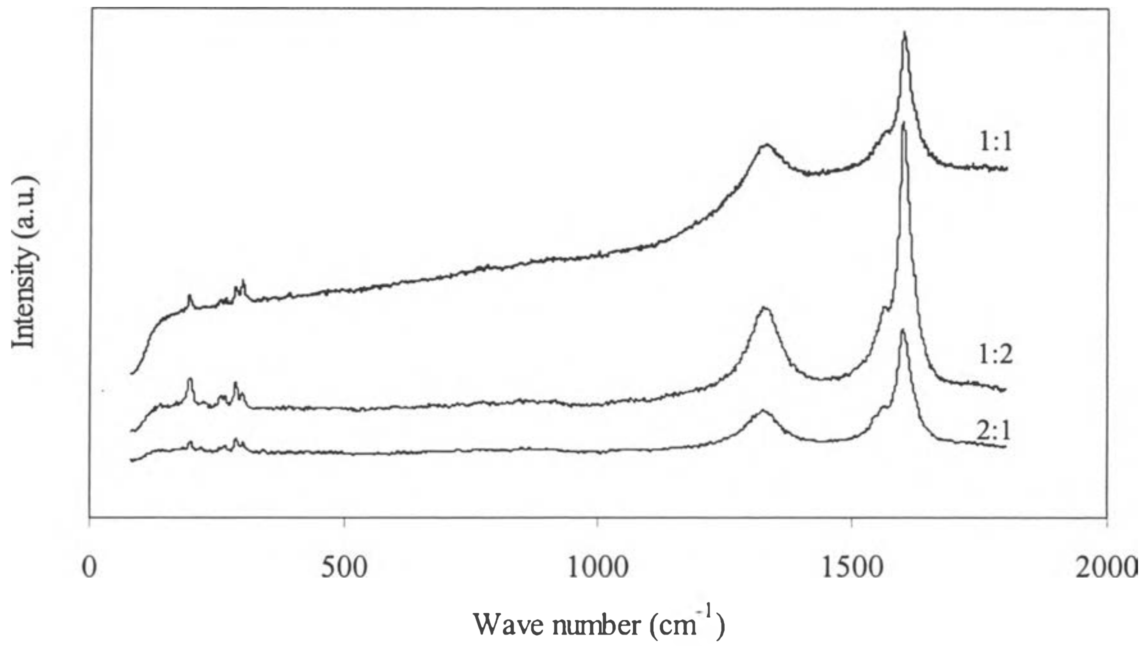

Figure 4.75 Raman spectra of carbon produced by FeMo at 1:1, 1:2, and 2:1 mole ratios over alumina support with CO at 750 °C.

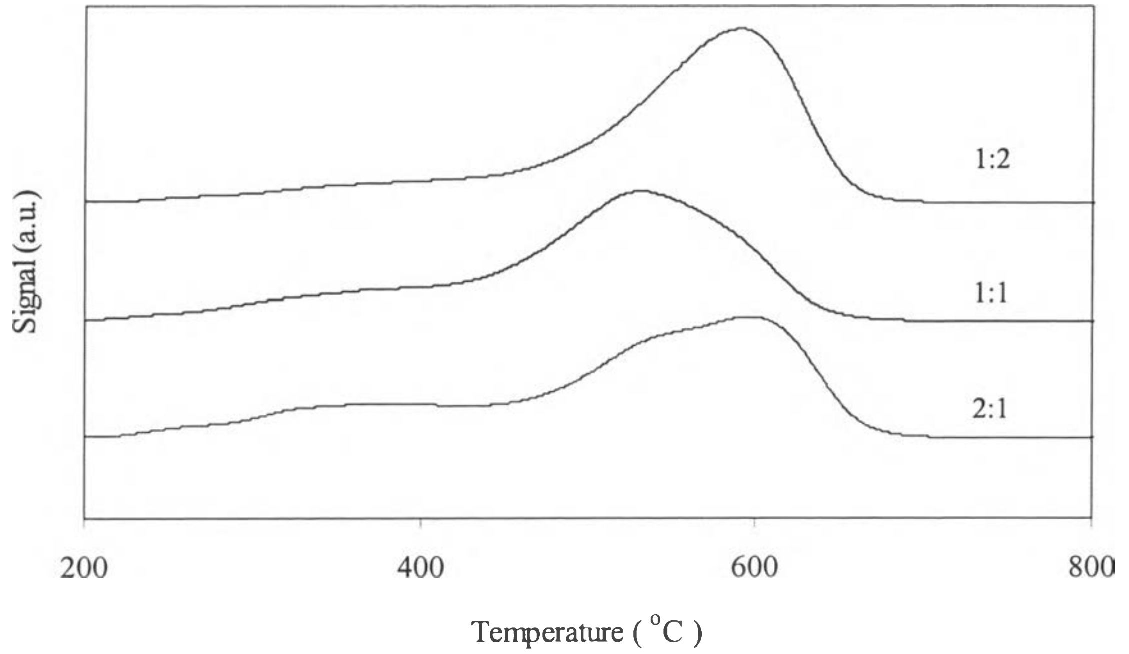

Figure 4.76 TPO profiles of carbon produced by FeMo at 1:1, 1:2, and 2:1 mole ratios over alumina support with CO at 750 °C.

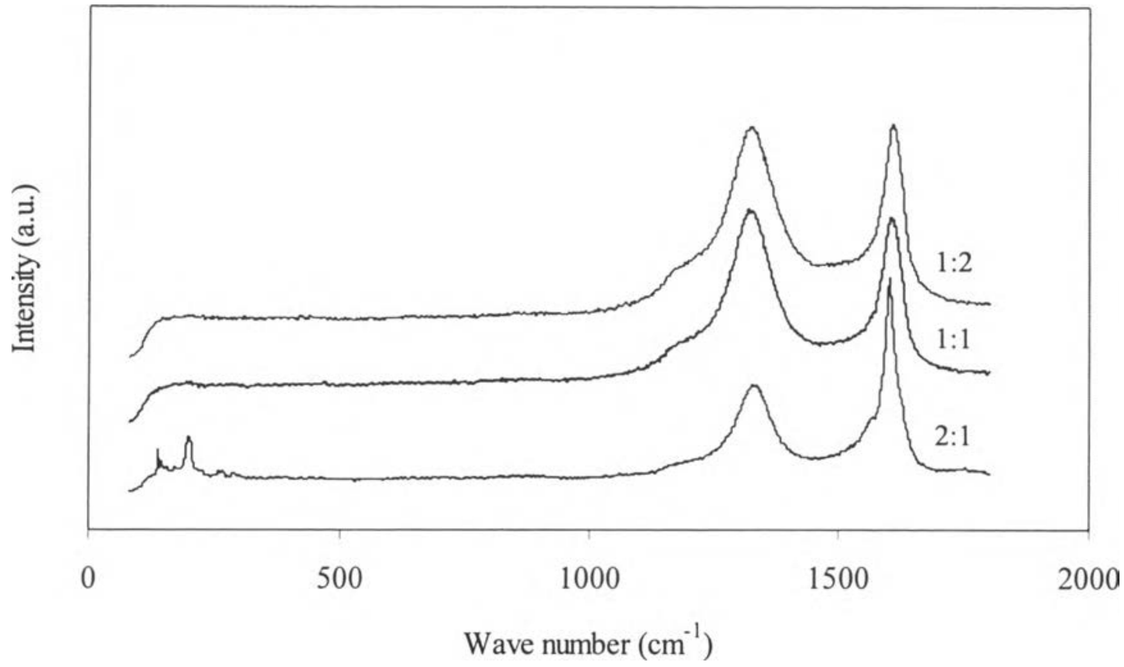

Figure 4.77 Raman spectra of carbon produced by FeMo at 1:1, 1:2, and 2:1 mole ratios over alumina support with mixture of CH_4 and CO at 750 °C.

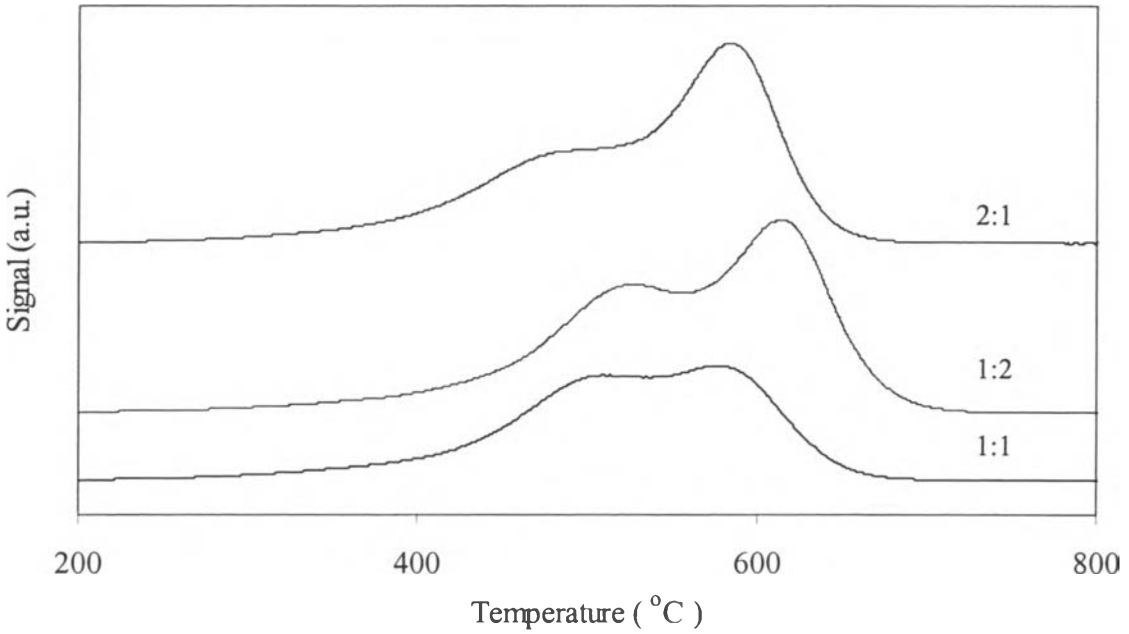

Figure 4.78 TPO profiles of carbon produced by FeMo at 1:1, 1:2, and 2:1 mole ratios over alumina support with mixture of CH_4 and CO at 750 °C.

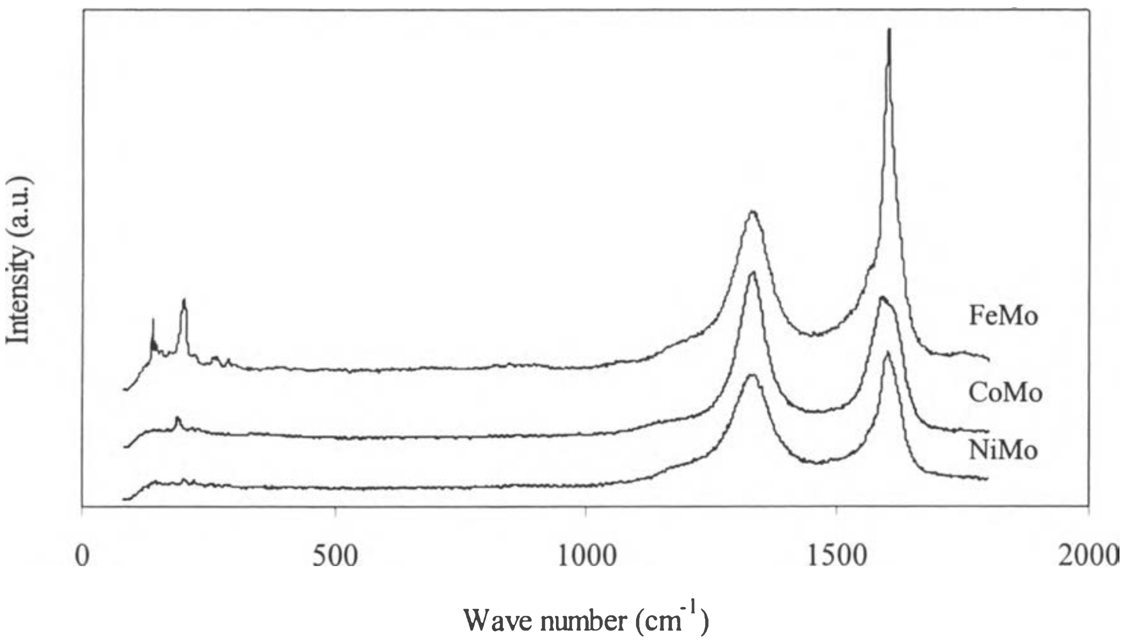

Figure 4.79 Raman spectra of carbon produced by NiMo, CoMo, and FeMo catalysts at 2:1 mole ratio over alumina support with mixture of CH_4 and CO at 750 °C.

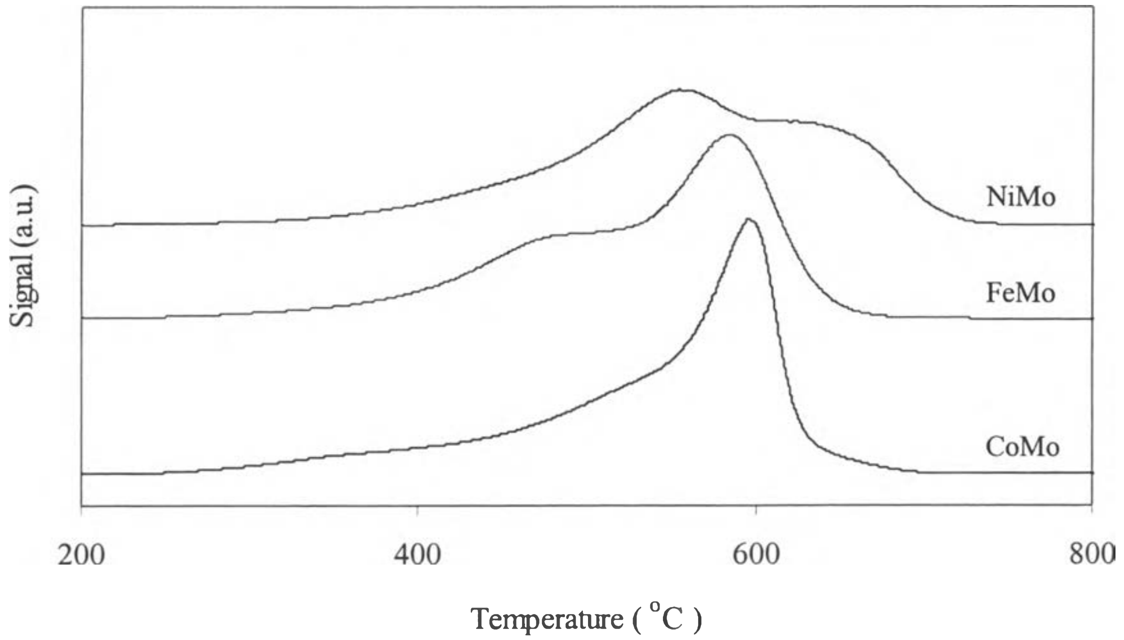

Figure 4.80 TPO profiles of carbon produced by NiMo, CoMo, and FeMo catalysts at 2:1 mole ratio over alumina support with mixture of CH_4 and CO at 750 °C.

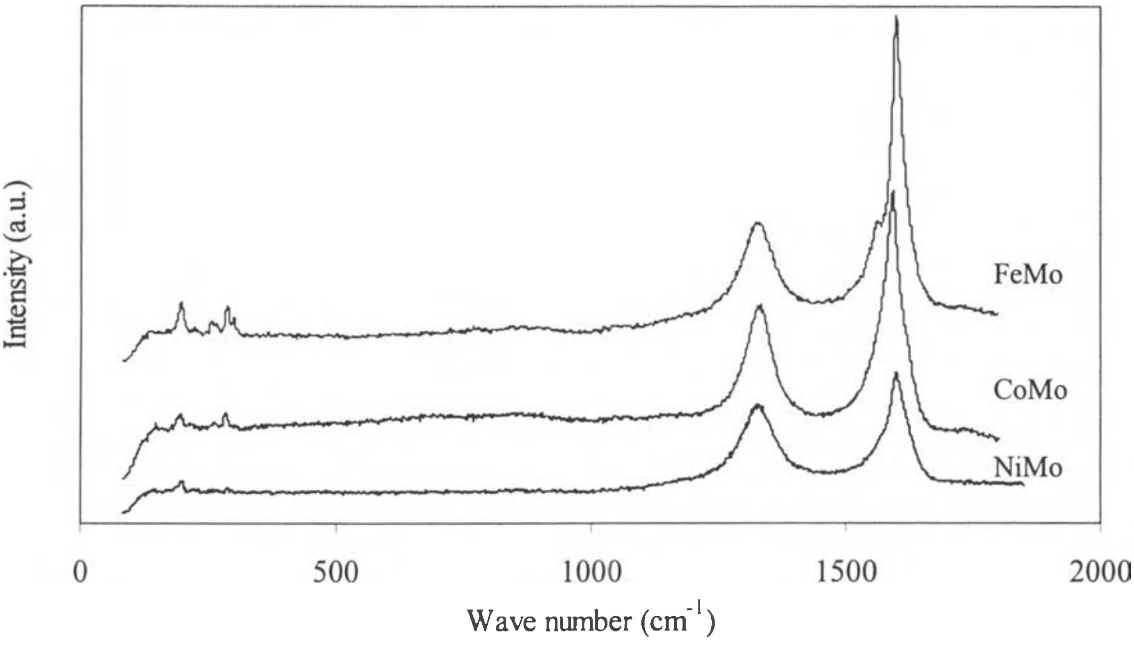

Figure 4.81 Raman spectra of carbon produced by NiMo, CoMo, and FeMo catalysts at 1:2 mole ratio over alumina support with CO at 750 °C.

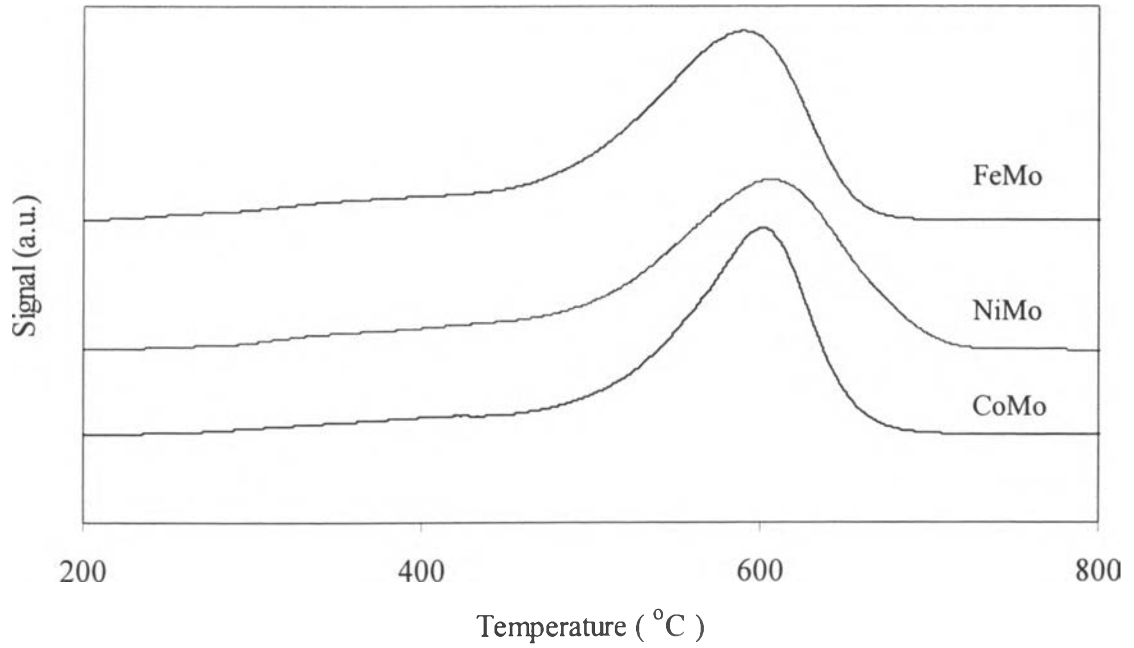

Figure 4.82 TPO profiles of carbon produced by NiMo, CoMo, and FeMo catalysts at 1:2 mole ratio over alumina support with CO at 750 °C.

The quality parameter of alumina support can be shown in Figure 4.83. Most of the deposited carbons produced by CO disproportionation not only presented the RBM signals but also gave high quality of SWNT. Interestingly, the quality parameter of carbon generated by CoMo 1:1 catalyst with CO disproportionation gaves a QP value close to one implying the highest quality of SWNT on deposited carbon. Moreover, some results show that carbon produced by mixture of CH_4 and CO showed the RBM signals and provided high quality of deposited carbon. The summary of carbon yields by comparing the different feed gases and catalyst formulations are shown in Figure 4.79. For the comparative bar chart of total carbon yield, the carbon obtained by CO disproportionation can produce high quality of SWNT, but provided the lowest yield of deposited carbon. The carbon samples that can produce SWNT, with increasing D/G ratios are summarized in Table 4.6. In this table, the distribution of diameter of SWNT is around 0.8–1.7 nm.

The TEM image of carbon species produced by FeMo 2:1 catalyst with CO disproportionation over alumina support presented SWNT as shown in Figure 4.80. In this image, the SWNT can be clearly seen on the alumina support.

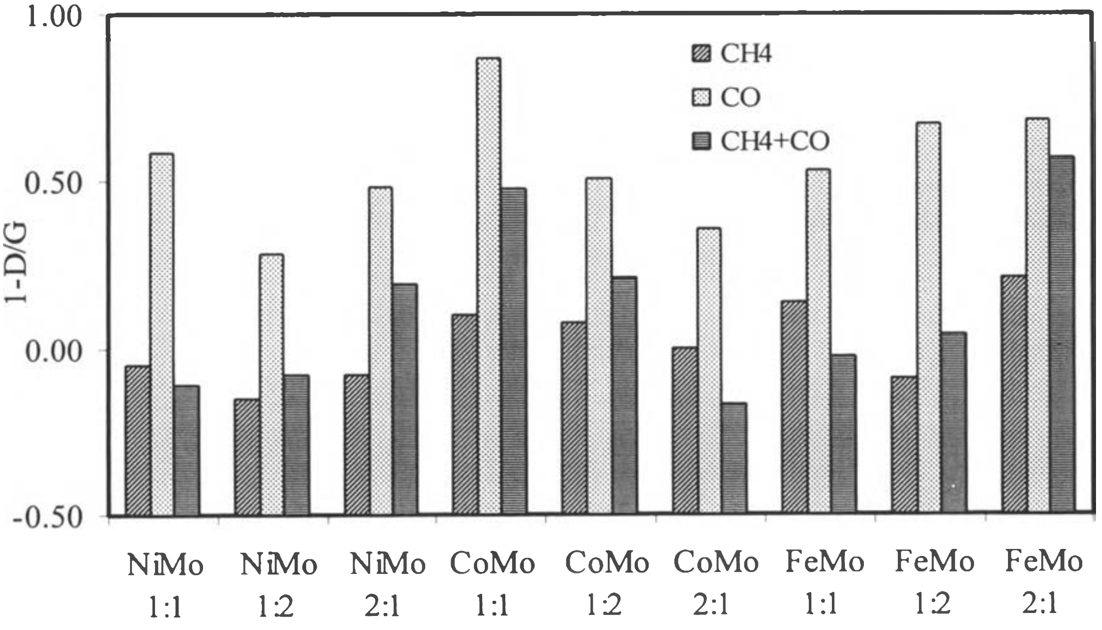

Figure 4.83 the quality parameter of carbon produced by different catalyst formulations over alumina support with CH_4, CO, and mixture at 750 °C.

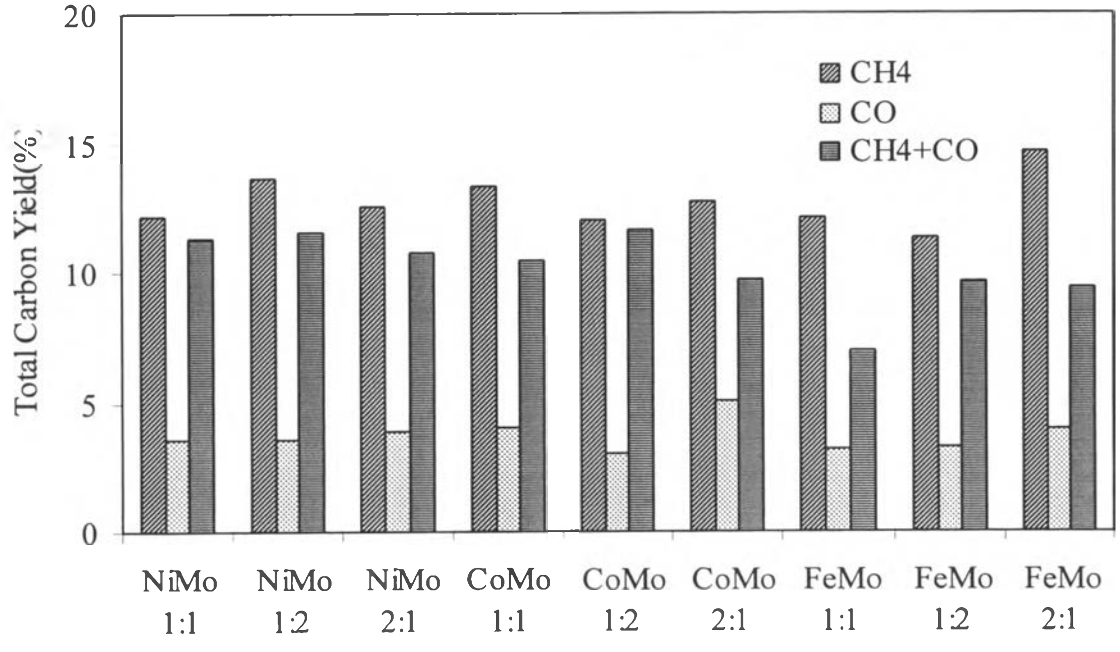

Figure 4.84 the total amount of carbon yield of carbon produced by different catalyst formulations over alumina support with CH_4, CO, and mixture at 750 °C.

Figure 4.85 TEM image showing SWNT produced by CO disproportionation on FeMo 2:1 catalyst over alumina support.

Table 4.6 Summary of SWNT formation on alumina support sorted by quality parameter

Samples	QP (1-D/G)	Carbon Yield (%)	diameter (nm)
CoMo 1:1/Al_2O_3 (CO, 750 °C)	0.86	4.03	0.83–1.25
FeMo 2:1/Al_2O_3 (CO, 750 °C)	0.68	3.94	0.76–1.20
FeMo 1:2/Al_2O_3 (CO, 750 °C)	0.67	3.29	0.78–1.18
NiMo 1:1/Al_2O_3 (CO, 750 °C)	0.59	3.56	0.82–1.23
FeMo 2:1/Al_2O_3 (CO+CH_4, 750 °C)	0.57	9.37	0.80–1.20
FeMo 1:1/Al_2O_3 (CO, 750 °C)	0.53	3.16	0.78–1.23
CoMo 1:2/Al_2O_3 (CO, 750 °C)	0.51	3.00	0.83–1.22
NiMo 2:1/Al_2O_3 (CO, 750 °C)	0.48	3.90	0.78–1.17
CoMo 1:1/Al_2O_3 (CH_4+CO, 750 °C)	0.48	10.43	1.20–1.23
NiMo 1:2/Al_2O_3 (CO, 750 °C)	0.28	3.60	1.20
CoMo 1:2/Al_2O_3 (CH_4+ CO, 750 °C)	0.21	11.65	1.24
FeMo 2:1/Al_2O_3 (CH_4, 750 °C)	0.21	14.67	1.22–1.55
NiMo 2:1/Al_2O_3 (CH_4+CO, 750 °C)	0.19	10.74	0.81–1.19
CoMo 1:1/Al_2O_3 (CH_4, 750 °C)	0.10	13.32	0.82–1.24
CoMo 1:2/Al_2O_3 (CH_4, 750 °C)	0.08	12.05	1.22–1.76

4.4 Effects of Silica, Magnesium Oxide, and Alumina supports on Carbon Nanotubes Formation

In order to select the support appropriate for selective catalyst, silica gel, magnesium oxide, and alumina supports were studied.

Figure 4.86–4.89 compare the Raman spectra of carbon over different supports. Results showed that silica and alumina are the prefered support to produce SWNT. On the other hand, the MgO support is not suitable in creating SWNT and gives high it also give quantity of undesirable forms of carbon.

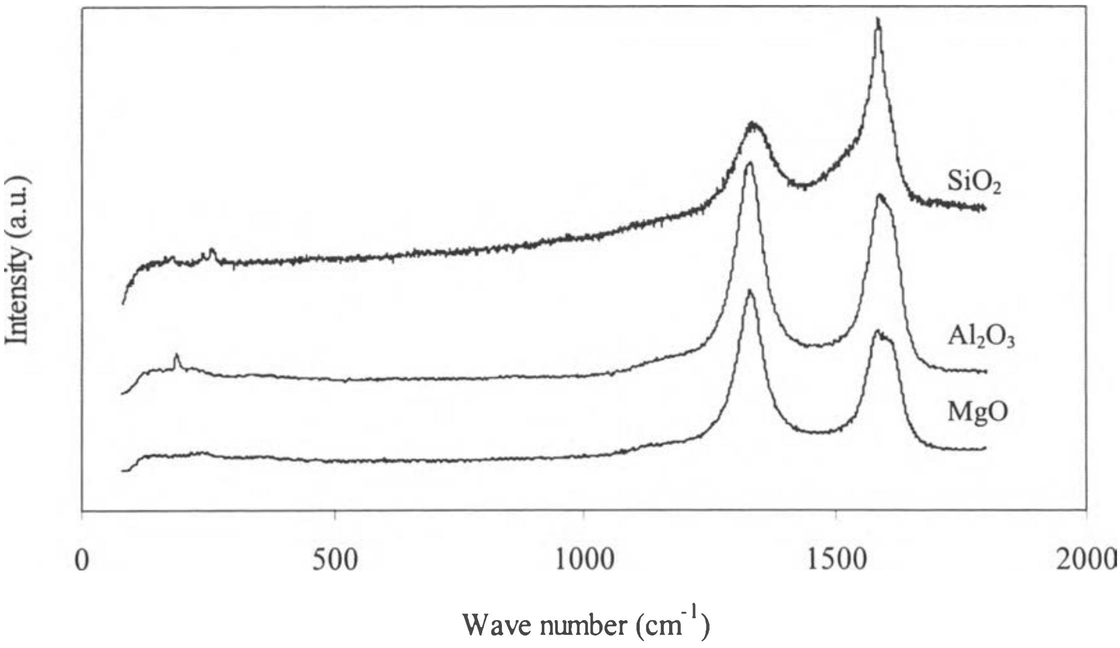

Figure 4.86 Raman spectra of carbon produced by CoMo 2:1 over silica, magnesium oxide, and alumina supports with mixture of CH_4 and CO at 750 °C.

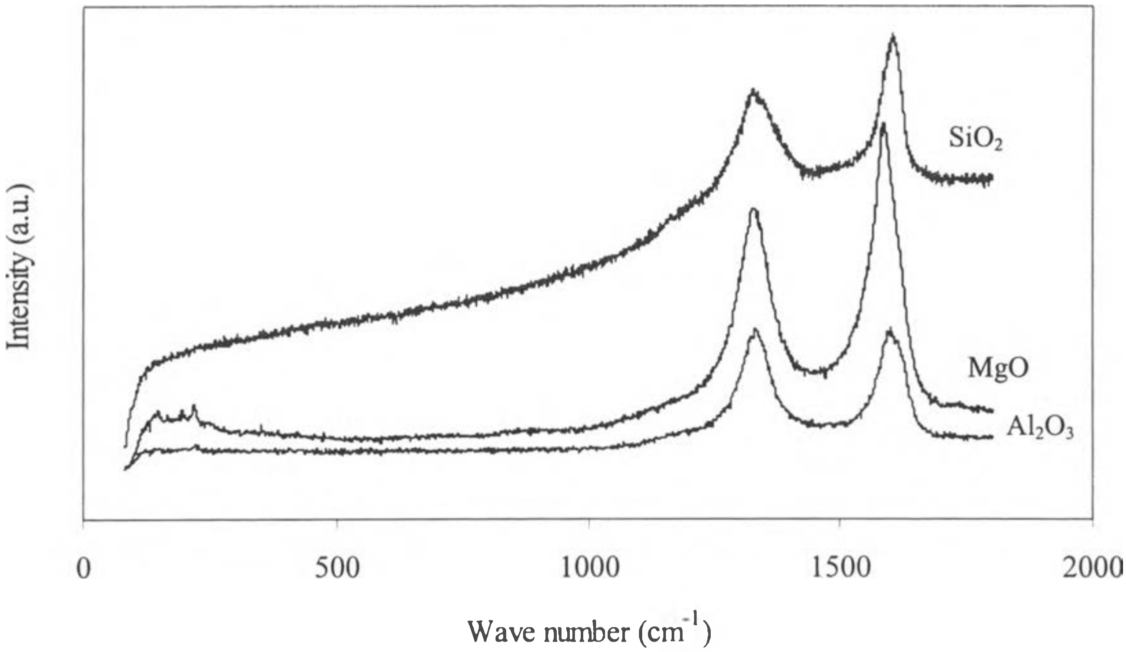

Figure 4.87 Raman spectra of carbon produced by CoMo 2:1 over silica, magnesium oxide, and alumina supports with CH_4 at 750 °C.

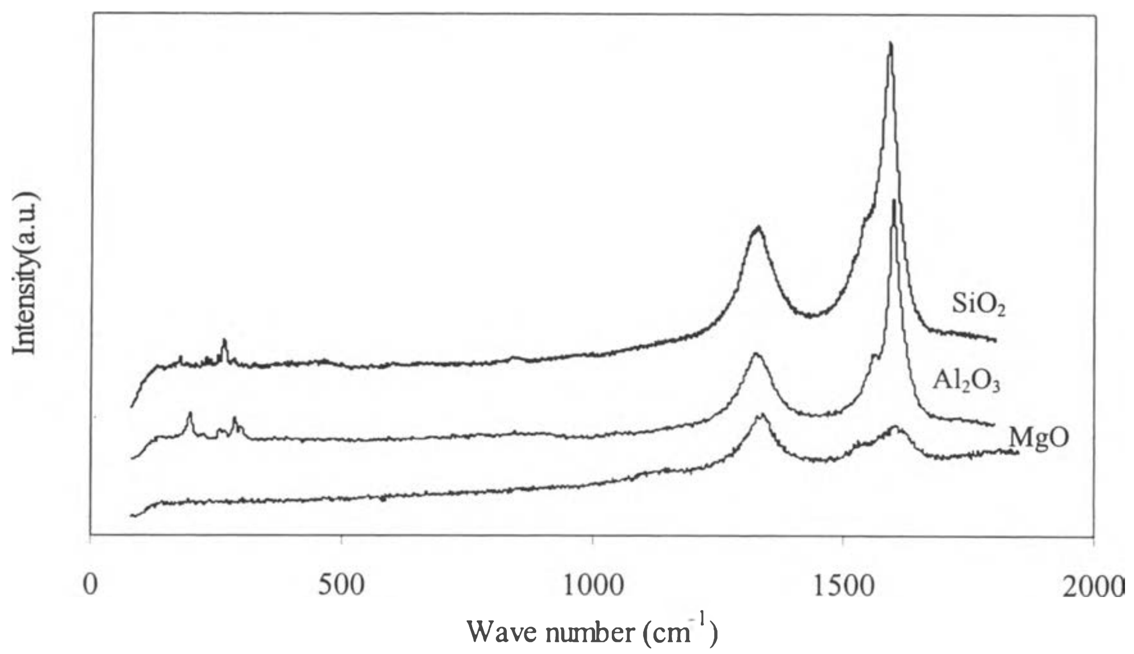

Figure 4.88 Raman spectra of carbon produced by FeMo 1:2 over silica, magnesium oxide, and alumina supports with CO at 750 °C.

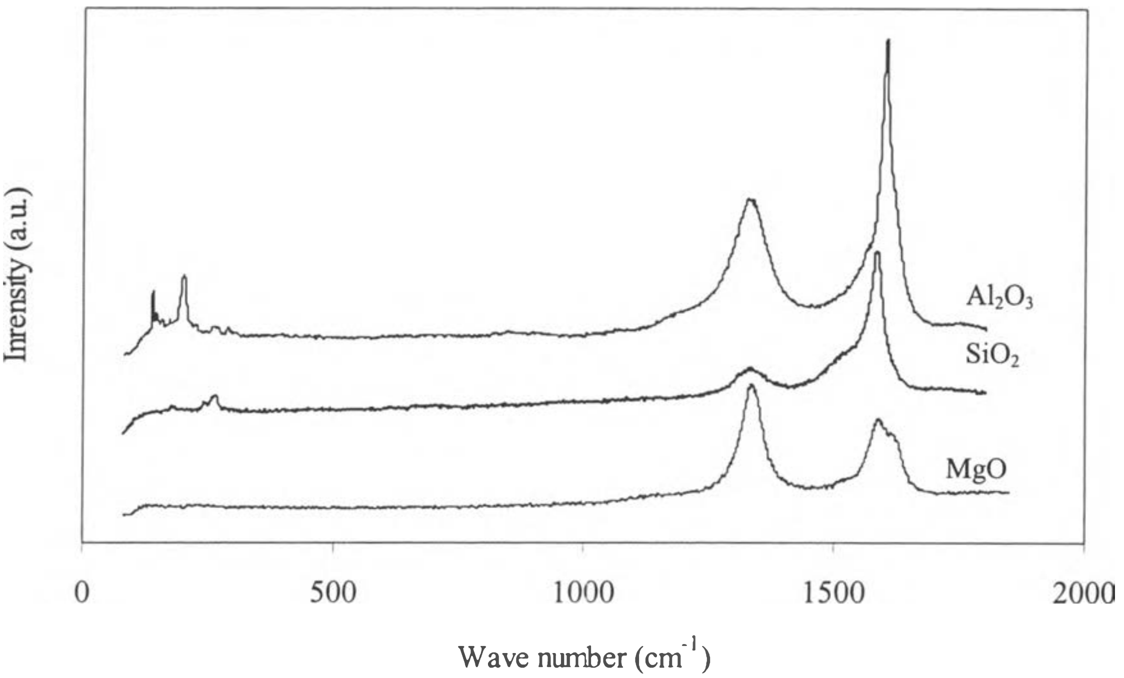

Figure 4.89 Raman spectra of carbon produced by FeMo 2:1 over silica, magnesium oxide, and alumina supports by mixtures of CH_4 and CO at 750 °C.